

Deutsches Rheuma-Forschungszentrum Berlin (DRFZ)  
and  
Research Center ImmunoSciences (RCIS)

**Migration and differentiation of murine germinal  
center derived B cell subsets in the course of the NP-  
specific immune response**

Dissertation zur Erlangung des akademischen Grades des  
Doktors der Naturwissenschaften (Dr. rer. nat.)

eingereicht am Fachbereich Biologie, Chemie, Pharmazie  
der Freien Universität Berlin

vorgelegt von

Mag. Atijeh Valai

aus Wien

im März 2012

1. Gutachter: Prof. Dr. Rudolf Manz
2. Gutachter: Prof. Dr. Rupert Mutzel

Disputation am 29.06.2012

<b>1</b>	<b><u>INTRODUCTION</u></b>	<b>4</b>
1.1	THE ADAPTIVE AND INNATE IMMUNITY	4
1.2	LYMPHOCYTES AND LYMPHATIC ORGANS	5
1.2.1	T CELLS AND THEIR TYPES AND FUNCTIONS	5
1.2.2	B CELLS; FUNCTIONS AND THEIR ANTIBODIES	6
1.2.3	PRIMARY LYMPHOID ORGANS	8
1.2.4	SECONDARY LYMPHOID ORGANS AND TISSUES	11
1.3	ACTIVATION OF B CELLS BY T-INDEPENDENT ANTIGENS	13
1.4	ACTIVATION OF B CELLS BY T-DEPENDENT ANTIGENS	14
1.5	SELECTION, SURVIVAL AND DIFFERENTIATION OF B CELLS IN THE T-DEPENDENT IMMUNE RESPONSE	15
1.5.1	THE EXTRAFOLLICULAR RESPONSE	16
1.5.2	THE GC REACTION	17
1.5.3	MEMORY B CELLS AND PLASMA CELLS	18
<b>2</b>	<b><u>OBJECTIVES</u></b>	<b>22</b>
<b>3</b>	<b><u>MATERIALS AND METHODS</u></b>	<b>23</b>
3.1	BUFFERS, REAGENTS AND SOLUTION	23
3.2	ANTIBODIES AND REAGENTS FOR FACS AND IMMUNOFLUORESCENCE	24
3.3	MICE, ANTIGEN AND IMMUNIZATIONS	25
3.4	IMMUNOFLUORESCENCE	25
3.5	ADOPTIVE TRANSFERS	27
3.6	FLOW CYTOMETRY	28
<b>4</b>	<b><u>RESULTS</u></b>	<b>29</b>
4.1	KINETIC OF NP-KLH SPECIFIC RESPONSE AFTER PRIMARY AND SECONDARY CHALLENGE	29
4.1.1	DIFFERENCES IN ABSOLUTE LYMPHOCYTE NUMBERS OF C57BL/6 MICE AFTER PRIMARY OR SECONDARY CHALLENGE DO NOT CORRELATE WITH THE STATE OF IMMUNE RESPONSE	29
4.1.2	KINETICS AND MATURATION OF NP-KLH INDUCED B CELL SUBSETS DURING PRIMARY AND SECONDARY IMMUNE RESPONSE	33

4.1.3 IDENTIFIED B CELLS WITH GC PHENOTYPE IN BLOOD ARE MATURE B CELLS WITH FOLLICULAR ORIGIN	38
4.1.4 DYNAMICS OF THE NP-KLH INDUCED PLASMA BLAST AND PLASMA CELL RESPONSE	42
<b>4.2 MIGRATORY BEHAVIOR OF BLOOD-DERIVED B CELL SUBSETS AFTER TRANSFER INTO AT AN EARLIER TIME POINT AFTER IMMUNIZATION</b>	<b>47</b>
4.2.1 TRANSFERRED B CELLS NUMBERS INCREASE AS EARLY AS 2 DAYS AFTER TRANSFER AND DO NOT VARY IN FREQUENCIES UNTIL DAY EIGHT	48
4.2.2 TRANSFERRED GC B CELLS HOME TO SECONDARY LYMPHOID ORGANS, KEEP THEIR PHENOTYPE BUT MAINLY DEVELOP FURTHER INTO POST GC B CELLS AND PLASMA CELLS	50
4.2.3 TRANSFERRED IGM <sup>+</sup> CD38 <sup>+</sup> PNA <sup>LO</sup> B CELLS HOME TO SECONDARY LYMPHOID ORGANS, SWITCH THEIR ISOTYPE AND INDUCE A STRONG BUT RATHER SHORT LIVED PLASMA CELL RESPONSE	53
4.2.4 TRANSFERRED IGG1 B CELLS HOME TO SPLEEN AND BONE MARROW AND DOWN-REGULATE SURFACE B220 AT LATER TIME POINTS	56
4.2.5 TRANSFERRED GC B CELLS ARE INITIALLY LOCATED ALONG THE T CELL BORDER AND PARTIALLY PROLIFERATE WITHIN THE B CELL ZONE AND INTERFOLLICULAR ZONE WHEREAS ANOTHER FRACTION ENTERS THE DARK ZONE AND SUBSEQUENTLY ACCUMULATES IN THE GC LIGHT ZONE	58
4.2.6 TRANSFERRED B220 <sup>+</sup> PNA <sup>LO</sup> CD38 <sup>H</sup> IGM <sup>+</sup> CELLS ACCUMULATE ALONG THE B/T BORDER AND WITHIN THE IF ZONE PRIOR TO ENTERING THE GC DARK AND LIGHT ZONES	63
<b>4.3 MIGRATORY BEHAVIOR OF BLOOD-DERIVED B CELL SUBSETS AFTER TRANSFER INTO RECIPIENTS AT THE TIME POINT AFTER IMMUNIZATION</b>	<b>68</b>
4.3.1 TRANSFERRED GC B CELLS AND IGM <sup>+</sup> B CELLS PROLIFERATE 2 DAYS AFTER TRANSFER IN SPLEEN AND BONE MARROW BUT DECREASE IN NUMBERS AFTERWARDS, WHEREAS IGG1 <sup>+</sup> B CELLS ARE ONLY DETECTED IN BONE MARROW AND REMAIN THERE AT STABLE FREQUENCIES	69
4.3.2 TRANSFERRED BLOOD GC B CELLS HOME TO SECONDARY LYMPHOID ORGANS, PARTIALLY KEEP THEIR PHENOTYPE BUT MAINLY DIFFERENTIATE FURTHER AND INDUCE A SHORT LIVED PLASMA CELL RESPONSE	73
4.3.3 TRANSFERRED BLOOD RESIDING IGM <sup>+</sup> CD38 <sup>+</sup> B CELLS CAN REGAIN A GC PHENOTYPE FOR A FEW DAYS AND INDUCE A STRONG SHORT LIVED PLASMA CELL RESPONSE	76
4.3.4 BLOOD-DERIVED IGG1 <sup>+</sup> CD38 <sup>+</sup> B CELLS ACCUMULATE IN THE BONE MARROW AND CHANGE THEIR SURFACE EXPRESSION OF B220 AT EARLY TIME POINTS OF IMMUNE RESPONSE	78
4.3.5 T CELL ASSOCIATED PROLIFERATION OF BLOOD-DERIVED GC B CELLS WITHIN THE FOLLICLE PRECEDES THEIR MIGRATION TO THE GC DARK ZONE FOLLOWED BY THEIR RECRUITMENT TO GC LIGHT ZONE	79

---

4.3.6	THE B CELL FOLLICLE IS THE MAIN ASSEMBLY SIDE OF TRANSFERRED BLOOD-DERIVED PNA <sup>LO</sup> CD38 <sup>HI</sup> IGM <sup>+</sup> B CELLS	84
<b>5</b>	<b><u>DISCUSSION</u></b>	<b>90</b>
<b>5.1</b>	<b>KINETIC OF NP-KLH INDUCED B CELL SUBSETS BY ANALYSIS OF THEIR EXPRESSION PROFILE OF CELL SURFACE MARKERS AFTER PRIMARY AND SECONDARY CHALLENGE</b>	<b>90</b>
5.1.1	IDENTIFICATION OF THE GC B CELL SUBSET	90
5.1.2	KINETIC OF THE GC B CELL SUBSETS	91
5.1.3	IDENTIFICATION OF THE MEMORY B CELL SUBSET	92
5.1.4	KINETIC OF THE MEMORY B CELL SUBSETS	92
5.1.5	IDENTIFICATION OF THE PLASMABLAST AND PLASMA CELL SUBSETS	93
5.1.6	KINETIC OF THE PLASMABLAST AND PLASMA CELL SUBSETS	93
<b>5.2</b>	<b>DETECTION OF GC B CELLS IN BLOOD OF NP-KLH IMMUNIZED C57BL/6 MICE</b>	<b>95</b>
<b>5.3</b>	<b>TRANSFERRED BLOOD GC B CELLS REPOPULATE PERSISTING GCs AND DIFFERENTIATE INTO PLASMA CELLS</b>	<b>96</b>
<b>5.4</b>	<b>TRANSFERRED IGM AND IGG1 POTENTIAL MEMORY B CELLS DISPLAY DIFFERENT MIGRATION PATTERNS</b>	<b>99</b>
<b>6</b>	<b><u>SUMMARY AND PERSPECTIVES</u></b>	<b>104</b>
<b>7</b>	<b><u>ZUSAMMENFASSUNG</u></b>	<b>107</b>
<b>8</b>	<b><u>ABSTRACT</u></b>	<b>109</b>
<b>9</b>	<b><u>REFERENCES</u></b>	<b>111</b>
<b>10</b>	<b><u>APPENDIX</u></b>	<b>117</b>

# 1 Introduction

## 1.1 The adaptive and innate immunity

Any immune response involves, firstly, recognition of the pathogen or foreign material, and secondly, a reaction to eliminate it. Broadly, the different types of immune response fall into two categories: innate (or non-adaptive) immune responses and adaptive immune responses. The important difference between these is that an adaptive immune response is highly specific for particular pathogen. Moreover, although the innate response does not alter on repeated exposure to a given infectious agent, the adaptive response improves with each successive encounter with the same pathogen: in effect the adaptive immune system “remembers” the infectious agent and can prevent it from causing disease later. For example, diseases such as measles and diphtheria induce adaptive immune responses which generate a live-long immunity following an infection. The two key features of the adaptive immune response are thus specificity and memory. (Roitt et al., 2001) The major component of the adaptive immune system is a specialized cell type called lymphocytes, to which we will refer in section 1.2.

Both the adaptive and innate immune system contains humoral and cellular components. The protective function of cell-mediated immunity is associated with cells such as macrophages, natural killer cells, antigen-specific cytotoxic T lymphocytes and cytokines which are released in response to antigen. These cells promote elimination of pathogen by inducing apoptosis through presentation of foreign antigen on their surface (T cells), directly destroying pathogens (macrophages and natural killer cells) or stimulating cells to secrete a variety of cytokines and influence the function of cells involved in adaptive or innate immune responses. Essentially, cell-mediated immunity is directed at microbes that survive phagocytes or infect non-phagocytic cells. It is also very effecting in removing virus-infected cells and involved in the defense against intracellular bacteria, protozoan and fungi. Humoral immunity, for which the protective function can be found in humor (serum), is mediated by antibodies, which are produced by antibody secreting cells (ASC), in particular plasmablasts and plasma cells. Antibodies play an important role in the defense against extracellular pathogens and their toxins. Their effector function is mediated by pathogen and toxin neutralization,

complement activation and opsonization of pathogens. Thus, humoral immunity refers to antibody production and its involved processes including cytokine production, germinal center (GC) formation and isotype switching, affinity maturation and generation of the memory B cell and plasma cell response.

This thesis deals with the following features of humoral immune response that play key roles in its progression and maturation:

- extrafollicular immune response: which is responsible for the fast production of antibodies after antigen encounter and takes place in lymphatic organs such as spleen and lymph nodes (MacLennan et al., 2003)
- GC reaction: is a micro-evolutionary process which takes place within GCs of secondary lymphatic organs during a T cell dependent (TD) immune response , resulting in the affinity maturation and production of high affinity plasma cells and memory B cells (MacLennan, 1994)

Each of the mentioned termini will be described more detailed in the following chapters and their roles in the orchestration of the TD immune response will be elucidated. Prior to that, the next section will introduce the properties of lymphocytes as the major arms of the humoral immune response and illustrate the architecture and migratory pathways in murine lymphatic organs.

## **1.2 Lymphocytes and lymphatic organs**

Lymphocytes are wholly responsible for the specific immune recognition of pathogen, so they initiate adaptive immune responses. All lymphocytes are derived from bone marrow stem cells, but T lymphocytes then develop in the thymus, while B lymphocytes develop in the bone marrow (in adult mammals).

### **1.2.1 T cells and their types and functions**

There are several different types of T cells, and they have a variety of functions. One group interacts with mononuclear phagocytes and helps them destroy intracellular pathogens; they are called type-1 T-helper cells or TH1 cells. Another group interacts with B cells and helps them to divide, differentiate and make antibody; these are the

TH2 cells. A third group of T cells is responsible for the destruction of the host cells which have become infected by viruses or other intracellular pathogens-this kind of action is called cytotoxicity and these cells are hence called T-cytotoxic (T<sub>c</sub>) cells. In every case, the T cell recognizes antigens, but only when they are presented on the surface of the other cell by so-called major histocompatibility complex (MHC) molecules. They use a specific receptor for this purpose, termed the T-cell antigen receptor (TCR). This is related, both in function and structure, to the surface antibody which B cells use as their antigen receptors. T cells generate their effects, either by releasing soluble proteins, called cytokines, which signal to other cells, or by direct cell-cell interactions (Roitt et al., 2001).

### **1.2.2 B cells; functions and their antibodies**

Each B cell is genetically programmed to encode a surface receptor specific for a particular antigen. Having recognized its specific antigen, the B cell multiply and differentiate into plasma cells, which produce large amount of the receptor molecule in a soluble form that can be secreted. This is known as antibody. These antibody molecules are large glycoproteins found in the blood and tissue fluids: because they are virtually identical to the original receptor molecule, they bind to the antigen that initially activated the B cells.

About 5.15% of the circulating lymphoid pool are B cells identified by the presence of surface immunoglobulin. They are constitutively produced and are inserted into the cell surface membrane where they act as specific antigen receptors. These receptors can be detected on the cell surface using fluorochrome-labeled antibodies specific for immunoglobulin.

#### **1.2.2.1 Cell surface immunoglobulin and signaling molecules form the B cell receptor complex**

The majority of B cells in peripheral blood express two immunoglobulin isotypes on their surface, IgM and IgD. On any B cell, the antigen binding sites of these isotypes are identical. Fewer than 10% of the B cells in the circulation express IgG, IgA or IgE, although these are present in larger numbers in specific locations of the body, for



example, IgA-bearing cells in the intestinal mucosa. Immunoglobulin associated with other molecules on the B cell surface forms the B cell antigen receptor complex (BCR). These “accessory” molecules consist of disulphide-bonded heterodimers of Ig $\alpha$  (CD79a) and Ig $\beta$  (CD79b). The heterodimers interact with trans-membrane segments of the immunoglobulin receptor, and are involved in cellular activation.

#### **1.2.2.2 Other B cell markers and subsets**

The majority of B cells carry MHC class II antigens, which are important for cooperative (cognate) interactions with T cells. These class II molecules consist of I-A and I-E in the mouse and HLA-DP, DQ and DR antigens in man. Complement receptors C3b (CD35) and C3d (CD21) are commonly found on B cells and are associated with activation and, possibly “homing” of these cells. CD19/CD21 interactions with complement associated with antigen plays a role in antigen induced B cell activation via the antigen binding B cell receptor. Fc receptors for exogenous IgG (Fc $\gamma$ RII, CD32) are also present and play a role in negative signaling to the B cell. CD19, CD20 and CD22 are the main markers currently used to identify human B cells. Other human B cell markers are CD72 and CD78. The CD72 molecule has also been described for murine B cells (Lyb-2) together with B220, a high molecular weight (220kDa) isoform of CD45 (Lyb-5). CD40 is an important molecule on B cells which is involved in cognate interactions between T and B cells. The combination of B220, CD21 and CD23 can be used to separate follicular B cells from marginal zone B cells in mouse (Wang et al., 2006).

#### **1.2.2.3 B cell differentiation leads to the formation of plasma cells and memory B cells**

Following B cell activation, many B cells mature into plasmablasts, which progress to terminally differentiated plasma cells. Some B blasts do not develop rough endoplasmic reticulum cisternae. These cells are found in GCs and are called GC B cells, which will be accurately described in the following sections. Under light microscopy, the cytoplasm of plasma cells is basophilic; this is due to the large amount of RNA being utilized for antibody synthesis in the rough endoplasmic reticulum. Plasma cells are infrequent in the blood, comprising less than 0.1% of circulating lymphocytes. They are normally restricted to secondary lymphoid organs and tissues but are also abundant in

the bone marrow. Antibodies produced by a single plasma cell are of one specificity and immunoglobulin class. Immunoglobulin can be visualized in the plasma cell cytoplasm by staining with fluorochrome labeled specific antibodies. Most of the plasma cells have a short lifespan, surviving for a view days and dying by apoptosis, whereas a subset of plasma cells with a long lifespan has been described in the bone marrow (Manz et al., 1998; Roitt et al., 2001). Another result of the TD response to primary antigenic exposure is the generation of memory B cells. Memory B cells are characterized as activated B cells which are cellular products of the GC response, larger than resting B cells and antigen specific. On antigen recall, memory response precursors expand rapidly with exaggerated differentiation into plasma cells to produce the high-titer, high-affinity antibody that typifies the memory B-cell response in vivo (McHeyzer-Williams and McHeyzer-Williams, 2004). Although IgM<sup>+</sup> and IgG<sup>+</sup> clones are usually observed during the first weeks after immunization, the study of long term memory has generally focused on IgG<sup>+</sup> memory, which can be detected in low numbers several months after immunization. IgG is considered a marker of B cell memory and can confer through its intra-cytoplasmic tail the signals necessary for long-term survival (Dogan et al., 2009).

### 1.2.3 Primary lymphoid organs

Primary lymphoid organs are the major sites of lymphocyte development. Here, lymphocytes differentiate from lymphoid stem cells, proliferate and mature into functional cells. In mammals, T cells mature in the thymus, B lymphocytes in the fetal liver and bone marrow. It is in the primary lymphoid organs that lymphocytes acquire the repertoire of specific antigen receptors in order to cope with antigenic challenges that individuals receive during their lifespan. In these primary lymphoid organs the cells with receptors for autoantigen are mostly eliminated, whereas in the thymus T cells also learn to recognize self-MHC molecules. There is evidence that some lymphocyte development occurs outside the primary lymphoid organs (Roitt et al., 2001).

### **1.2.3.1 The thymus is the site of T cell development**

The thymus in mammals is a bilobed organ, located in the thoracic cavity, overlying the heart and major blood vessels. Within each lobule lymphoid cells (thymocytes) are arranged into an outer cortex and an inner medulla. The tightly packed cortex contains the majority of immature proliferating thymocytes; more mature cells are found in the medulla, implying a differentiation gradient from the cortex to the medulla. There is a network of epithelial cells throughout the lobules which play a role in the differentiation process from bone marrow-derived prethymic cells to mature T lymphocytes.

### **1.2.3.2 Mammalian B cells develop in the bone marrow and fetal liver**

Mammals do not have a specific discrete organ for B cell lymphopoiesis. Instead, the cells develop directly from lymphoid stem cells in the hematopoietic tissue of the fetal liver from 8 to 9 weeks from gestation in humans, and by about 14 days in the mouse. Later, the site of B cell production moves from the liver to the bone marrow, where it continues through adult life. This is also true of the other hematopoietic lineages, giving rise to erythrocytes, granulocytes, monocytes and platelets.

B cells do not develop in indistinct domains of the bone marrow. B cell progenitors are seen adjacent to the endosteum of the bone lamellae. Each B cell progenitor may produce up to 64 progeny at the stage of immunoglobulin gene rearrangement. These migrate towards the center of each cavity and reach the lumen of a venous sinusoid. In the bone marrow B cells mature in close association with stromal reticular cells, which contribute to their maturation by producing IL-7 (Figure 1). The majority of B cells (over 75%) maturing in the bone marrow, do not reach the circulation, but undergo a process of programmed cell death or apoptosis and are phagocytosed by bone marrow macrophages. It has been suggested that B cell-stromal interactions may mediate a form of positive selection that rescues a minority of B cells with productive rearrangements of their immunoglobulin genes from programmed cell death. Negative selection of autoreactive B cells may occur in the bone marrow or in the spleen, the site to which the majority of newly produced B cells are exported during fetal life. From kinetic data, it is estimated that about  $5 \times 10^7$  murine B cells are produced each day. Since the mouse spleen contains  $7.5 \times 10^7$  B cells, a large proportion of B cells must die, probably at the

pre-B cell stage due to non-productive rearrangements of receptor genes or because of expressing self-reactive antibodies.

Lymphoid stem cells expressing terminal deoxynucleotidyl transferase (TdT) proliferate, differentiate and undergo immunoglobulin gene rearrangements to emerge as pre-B cells which express  $\mu$  heavy chains in the cytoplasm. Some of these pre-B cells bear small numbers of surface  $\mu$  chains, associated with surrogate light chains  $V_{pre-B}$  and  $\gamma 5$ . Allelic exclusion of either maternal or paternal immunoglobulin genes has already happened by this time. Once a B cell has synthesized light chains, which may be either  $\kappa$ - or  $\lambda$ - type, it becomes committed to the antigen binding specificity of its surface IgM antigen receptor. Thus, one B cell can make only one specific antibody, a central tenet of the clonal selection theory for antibody production. A sequence of immunoglobulin gene rearrangements takes place during B cell ontogeny. Heavy chain gene rearrangements occur in B cell progenitors and represent the earliest indication of B-lineage commitment. This is followed by light chain rearrangements which occur at later pre-B cell stages (Figure 1).

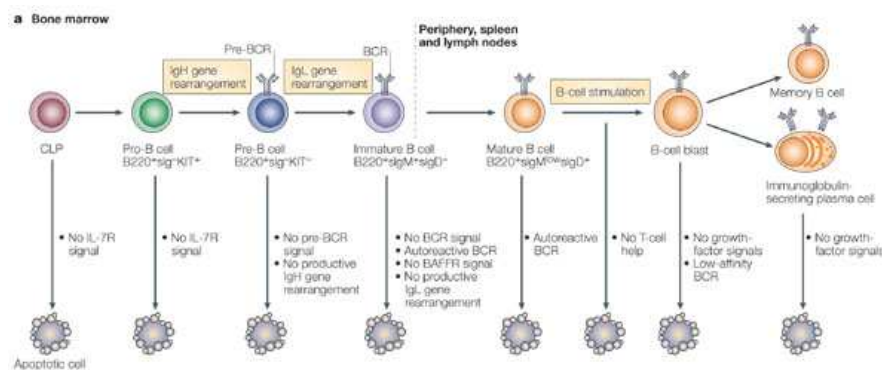


Figure 1: B cell development in bone marrow and secondary lymphoid organs (Strasser, 2005).

After the differentiation steps mentioned above, B cells migrate to the secondary lymphoid organs. Early B cell immigrants into fetal lymph nodes are surface IgM<sup>+</sup> and are B-1 cells. Following antigenic stimulation, mature B cells can develop into memory cells or ASC. Surface immunoglobulins are usually lost in plasma cells, since their function as a receptor is no longer required (Roitt et al., 2001).

## 1.2.4 Secondary lymphoid organs and tissues

The generation of lymphocytes in primary lymphoid organs is followed by their migration into peripheral secondary tissues. The secondary lymphoid tissues comprise well organized encapsulated organs, the spleen and lymph nodes.(systemic organs) and non-encapsulated accumulations of lymphoid tissue like the mucosal associated tissue (MALT). Systemic organs and the mucosal tissue have different functions in immunity. The spleen is responsive to blood borne antigens and patients who have had removed their spleen are much more susceptible to pathogens that reach the blood stream. The lymph nodes protect the body from antigens that come from skin or from internal surfaces and are transported via the lymphatic vessels. Response to antigens encountered via these routes result in secretion of antibodies into circulation and in local cell-mediated responses. It is not surprising that the bulk of the body's lymphoid tissues (>50%) is associated with the mucosal system, since this is a major pathway for entry of external antigens,. Likewise, IgA is the most abundant immunoglobulin in the body.

### 1.2.4.1 The systemic immune system: the spleen

The spleen lies at the upper left quadrant of the abdomen, behind the stomach and close to the diaphragm. The adult spleen is around 13 x 8 cm in size and weighs about 180-250 g. Its outer layer consists of a capsule of collagenous bundles of fibers which enter the parenchyma of the organ as short trabeculae. These, together with a reticular framework, support two main types of splenic tissue-the white pulp and the red pulp.

The white pulp: The white pulp consists of lymphoid tissue, the bulk of which is arranged around a central arteriole to form the periarteriolar lymphoid sheaths (PALS). PALS are composed of T and B cell areas. The T cells are found around the central arteriole; the B cells may be organized in either primary unstimulated follicles (aggregates of naïve, resting B cells) or secondary, stimulated follicles (which possess GCs). The GCs also contain follicular dendritic cells (FDC) and phagocytic macrophages. Specialized macrophages and a subset of B cells, responding to type II thymus independent antigens i.e. polysaccharides, are found in marginal zones, the areas overlying the mantle of secondary follicles. Macrophages and FDCs present antigen to B cells in the spleen. B cells and other lymphocytes are free to leave and enter the PALS via capillary branches of the central arterioles that enter the marginal

zone. Some lymphocytes, especially plasmablasts, can pass across the marginal zone via bridges into the red pulp (Cesta, 2006).

The red pulp: This tissue consists of venous sinuses and cellular chords containing resident macrophages, erythrocytes, platelets, granulocytes, lymphocytes and numerous plasma cells. In addition to immunological functions, the spleen serves as a reservoir for platelets, erythrocytes and granulocytes. Aged platelets and erythrocytes are destroyed in the spleen. This process is carried out in the red pulp and called haemocatheresis. These functions are possible by the vascular organization of the spleen. Central arteries, surrounded by PALS, end with arterial capillaries, which open freely into the red pulp cords. Thus, circulating cells reach these cords and get trapped. Aged platelets and erythrocytes are recognized and phagocytosed by macrophages. Blood cells that are not ingested and destroyed can enter the blood circulation by squeezing through holes in the discontinuous endothelial wall of the venous sinuses, whereas plasma flows freely through them.

#### 1.2.4.2 Lymph nodes and the lymphatic system

The lymph nodes filter antigen from the interstitial tissue fluid and lymph during its passage from the periphery to the thoracic duct and the other major collecting ducts. Lymph nodes frequently occur as branches of the lymphatic vessels. Clusters of lymph nodes are strategically placed in areas such as the neck, axillae, groin, mediastinum and the abdominal cavity. Lymph nodes protect the skin and mucosal surfaces of the respiratory, digestive and genitourinary tracts.

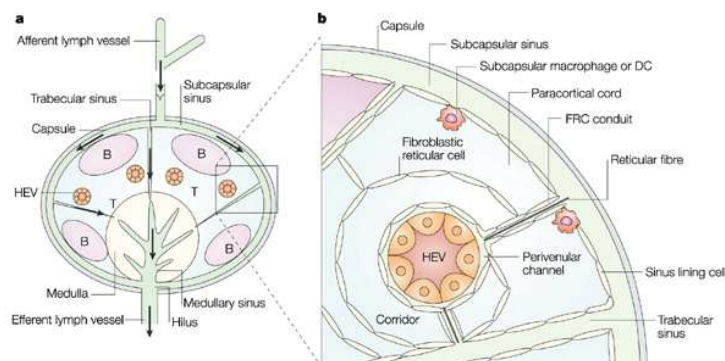


Figure 2: Schematic structure of a lymph node (von Andrian and Mempel, 2003)

Lymph arrives at the lymph node via several afferent lymphatic vessels, and leaves the node through one efferent lymphatic vessel at the hilus. As shown in Figure 2, a typical lymph node is surrounded by collagenous capsule. Radial trabeculae together with reticular fibers support the various cellular components. The lymph node consists of a B cell area (cortex) a T cell area (paracortex) and a central medulla, consisting of cellular cords containing T cells, B cells, abundant plasma cells and macrophages. The paracortex contains many antibody presenting cells (APCs) which express high levels of MHCII surface antigens. These are cells migrating from the skin (Langerhans cells) or from mucosa (dendritic cells), which transport processed antigens into the lymph nodes from the external and internal surfaces of the body. The bulk of the lymphoid tissue is found in the cortex and the paracortex. The paracortex contains specialized post capillary vessels – high endothelial venules (HEV) that allow traffic of lymphocytes out of the circulation into the lymph node. The medulla is organized into cords, separated by lymph (medullary) sinuses which drain into a terminal sinus, the origin of the lymphatic vessel. As the lymph passes across the nodes from the afferent to the efferent lymphatic vessels, particulate antigens are removed by the phagocytic cells and transported into the lymphoid tissue of the lymph node.

The cortex contains aggregates of B cells in the form of primary and secondary follicles, whereas the T cells are mainly found in the paracortex. Thus, if an area of skin and mucosa is challenged by a T-dependent antigen, the lymph nodes draining that particular area show active T cell proliferation in the paracortex. Germinal centers in secondary follicles are seen in antigen-stimulated lymph nodes. These are similar to the GCs found in the B cell areas of the splenic PALS and MALT.

### **1.3 Activation of B cells by T-independent antigens**

Naïve mature B cells are free to exit the bone marrow and migrate into the periphery. If these cells do not encounter antigen, they die within a few weeks by apoptosis. If they, however, encounter specific antigen, they undergo activation, proliferation and differentiation leading to the generation of plasma cells and memory B cells

There are a small number of antigens activating B cells without MHCII restricted T cell help, referred to as T cell independent (TI) antigens. Importantly, many TI antigens are

particularly resistant to degradation. TI antigens can be divided into two groups (TI-1 and TI-2) based on the manner they activate B cells. TI-1 antigens are predominantly cell wall components. The prototypical TI-1 antigen is lipopolysaccharide (LPS), a component of the cell wall of Gram-negative bacteria. TI-2 antigens are predominantly large polysaccharide molecules with repeating antigenic determinants. Bacterial cell wall polysaccharides, polymeric bacterial flagellin, and poliomyelitis virus are examples of such. Many TI-1 antigens possess the ability in high concentrations to activate B cell clones that are specific for other antigens, a phenomenon known as polyclonal B cell activation. However, in lower concentrations they only activate B cells specific for themselves. TI-1 antigens do not require a second signal. TI-2 antigens, by the other hand, are thought to activate B cells by clustering and cross-linking Ig molecules on the B cell surface, leading to prolonged and persistent signaling. TI-2 antigens require residual non-cognate T cell help such as cytokines. Several signal transduction molecules are necessary for mediating T-independent antigen response in B cells. These include CD19, HS1 protein, lymphotoxin  $\alpha$ , and TNF $\alpha$ . Primary responses to TI antigens are slightly weaker than those to TD antigens and generate mainly IgM. The secondary response to TI antigens resembles the primary response, thus does not induce a maturation leading to class switching or increasing the antibody affinity. This is most likely due to the lack of CD40 activation. Memory induction to TI antigens is also relatively poor. However, they have the advantage of being rapid, as they do not depend on complex interactions. TI antigens mainly activate the B-1 cells found mainly in the peritoneum. These B-1 cells can be identified by their expression of CD5, which is induced upon binding to TI antigens.

## 1.4 Activation of B cells by T-dependent antigens

In the late 1960s Mitchison and others showed that to induce an optimal secondary antibody response to a small chemical group or hapten, the experimental animal must be immunized with the same hapten-carrier conjugate, not just the same hapten. This was referred to as the carrier effect. Furthermore, it was shown that Th cells recognize the carrier, whereas B cells recognize the hapten. One consequence of this system is that an individual B cell can receive help from T cells specific for different antigenic peptides,



provided that the B cell can present those determinants to each T cell. In an immune response in vivo, it is believed that the interactions between B cells and T cells which drive B cell division and differentiation involve T cells that have already been stimulated by contact to the antigen presented on other APCs. Antigen entering the body is presented by cells which present the antigen in highly immunogenic form to the Th cells and B cells. The T cells recognize determinant on the antigen which are distinct from those recognized by the B cells. Two processes are required to activate a B cell: i) antigen interacting with B cell Ig receptors. This involves naïve antigen, ii) stimulating signals from Th cells that respond to processed antigen bound to MHCII class molecules. The initial interaction between a naïve B cell and a cognate antigen via the BCR in the presence of cytokines or other growth stimuli induces activation and proliferation of the B cell. This then leads to processing of the TD antigen and presentation to T cells. The interaction between T and B cells is a two way process, in which B cells present antigen to T cells and receive signals from the T cells for division and differentiation. The central, antigen specific interaction is that between the MHC class II-antigen complex and the TCR. It is known that CD40, a member of TNF $\alpha$  receptor family, delivers the most potent activating signal to B cells, even more potent than signals transmitted via surface Ig. Upon activation, T cells express CD40L, which interacts with CD40. This interaction helps to drive B cells into cell cycle. Transduction of signals through CD40 also induces upregulation of CD80/CD86 and thus, provides costimulatory signals to the responding T cells. Signaling through CD40 is also essential for GC development and antibody responses to TD antigens. This is confirmed by hyper-IgM syndrome, an immunodeficiency disease caused by a genetic mutation of CD40L. This disorder is characterized by a failure to form GCs and absence of isotype switch to IgG, IgE or IgA production (Roitt et al., 2001).

## **1.5 Selection, survival and differentiation of B cells in the T-dependent immune response**

Immunization results in a limited number of B-cell clones being activated. Excluding factor such as location within the body as a variable, the distinction between those B cells that respond to the antigen and those which do not, seems to be made on basis of

affinity for cognate epitopes. There is clearly a threshold for activation below which B cells remain ignorant of challenge. There is also significant competition among those above this threshold. Thus, while low affinity B cells initiate a response and give rise to characteristic TD GCs and foci of plasma cells, this only occurs in the absence of higher affinity competitor B cells (Dal Porto et al., 1998; Shih et al., 2002). This competition does not mean that only a single clone will participate, but does result in pauci-clonal responses (Jacob et al., 1991). Thus, already at this earliest stage of the response, selection operates to ensure that clones with the highest affinity for antigen are enriched among the responding population. Importantly, this is not an absolute measure of affinity but a relative one such that the response that is initiated represents the best possible.

### **1.5.1 The extrafollicular response**

The initial interaction of antigen-specific B cells with T cells at the T/B cell zone borders of secondary lymphoid organs leads to bifurcation of the B cell differentiation. One pathway leads into the follicle and the formation of GCs, while the alternative pathway leads to the development of plasma cell foci in the extrafollicular regions. This happens either at the bridging channels of spleen or along the medullary chords of lymph nodes (MacLennan et al., 2003). Early work examining the variable (V) region gene structure of the B cells in foci and adjacent GCs concluded that the same clone could establish both, thus interpreted that the entry of B cell clones into GC and foci is rather stochastic (Jacob et al., 1991). However, other work has noted a significant difference in the length of the third complementary determining region (CDR3) of the VH genes of early GCs compared to contemporaneous plasma cells, presumed to be extrafollicular because of the early stage of the response (McHeyzer-Williams et al., 1993). While the CDR3 length did not lead to different affinity, the results were interpreted such that a shorter CDR3 provides a selective advantage. An equivalent study showed that the foci were relatively heterogeneous in their VH gene representation while the GCs were more restricted. However, definite evidence was provided by Brink and colleagues by adoptive transfer experiments (Paus et al., 2006). They found that high affinity interactions preferentially induced differentiation along the plasma cell pathway, while the lower affinity interactions induced the B cells to

form GCs. However, it should be remembered that in their work affinity was not measured but rather inferred. A discordant result was provided by Shih and colleagues in which two types of engineered B cells with different affinity for one antigen were co transferred into recipients and then exposed to antigen (Shih et al., 2002). In this system, however the high affinity receptor dominated the GC response from early time points and increased the dominance as the response progressed. However, there was no indication in this study of the representation of different affinity B cells in the plasma cell foci. There are of course different experimental systems using different antigens, a protein in one (Paus et al., 2006) case and a hapten in the other (Shih et al., 2002).

### **1.5.2 The GC reaction**

While the foci of plasma cells are short-lived, the alternate differentiation pathway leading to GC formation results in the formation of long lived antigen specific clones. These cells comprising the memory B cell and plasma cell compartment are enriched for improved affinity, as results of selective expansion of B cell clones.

The GC initially contains only dividing centroblasts. Shortly thereafter, the GC polarized into a dark zone containing centroblasts and a light zone containing non dividing centrocytes. Centroblasts rapidly proliferate within the dark zone and downregulate their surface immunoglobulin. Somatic hypermutation of the immunoglobulin V genes generates diversity by giving rise to variants with different affinities from one single clone. Many of these mutations will be deleterious to the B cell, leading to either an unexpressible receptor or one with greatly reduced affinity for antigen, such that it will be unable to bind. Other changes, however, will result in improved binding of antigen. Recently it was shown that somatic mutations not only can improve affinity but can also lead to stabilization of the BCR (Weiser et al., 2011). The rate of somatic mutation in Ig genes is about  $10^3$  to  $10^4$  higher than the spontaneous rate of mutation in other genes, a fact that somatic hypermutation owes its name. Merging the estimated rate of somatic hypermutation ( $10^{-3}$ /bp per cell/generation) (Clarke et al., 1985) and the total number of base pairs encoding the variable region of the antibody (n=700) results in an average rate of 1 mutation/cell division.

Following these developmental changes, the centroblasts migrate to the light zone where antigen is presented on the surface of FDCs and give rise to centrocytes which express surface Ig BCR. In the light zone, centrocytes encounter antigen from the FDCs and T cells interact with centrocytes through surface molecules such as BCR, CD40, CD80, CD86, ICAM-1, VCAM-1 and others. While the occurrence of somatic mutation and the retention of high affinity clones are well documented, the means by which individual clones are selected remains unclear. There remain two conundrums. First, the improved affinity of GC B cells late in the response implicates antigen binding as the selective criterion. This suggests that clones within the GC compete for limited amount of antigen; however, the experimental data supporting this view directly remain weak. In fact, reducing antigen to extremely low levels made little difference to B cell selection compared to situations where antigen is excessively available (Hannum et al., 2000). However, this may be context dependent, since similarly designed experiments using a different system produced results consistent with antigen levels (González-Fernández and Milstein, 1998).

The second conundrum surrounds the pathway that mediates B cell selection. Upon antigen binding, the BCR transmits a signal which could change depending on the affinity of binding. Alternatively, selection could operate depending on T cell help. High affinity BCR may lead to increased antigen capturing, thus more peptide is presented on the B cell surface in the context of MHCII to the Th cells. In this scheme, GC B cells are not competing for the antigen alone, but rather for access to T cells (Tarlinton, 2008). Recently, *in vivo* imaging of GC B cells has shown that they pause only briefly when in contact with FDCs, but remain for much longer in contact with the limited number of T cells (Hauser et al., 2007; Schwickert et al., 2009; Beltman et al., 2011). These data suggest that selection within the GC is mediated by competition for access to T cells and indirectly for binding to antigen in terms of delivering a survival advantage to B cell binding antigens.

### **1.5.3 Memory B cells and Plasma cells**

The output of the GC reaction is long lived memory, comprising of circulating memory B cells and sessile plasma cells mainly located within the bone marrow. Whereas plasma cells are well defined, the resolution of memory B cells from antigen specific B

cells outside the GC remains intricate. In the first instance, one has to resolve them from antigen binding naïve B cells. The simplest way of achieving this is to choose antigen reactive cells which have undergone class switch recombination, as isotype switch is a post activation feature of the B cell response. However, there are well defined IgM<sup>+</sup> memory B cells in human and in mouse (Klein et al., 1998; White and Gray, 2000), such a population would be excluded by the stated conditions. Therefore, Tarlinton and colleagues claim that distinguishing the memory B cell subset from other cell types with 100% efficiency is only possible by examining the V genes for the presence of somatic mutation (Tarlinton, 2008). However, the somatic hypermutation in memory B cell has been a matter of debate, although some work suggested somatic hypermutation to occur in memory B cells during the first weeks of GC reaction (Siekevitz et al., 1987), others assigned them the ability of undergoing new round of hypermutation upon antigenic stimulation (Berek and Milstein, 1987). A consensus now exists that suggests memory B cells are formed during the early phase of the GC reaction, with some of them bearing unmutated V gene segments. Yet somatic mutation can continue until the GC reaction wanes out, with the corresponding centroblasts accumulating more mutations than their memory B cell counterparts (Ridderstad and Tarlinton, 1998; Takahashi et al., 2001; Anderson et al., 2007).

Furthermore, the impact of antigen presentation on the survival of memory B cells was subjected to a lot of controversies during the last years. Several groups has reported that homeostasis of memory B cells is dependent of the persistence of antigen in secondary lymphoid organs (Gray and Skarvall, 1988), (Bachmann et al., 1996). Contrary, it has been shown that memory B cells can survive in the absence of their antigen (Schitteck and Rajewsky, 1990).

Recently, Weill and colleagues delivered the interesting finding that B cell memory can be composed of several layers, with an antigen independent layer located outside the follicles in spleen, blood and lymph nodes and an antigen dependent layer of proliferating centroblasts in GC like structures. Both of these layers were composed of IgM<sup>+</sup> and IgG1<sup>+</sup> cells. After challenge, the IgG1<sup>+</sup> subset showed immediate effector and protective functions, whereas the IgM<sup>+</sup> cells migrated into GCs and were capable of switching into IgG1. Thus, the IgM<sup>+</sup> subset did not contribute much to the immediate

antibody line of defense, but instead, induced a delayed effector response after encountering further antigen (Dogan et al., 2009).

Memory B cells, however, can be functionally distinguished from the long lived plasma cells. Long lived plasma cells are terminally differentiated cells that are produced by continually produce high affinity antibody and that will not be drawn into a secondary response (McHeyzer-Williams et al., 2006). These cells generate higher affinity antibodies through affinity maturation (Radbruch et al., 2006). Acute ablation of the GC by anti CD40 treatment halts generation of new plasma cells and prevents further improvements of antibody affinity (Takahashi et al., 1998).

Plasma cells are identified by syndecan-1 surface expression, have an extensive rough endoplasmic reticulum (ER), and are enriched within the red pulp of the spleen, in the medullary cords of the lymph nodes, and in the bone marrow. The precursors of plasma cells are called plasmablasts; these are dividing cells that are found in the B cell follicles in addition to red pulp and medullary chords, but not in the bone marrow. Plasma cells and plasmablasts are collectively referred to as antibody secreting cells (ASCs) or antibody forming cells (AFCs) based on their ability to secrete antibody, which is often class switched. Plasma cell differentiation is dependent on a key transcriptional repressor, BLIMP-1, which inhibits many B cell lineage and GC specific genes. By expressing Pax5, BLIMP-1 allows expression of XBP-1, a transcriptional factor essential to survive ER stress associated with massive antibody secretion. It was shown that BLIMP-1 is an early marker of plasma cell development. Plasmablasts express lower levels of BLIMP-1 than fully differentiated plasma cells and are heterogeneous for syndecan-1 expression.

Within secondary lymphoid organs, both short lived and long lived plasma cells localize to medullary cords in lymph nodes and within the red pulp of the spleen, where they are thought to secrete antibody. Within these anatomic locations, plasma cells are largely sessile. Plasma cell migration to these regions has never been visualized directly, but chemokines receptors are thought to play a role because expression of CXCR4, CCR6, and EBI2 increases and CXCR5 is reduced during plasma cell differentiation. In addition, *in vitro* experiments have shown chemotaxis of spleen red pulp PCs to the chemokines S1p and CXCL12, which are ligands of S1p1/S1p3 and CXCR4 receptors,

respectively. Consistent with this idea, CXCL12 is expressed in red pulp and medullary cords, and genetic ablation experiments showed that CXCR4 deficient plasma cells failed to accumulate in red pulp or bone marrow but were enriched in blood and normal in lymph nodes, compared to CXCR4 sufficient cells, suggesting a role for CXCL12 for plasma cell homing (Fooksman et al., 2010).

Long lived plasma cells egress from lymph nodes, and homing to the bone marrow is critical for their long term survival. S1p expression is high in blood and low in secondary lymphoid organs, providing a gradient that may be used for egress (Schwab and Cyster, 2007). Intercellular adhesion molecule-1 (ICAM-1) is highly expressed in medullary cords, which are the exit sites of plasma cells from lymph nodes.

## 2 Objectives

Germinal centers are transient structures that are formed in response to TD antigens in secondary lymphoid tissues. The major function of GCs is to ensure sustained immune protection and rapid recall responses against encountered antigens by production of high-affinity antibody secreting plasma cells and memory B cells.

The main objective of this thesis is to describe the migration pattern and dynamics of GC-derived B cells subsets upon challenge with NP-KLH, providing a comprehensive overview of the GC response.

In a nutshell, this work has the following specific aims:

- Characterization of the B cell-specific developmental processes occurring during the GC reaction.
  - An extensive kinetic of GC B cells, memory B cells and plasma cells will be conducted by multi-color flow cytometric and immunofluorescence microscopy methods in the course of primary and secondary immune response of C57BL/6 mice to NP-KLH.
  - In order to delineate the GC response, the GC B cell and plasma cell compartment in spleen, blood and bone marrow will be resolved into subsets, based on the differential expression of developmental markers, surface immunoglobulins and hapten-specificity.
- Establishment of an efficient transfer system of blood derived B cell subsets.
  - In order to predict the occurring processes within a “wild type” system, an efficient experimental procedure will be established allowing transferring as few cells as possible.
  - To address the impact of the state of the immune response on the migration and differentiation of B cells, donor cells will be transferred into recipients at an early stage and shortly before the peak of the GC response.
- Last but not least, the results will be discussed in the light of the current theoretical models for the formation and progress of the GC response.



### 3 Materials and methods

#### 3.1 Buffers, reagents and solution

<b>Buffer/Solution</b>	<b>Components</b>
50xTAE buffer	242 g/L Tris, 57.1 ml/L 96% acetic acid, 10% EDTA 0.5 pH 8.6
FACS buffer	PBA, 4nM EDTA, pH 8.0
PBA	PBS, 0.5% BSA (Fraction V, Sigma)
PBS	130 mM NaCl, 10 mM sodium phosphate buffer
Blocking buffer	PBS, 5% BSA, 0.1% Tween-20, 10% rat serum
Washing buffer	PBS, 5% BSA, 0.1% Tween-20
TNT washing buffer	0.1% Tris/HCl pH 7.5, 0.15 M NaCl, 0.05% Tween-20
TNT blocking buffer	0.1% Tris/HCl pH 7.5, 0.15 M NaCl, 0.5% blocking reagent
Transfer buffer	PBS, 10 mM Hepes, 50 U/ml penicillin/streptomycin, 2.5% ACDA

### 3.2 Antibodies and reagents for FACS and immunofluorescence

Specificity	Clone	Conjugate	Origin
B220	RA3.6B2	A405	eBioscience
CD138	281-2	PE	BD Pharmingen
PNA	FITC		Vector Labs
NIP	-	PE	Self made
CD38		APC	eBioscience
IgG1		Bio	BD Pharmingen
IgM		A700	House made
CD22.2	Cy34.1	Bio	BD Pharmingen
MHCII	M5/114	APC	Ebioscience
DAPI			Molecular probes
Bcl-6	GI191E	purified	eBioscience
Ki67	TEC-3		Dako
CD3	KT-3		ABD Serotec
F4/80			House made
SA		A546	Mol. Probes
Kappa	187.1	A405	BD Pharmingen
Lambda	JC5-1		BD Pharmingen
TSA Kit			Perkin Elmer
IgG ( $\alpha$ rat)		A647	Invitrogen
CD45.2	104	APC	eBioscience
CD45.1	A20	A700	eBioscience

### 3.3 Mice, antigen and immunizations

Six to 8-wk-old female C57BL/6 mice were from The Jackson Laboratory. All animal experimentation protocols were approved by the relevant Animal Ethics Committee. Primary immunization was with a single i.p. injection of 100  $\mu$ l NP coupled to KLH in the ratio of 1:23 (purchased from Biocat) in Alum (obtained from Thermo Scientific). The secondary response was elicited by i.p. immunization of mice which were primarily immunized at least 6 wk before with 50  $\mu$ l NP-KLH in Alum.

### 3.4 Immunofluorescence

A major challenge of this thesis was to establish a high-throughput immunofluorescence staining system which allows the detection of single donor cells and their subsequent evaluation with respect of their morphology and localization in several whole cryosectioned mesenteric lymph nodes. To serve the mentioned purpose, applied standard protocols were modified and adapted to commercial signal amplification systems. A comprehensive description of these protocols is given as follows:

Mesenteric lymph nodes were immersed in OCT and snap-frozen in liquid nitrogen. Tissue sections of 8- $\mu$ m thickness were cut in a cryostat and fixed with acetone. For detection of GC B cells Ki67 (DAKO),  $\alpha$  rat IgG-Alexa647 (BD) and B220-A405 (Ebioscience) were used. Isotype switch was shown with IgG1-FITC (BD) and plasma cells were detected with anti Kappa and Lambda antibodies (BD). T cells were identified with CD3-A488 (Serotec). Follicular dendritic cells were stained with M2-A546 (donation of Berek laboratory) or CD21-A546 (house manufactured) and antigen specific cells were visualized with PE conjugated NIP (house manufactured). Donor CD45.2<sup>+</sup> cells were detected with CD45.2-bio antibody (Ebioscience). For multiple signal amplification TSA cyanine 3 System (PerkinElmer) was used. Images were acquired with confocal microscope (Zeiss) and pictures were analyzed with ZEN, Image J and Adobe Photoshop software.

#### Standard protocol for immunofluorescence staining:

- Acetone fixation of tissue sections:

NOTE: if fluorescent proteins are to be visualized in situ, acetone-fixation does not work, use PLP-fixation instead.

Consecutive sections were cut with 7  $\mu\text{m}$  thickness, fixated to poly-l-lysine coated slides (positively charged, for example Fisher Super frost Plus) and allowed to dry at room temperature (RT) for 15-30 min. Slides were put into ice-cold acetone for 10 min and allowed to dry at room temperature over night. Dried slides can be stored at  $-80^{\circ}\text{C}$ .

- Stainings of tissue sections:

Sections were allowed to warm up to room temperature (if stored at  $-80$ ). A line with PAP pen was drawn around the sections and allowed to dry for 10 min. This prevents antibody dilutions from spreading all over the slide. Slides were rehydrated in PBS for 20 min. A blocking step was performed using block solution for 20 min. Liquid was tapped off and 100-200  $\mu\text{l}$  of primary antibody mix in washing buffer was carefully applied on the tissue. Stainings were incubated for 60 min in a humidified chamber and washed afterwards by adding  $\sim 100$   $\mu\text{l}$  washing buffer for 10 min. This step was repeated 3 times. If necessary, a secondary reagent was incubated on washed tissue for additional 60 min. After 3 wash steps liquid was tapped off,  $\sim 100$   $\mu\text{l}$  fluoromount G (Southern Biotec) was added and slides were carefully covered with a cover slip.

For intracellular staining such as Ki67, tissue was fixated with 1% cytofix (BrDU Kit, BD Pharmingen) in PBS for 20 min prior to first staining with antibodies. Slides were washed in PBS on a shaker at room temperature for 10 min. Cells were blocked for unspecific binding and stained with the primary antibodies. After the washing, the tissue was permeabilized with 1% Na-Citrate and 1% Triton X-100 (in  $\text{H}_2\text{O}$ ) 10 min on ice. Slides were washed extensively and stained with Ki67 (in PBS/BSA/Tween) for 60 min. After 3 wash steps, tissue was incubated with secondary antibody ( $\alpha$  rat IgG-Alexa647, for instance) for 60 min. Slides were washed and covered as described in the standard procedure.

Modified protocol for staining of acetone fixated tissue with TSA signal amplification system in combination of Bcl-6 or Ki67 intracellular staining:

Sections were allowed to warm up to room temperature (if stored at  $-80$ ). A line with PAP pen was drawled around the sections and allowed to dry for 10 min. This prevents

antibody dilutions from spreading all over the slide. Slides were rehydrated in PBS for 20 min. Tissue was permeabilized by incubation with 100  $\mu$ l cytofix (BrdU flow Kit, BD)/slide for 20 min followed by an extensive wash step in a with PBS filled container placed on shaker for 10 min. Endogenous peroxidase was quenched by 0.3 %  $H_2O_2$  in PBS for 10 min.  $H_2O_2$  was removed by a wash step in PBS/BSA/Tween (see previous standard protocol). Endogenous biotin was quenched using avidin/biotin blocking Kit (Vector Labs). An additional blocking step was performed using TNB block solution for 20 min. This step can be combined with the biotin incubation step. Liquid was tapped off and 100-200  $\mu$ l of primary antibody mix in TNT washing buffer was carefully applied on the tissue. Stainings were incubated for 60 min in a humidified chamber and washed afterwards by adding  $\sim$ 100  $\mu$ l TNT for 10 min. This step was repeated 3 times. Next, 100  $\mu$ l SA-HRP (1:100) in TNB buffer was applied on slides and incubated for 30 min. An additional wash step with TNT buffer was repeated 3 times. To amplify the detection signal tyramid solution (1:50) was incubated on tissue for 5 min and removed with a 3 times wash step (TNT buffer). After washing, the tissue was permeabilized with 1% Na-Citrate and 1% Triton X-100 (in  $H_2O$ ) 10 min on ice. Slides were washed extensively (TNT) and stained with Ki67 (in PBS/BSA/Tween) or likewise Bcl-6 for 60 min. If necessary, after 3 wash steps, tissue was incubated with secondary antibody ( $\alpha$  rat IgG-Alexa647, for instance) for 60 min. After 3 wash steps liquid was tapped off,  $\sim$ 100  $\mu$ l fluoromount G (Southern Biotech) was added and slides were carefully covered with a cover slip.

### **3.5 Adoptive transfers**

Total blood from C57BL/6 mice was collected via retro orbital bleeding 8 days after immunization with NP-KLH. Lymphocytes were isolated with Histopaque (Sigma Aldrich) according to producer's protocol. Mature B cells were negatively enriched by adding an erythrocyte specific antibody (Ther-119) to the standard EasySep untouched B cell isolation Kit (StemCell Technologies) and modification of the biotin selection and antibody mix components to 1.25% of the originally recommended volumes in the protocol.  $IgM^+$ ,  $IgG1^+$  potential memory and GC B cell subsets were FACS sorted after exclusion of  $IgD^+$  B cells,  $CD138^+$  plasmablasts and plasma cells (DUMP channel) with

BD Diva FACS-SORT facility and transferred into CD45.1 recipients immunized either 4 or 8 d before. Approximately  $3 \times 10^3$  -  $8 \times 10^3$  cells were transferred per recipient. In control experiments  $10^5$  blood-derived IgD<sup>+</sup> B cells were transferred. Spleen and bone marrow were analyzed with flow cytometric methods. Mesenteric lymph nodes were isolated and prepared as described for immunofluorescence analysis.

### 3.6 Flow cytometry

To stain lymphocytes for multi-parameter flow cytometry analysis, cells suspended in PBS/BSA were added to 20 µg anti-FcYR to prevent unspecific staining mediated by FcR binding. The following antibodies were added to the cells; B220 (RA3-6B2)-pacific blue, PNA-FITC (Vector), NIP-PE (house manufactured), IgG1-biotin (BD Biosciences), SA-PerCPCY5.5 (Ebioscience), CD38-APC (Ebioscience), IgM-A700 (house manufactured), Lambda-FITC (BD Bioscience), CD138-PE (BD Bioscience), CD22.2-biotin (BD Bioscience), MHCII-APC (eBioscience), Kappa-A700 (house manufactured) and incubated 20min on ice. For intracellular staining, cells were washed with PBS/BSA, fixated with Cytofix/Cytoperm (BD Biosciences) and washed with Perm/Washing buffer (BD Biosciences). For measurement, cells were suspended in PBS/BSA/EDTA. Flow cytometric analysis was performed on BD LSRII flow cytometer. All samples were fluorescence compensated with positive controls to exclude spectral overlap. A total of  $4 \times 10^6$  -  $5 \times 10^6$  cells were analyzed per sample. Data were acquired using DIVA software (BD Biosciences) and analyzed with Flow Jo software (Tree Star).

## 4 Results

### 4.1 Kinetic of NP-KLH specific response after primary and secondary challenge

#### 4.1.1 Differences in absolute lymphocyte numbers of C57BL/6 mice after primary or secondary challenge do not correlate with the state of immune response

To better understand the differentiative processes of B cells occurring during the murine immune response, multiparameter flow cytometric analysis of B cell subsets from different organs of C57BL/6 mice challenged with NP-KLH was performed at consecutive time points following primary and secondary immunization (Figure 3). To facilitate subsequent phenotypic characterization of various stages of the primary immune response, lymphocytes numbers were recorded in different organs. Using MACS Quant technology, lymphocytes from spleen, blood and bone marrow of C57BL/6 mice were identified and enumerated 4-50 days after intra peritoneal (i.p.) immunization with NP-KLH in alum. The counted cell numbers of the organs did not uniformly increase at the peak and decrease with attenuation of the immune response.

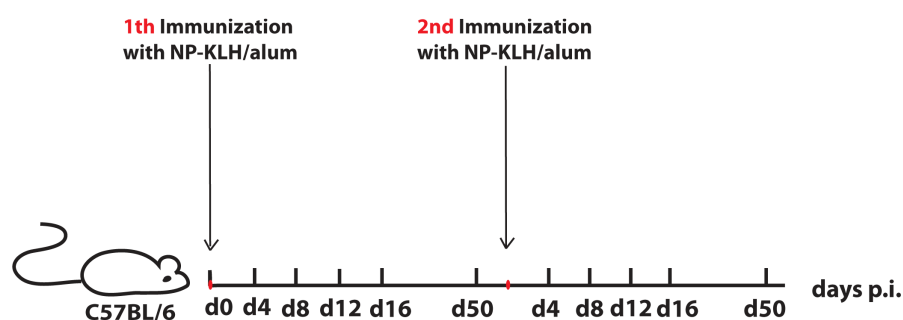


Figure 3: Experimental setup for NP specific immune response after primary and secondary immunization. Six to 8 wk old mice were immunized i.p. with 100  $\mu$ g NP-KLH in alum. Spleen, pooled blood and bone marrow were isolated at 5 consecutive time points after primary or secondary immunization, harvested and processed to single cell suspensions. Cells were stained with two different antibody cocktails and analyzed with flow cytometry

As shown in Figure 4A, at day 50 after primary challenge splenic lymphocytes had increased and were significantly higher than lymphocyte numbers of naive animals and those analyzed at day 12 after immunization. In bone marrow, a significant decrease of numbers was observed comparing day 4 and day 8, by day 12 however, the measured numbers dropped to approximately  $4 \times 10^7$  and remained mostly unchanged until day 50

p.i. Counting of lymphocytes recovered from blood showed a slight increase at day 8 p.i. Since due to limited lymphocyte numbers pooled blood had to be used, no statistical analysis could be performed, thus, the significance of the latter observation remains unclear.

Figure 4B shows that in contrast to the primary challenge, lymphocyte numbers in spleen peaked at day 4 after secondary immunization. After a significant decrease at day 12, splenic lymphocytes continuously increased towards day 16 and day 50 after immunization. Analysis of the bone marrow compartment revealed that the resident lymphocyte population undergoes minor changes over time. However, a significant increase of lymphocyte numbers was observed between day 16 and day 50 after secondary challenge.

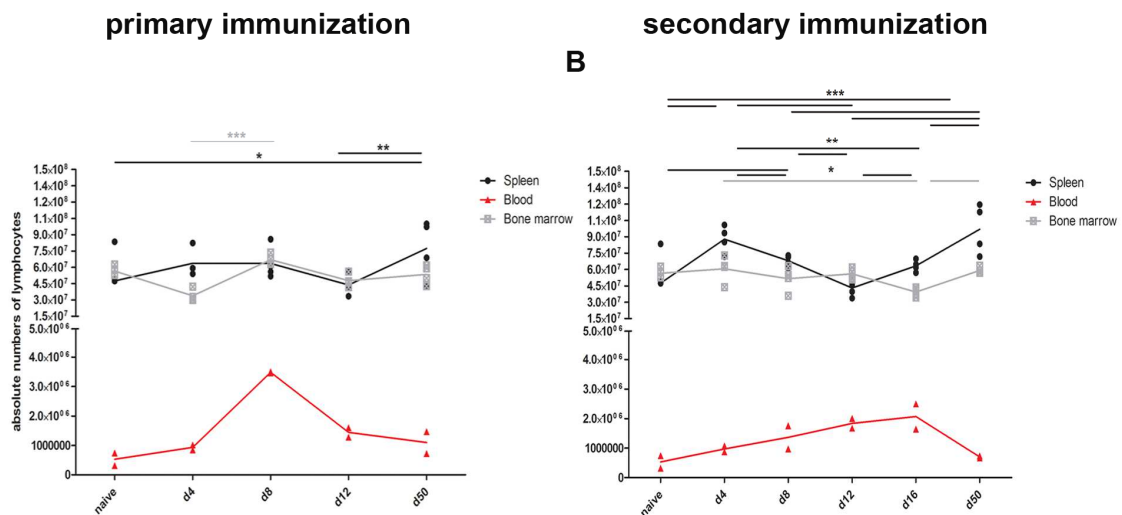


Figure 4: Absolute numbers of lymphocytes in spleen, blood and bone marrow of C57BL/6 mice at 5 consecutive time points after primary (A) and secondary (B) immunization. Spleen, collected blood and bone marrow of immunized and unimmunized groups of mice were isolated, harvested and prepared for FACS analysis. Absolute numbers of lymphocytes from each organ of mice were determined by MACS Quant analyzer at day 4, 8, 12, 16 and 50 after immunization. Significant differences of obtained cells numbers were determined with 2Way Anova. \* equals  $P < 0.05$ . \*\* equals  $P < 0.01$  and \*\*\* equals  $P < 0.001$ . Each point represents one mouse. Blood samples were pooled from groups of 6 mice and measured in two independent experiments, thus only two red rectangles are depicted at each time point

To determine whether an efficient and specific NP-KLH immune response was induced, frequencies of hapten-binding B cells from NP-KLH immunized animals were determined by their binding to NIP-PE and compared to the obtained frequencies from naïve animals (Figure 5). The results confirmed an induced NP response, reflected in a



newly generated B220<sup>+</sup> NIP binding population as soon as 4 days post challenge. This population peaked at the analyzed time points between 12-16 days after immunization and had declined by day 50 p.i.

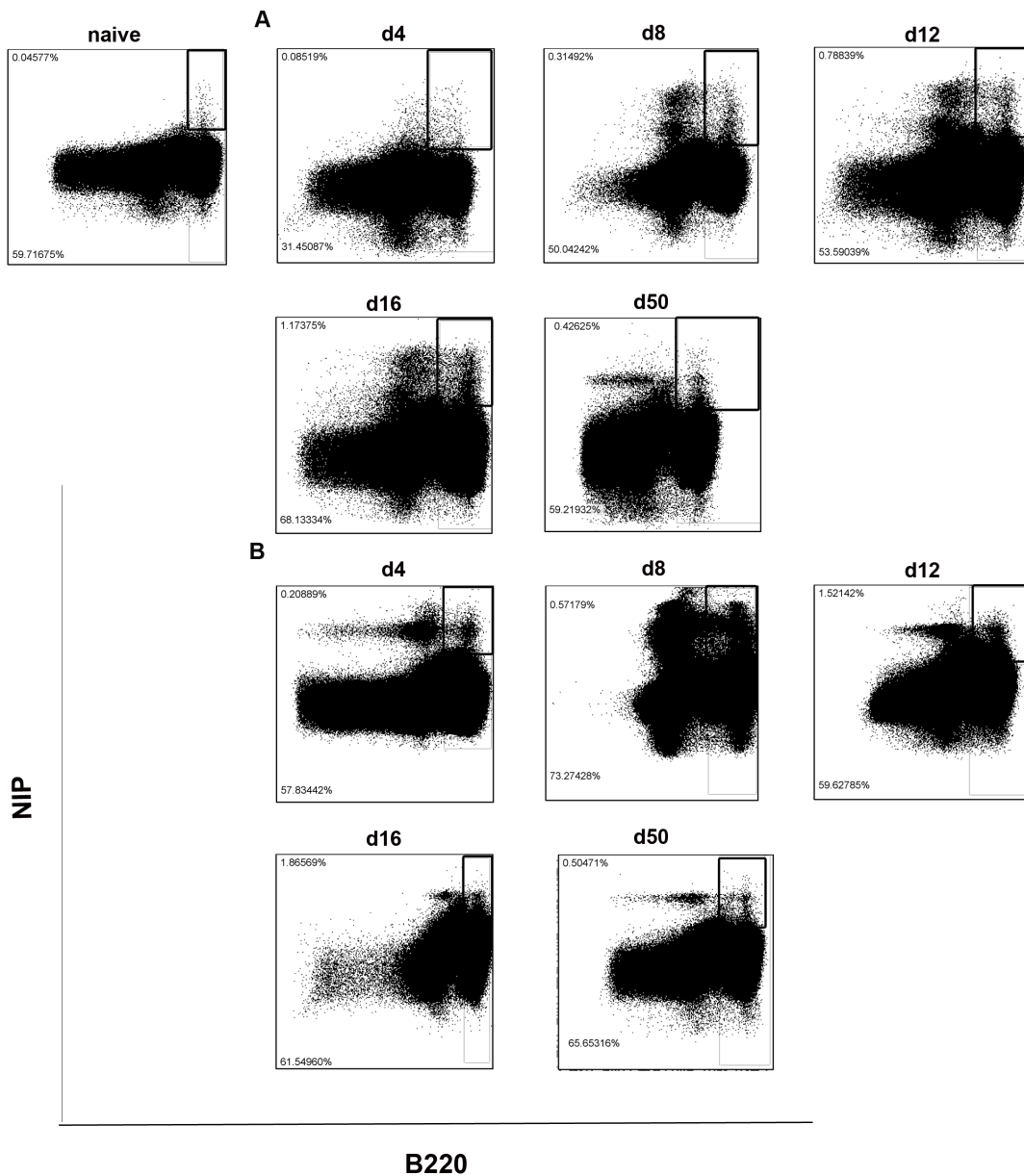


Figure 5: Kinetics of B220<sup>+</sup>NIP<sup>+</sup> population elicited by NP-KLH immunization. On the indicated days post immunization, splenocytes from animals challenged once (A) or twice (B) with NP-KLH were isolated and mononuclear cells were stained with B220-A405 and NIP-PE. The first dot plot represents the B220 and NIP staining of naïve lymphocytes and illustrates background staining directed against NIP. Numbers within the dot plots are percentages of viable mononuclear cells with a B220<sup>+</sup>NIP<sup>+</sup> phenotype observed at the respective time point and are representative of 3 independent experiments with 4 mice in each group.

To further analyze the effect of immunization with NP-KLH on the architecture of the lymphoid tissue, mesenteric lymph nodes of immunized mice were isolated at determined time points and tested for binding to GC specific markers by immunofluorescence microscopy (Figure 6A). The obtained results confirmed previous

studies conducted in the spleen (Figure 5). Small PNA binding GC structures were detected within the B cell follicle as soon as 4 days after immunization. These structures grew in size and were subsequently easier detectable as the response progressed until day 16 p.i. However, hapten-specific GCs were visualized as early as 1 wk after challenge (Figure 6B) and were detectable throughout all subsequent analyzed time points.

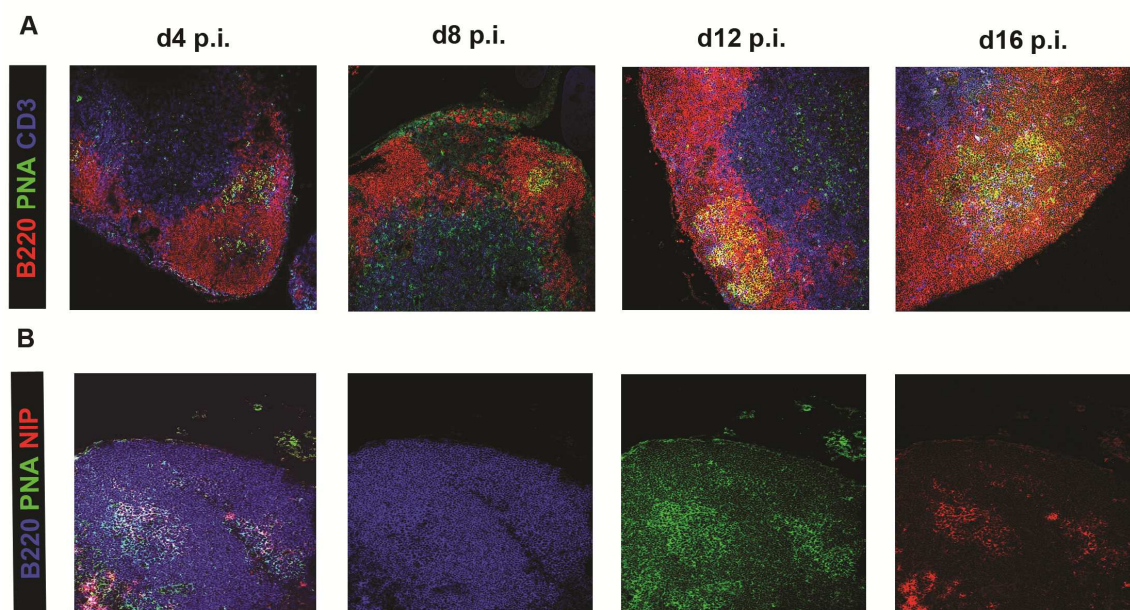


Figure 6: Immunofluorescence analysis of GCs within mesenteric lymph nodes elicited by NP-KLH immunization. Lymph nodes were isolated and prepared at consecutive time points after primary immunization. GCs were visualized with PNA with respect to the B cell zone and T cell zone. Representative pictures were taken at 4, 8, 12 and 16 days after primary immunization (A). Picture B shows an overlay of a hapten-specific GC, detected at day 12 after primary immunization by incubation with NIP-PE, B220 and PNA (B). Pictures were taken with 20x magnification.

#### 4.1.2 Kinetics and maturation of NP-KLH induced B cell subsets during primary and secondary immune response

To characterize the fate of post-GC B cell populations, spleen, blood and bone marrow were examined by flow cytometry for binding to a combination of different antibodies. Animals were examined at 4, 8, 12, 16 and 50 days after primary and secondary immunization and compared to naïve controls. Spleen, blood and bone marrow were harvested; leucocytes were recovered and stained with a cocktail of different antibodies. Detected lymphocytes by forward and sideward scatter were partitioned into B220 expressing and not expressing cells. Among the positive population, cells were

identified that bound high amounts of PNA, thus were GC B cells (Figure 7A). Further, detected GC B cells were analyzed for expression of CD38, IgG1, IgM and binding to NIP. Among B220 expressing B cells, frequencies of NIP binding, CD38<sup>+</sup>IgG1<sup>+</sup> or CD38<sup>+</sup>IgM<sup>+</sup> cells were determined (Figure 7B, referred to as IgG1<sup>+</sup> and IgM<sup>+</sup> B cells). In a parallel approach, detected lymphocytes were partitioned into CD138<sup>+</sup> cells that did or did not stain with a cocktail of B220, CD22.2, MHCII and Lambda (Figure 7C).

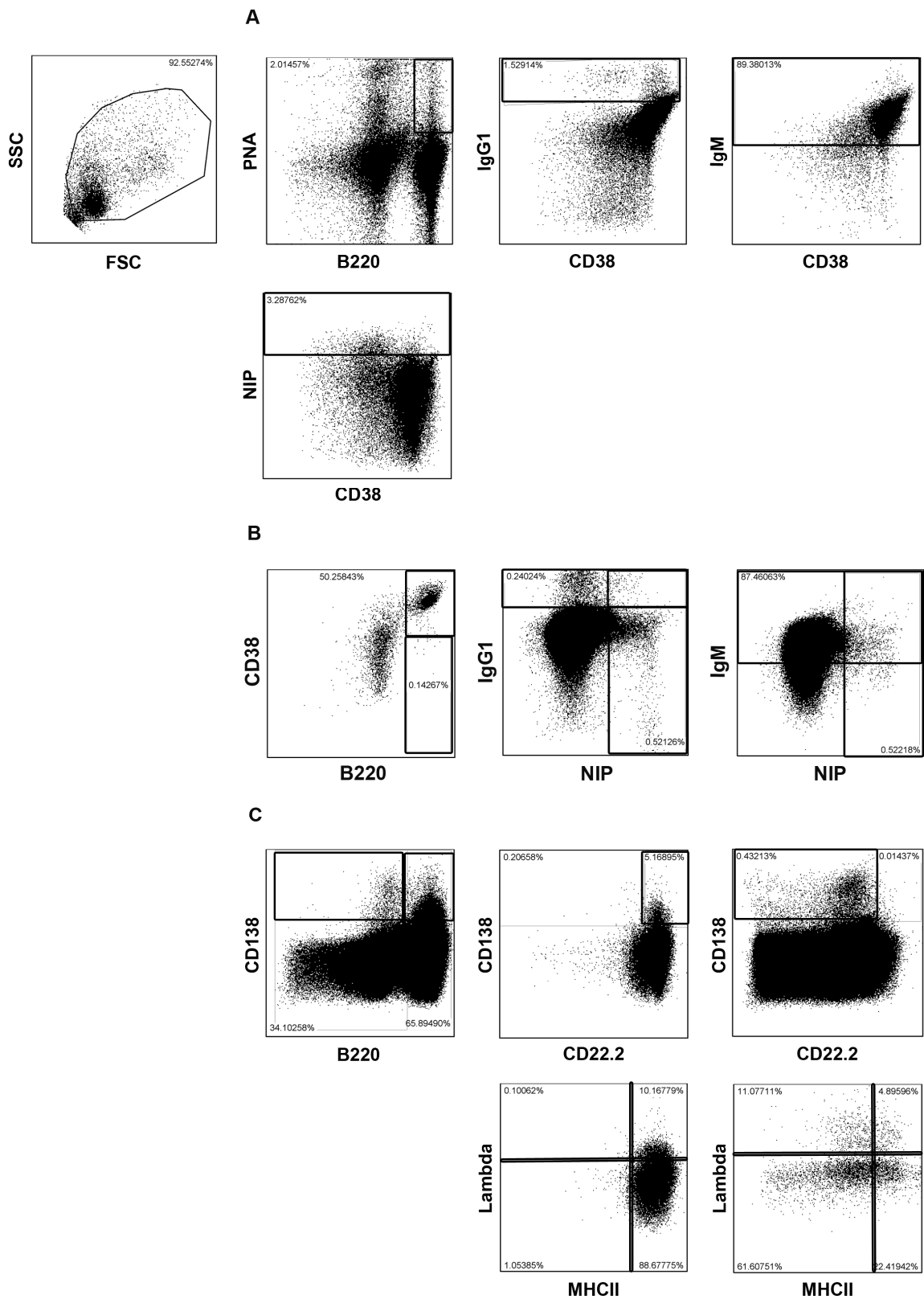


Figure 7: Identification of different B cell subsets during the NP-KLH specific immune response. Spleen, pooled blood and bone marrow (femur and tibia) of immunized C57BL/6 mice were isolated and lymphocytes were recovered. Single cell suspensions were stained either with B220, PNA, NIP, CD38,

IgM and IgG1 for the detection of different B cell subsets, or with B220, CD138, CD22.2, MHCII, Lambda and Kappa for identification of plasmablasts and plasma cells, respectively. From each sample  $5 \times 10^6$  lymphocytes were analyzed with flow cytometry. Data represent gating strategy of one representative lymphocyte sample from spleen at day 8 after primary immunization. GC B cells were detected among lymphocytes by expression of B220 and binding high amounts of PNA. GC B cells (A) and B220 expressing B cells (B) were further analyzed for the expression of CD38, IgG1, IgM and binding to NIP. CD138<sup>+</sup> B220 expressing (C, first and second pot) or not expressing (C, first and third pot) cells were examined for expression of CD22.2, MHCII and Lambda.

As shown in Figure 8, B220<sup>+</sup> PNA<sup>hi</sup> cells, previously defined by flow cytometry and immunofluorescence as GC B cells, appeared in spleen as early as day 4 after primary immunization, reached their maximum frequency by day 8-12 p.i. and decreased slightly afterwards. GC B cells could still be identified into the seventh week postimmunization. Kinetics of the GC reaction during the secondary response differed from the primary response, as the peak was reached between days 4 and 8. Importantly, a population of B220<sup>+</sup> PNA<sup>hi</sup> cells was also seen in blood (Figure 8), and their kinetics resembled the kinetics of splenic GC B cells. Such cells were also found in naïve animals but increased to higher numbers upon immunization. However, the question whether these newly detected blood-derived B220<sup>+</sup> PNA<sup>hi</sup> cells originated from the follicle and are bona fide GC B cells will be addressed in the following sections.

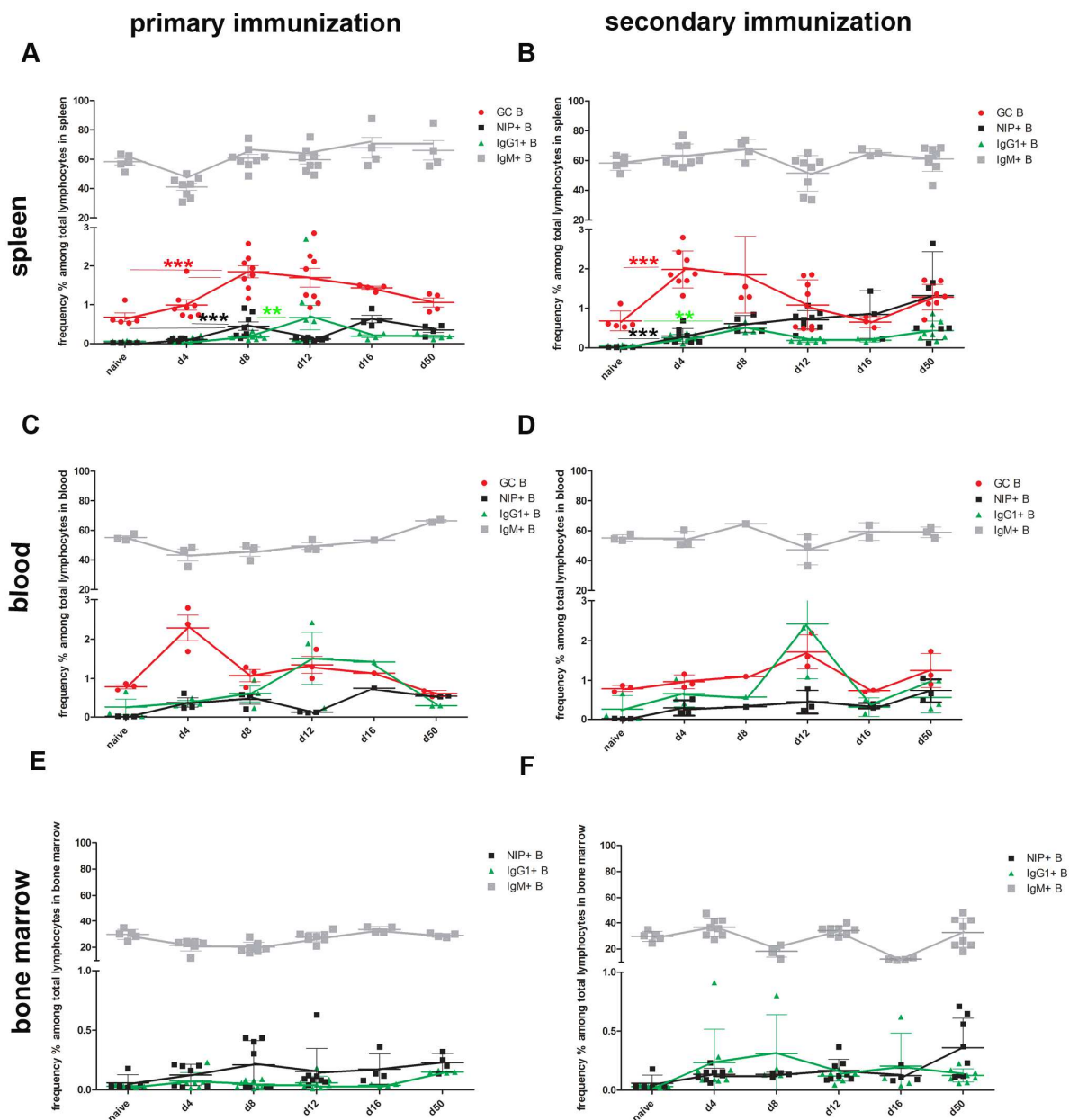


Figure 8: Kinetics and maturation of B cell subsets during primary or secondary immune response. Spleen (first row), blood (second row) and bone marrow (third row) of C57BL/6 mice were isolated at regular intervals after primary (A, C, E) or secondary (B, D, F) immunization and compared to naïve controls. Frequencies of GC B cells, hapten-binding, IgG<sub>1</sub><sup>+</sup> or IgM<sup>+</sup> B cells, plasmablasts and plasma cells within the lymphocyte population are shown. Bar graphs represent means  $\pm$  SD. 8 mice were analyzed at each time point. Statistical significance was tested for spleen and bone marrow by One-way Anova.

A population of hapten-binding B cells appeared at detectable levels as soon as 4 days after immunization in all analyzed organs and was only subjected to minor changes in frequency across analyzed time points. Taking into account the increasing absolute numbers in spleen (Figure 4) and bone marrow until day 50 p.i., it appears that with the immunization protocol used in this work, the numbers of hapten-binding B cells in

spleen and bone marrow increase over the time while their frequency remains constant. B220, CD38 and IgG1 were used as markers for isotype-switched B cells that could potentially belong to the memory B cell pool. These cells were rarely detectable in naïve animals. By day 12 after primary immunization, however, their frequency increased to 0.5% of total lymphocytes in spleen, dropped to 0.2% by day 16 and remained at stable frequencies until day 50 p.i. Induction of a secondary immune response resulted in a similar kinetic within spleen, however, by day 8 numbers of B220<sup>+</sup>CD38<sup>+</sup>IgG1<sup>+</sup> cells increased to 0.5%. Four days later, the observed frequencies had decreased to 0.2% and remained constant until the very last time point of analysis. Quantification of the isotype-switched B cell compartment in blood confirmed the retrieved data from spleen, notably the sudden increase of these cells was assessed with some delay, at day 12 after secondary immunization. Another feature of the IgG1<sup>+</sup> B cell kinetic during secondary immune response was the higher frequency of this subset in bone marrow. However, a statistically significant difference to naïve animals could not be detected before 50 days after immunization.

For quantification of nonswitched B cells which could possibly join the memory B cell pool, frequencies of the B220<sup>+</sup>CD38<sup>+</sup>IgM<sup>+</sup> subset were determined. Consistent with the B220<sup>+</sup>CD38<sup>+</sup>IgG1<sup>+</sup> kinetics, the relative frequency of IgM<sup>+</sup> B cells remained nearly constant at all analyzed time points.

Further statistical validation supported the previous results in that during the NP-KLH induced immune response the kinetics of the B220<sup>+</sup>CD38<sup>+</sup>IgM<sup>+</sup>, B220<sup>+</sup>CD38<sup>+</sup>IgG1<sup>+</sup> subsets underlie minor changes. Taken together, these data suggest a rather steady state between switched and non switched B cells but an increase of hapten-specific B cells during the NP-KLH specific immune response.

#### **4.1.3 Identified B cells with GC phenotype in blood are mature B cells with follicular origin**

To confirm the B220<sup>+</sup> PNA<sup>hi</sup> cells in blood as an exclusive GC B cell population, the conditions were defined under which cells of this phenotype could be elicited. GCs are antigen inducible, thus hapten-specific GC B cells should appear following immunization. To determine whether the kinetic of blood-derived GC B cells applies to the NP-induced GC response in spleen, splenic GC B cells from primary or secondary



NP-KLH immunized C57BL/6 mice were subjected at following time points to multiparameter flow cytometry analysis and were compared to the B220<sup>+</sup> PNA<sup>hi</sup> population in blood (Figure 9A). As shown in Figure 9A, the analysis revealed the similar kinetics of the GC B cell subset in these two organs. However, B cells with B220<sup>+</sup> PNA<sup>hi</sup> phenotype were not detected in bone marrow at any time point of analysis. As shown in Figure 9C, NP-specific GC B cells appeared in blood as soon as 4 days after immunization and were absent in naïve animals, confirming the observations in spleen. Induction of a secondary response to NP-KLH led to a longer persistence of this subset in blood, accordingly by day 50 after secondary immunization blood-derived B220<sup>+</sup> PNA<sup>hi</sup> cells were found with similar frequencies to splenic GC B cells (Figure 9B, D).

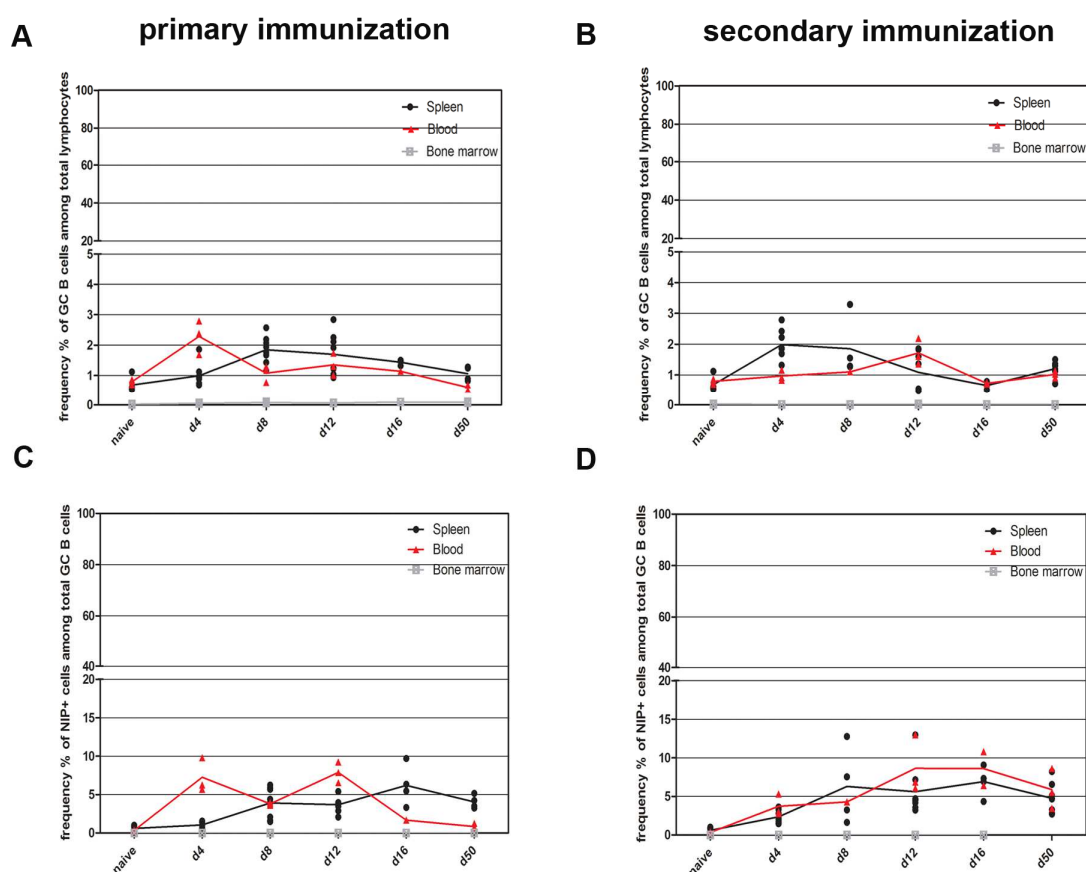


Figure 9: Kinetics and maturation of the GC B cell response and NP specific GC B cell response after primary or secondary immunization of C57BL/6 mice. Lymphocytes from spleen (black dots), pooled blood (red triangles) and bone marrow (grey boxes) from primary (A, C) or secondary (B, D) immunized

mice were isolated at the designated time points post challenge. Frequencies of total GC B cells among lymphocytes were determined and the percentage of hapten binding GC B cells was calculated respectively. Each dot represents one mouse. Each red dot represents obtained results obtained from pooled blood of 4 mice

To further validate the identity of the blood-derived  $B220^+ PNA^{hi}$  cells, the phenotype of this population was characterized more thoroughly. The  $B220^+ PNA^{hi}$  were determined to be mature B cells with follicular origin, as they expressed the B cell lineage markers CD21 and CD23 (Debnath et al., 2007) on their surface and did not bind CD93 which is expressed on transitional B cells released from bone marrow (Figure 10) (Rumfelt et al., 2006).

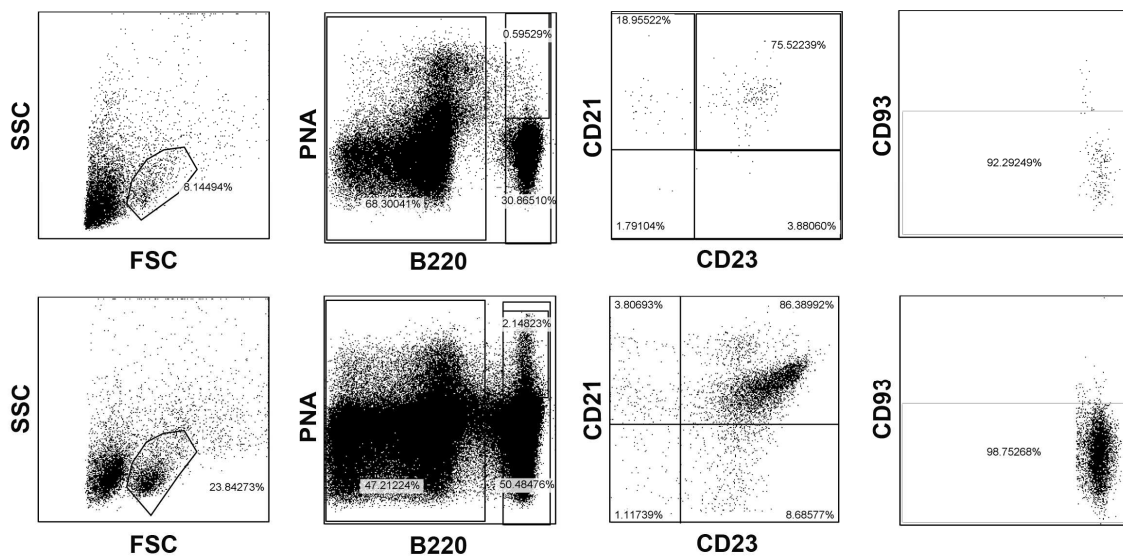


Figure 10: Comparison of blood-derived B cells with GC phenotype with splenic GC B cells. C57BL/6 mice were immunized with NP-KLH in alum. Leucocytes were isolated after 8 days from pooled blood (first row) and spleen (second row) and stained with B220, PNA, CD23, CD21 and CD93. The dot plots show the correlated expression of surface CD21, CD23 and CD93 by blood or spleen derived  $B220^+ PNA^{hi}$  cells. The numbers within the plots represent the percentages of total cells and are representative of three independent experiments.

In light of the above evidence suggesting that the blood residing  $B220^+ PNA^{hi}$  population has follicular origin and is antigen inducible, studies were performed to more thoroughly analyze the phenotype of these cells by investigating the expression of the GC relevant surface marker CD38 (Ridderstad and Tarlinton, 1998). Because GCs are associated with isotype switching, the distribution of IgM and IgG<sub>1</sub> were evaluated following primary and secondary immunization and compared to the obtained values from spleen. As shown in Figure 11, although the NP specific GC B cell response in blood and spleen expands and subsequently diminishes over time, the percentage of

total IgM<sup>+</sup> and IgG1<sup>+</sup> cells remained largely unchanged throughout the whole response. Notably, the frequencies of IgG1 expressing and hapten binding GC B cells after both immunizations significantly differed from naïve animals. This difference was apparent as early as 8 days after primary and 4 days after secondary challenge. Another common feature of both subsets was the relatively constant levels of CD38 expression in both immunization systems.

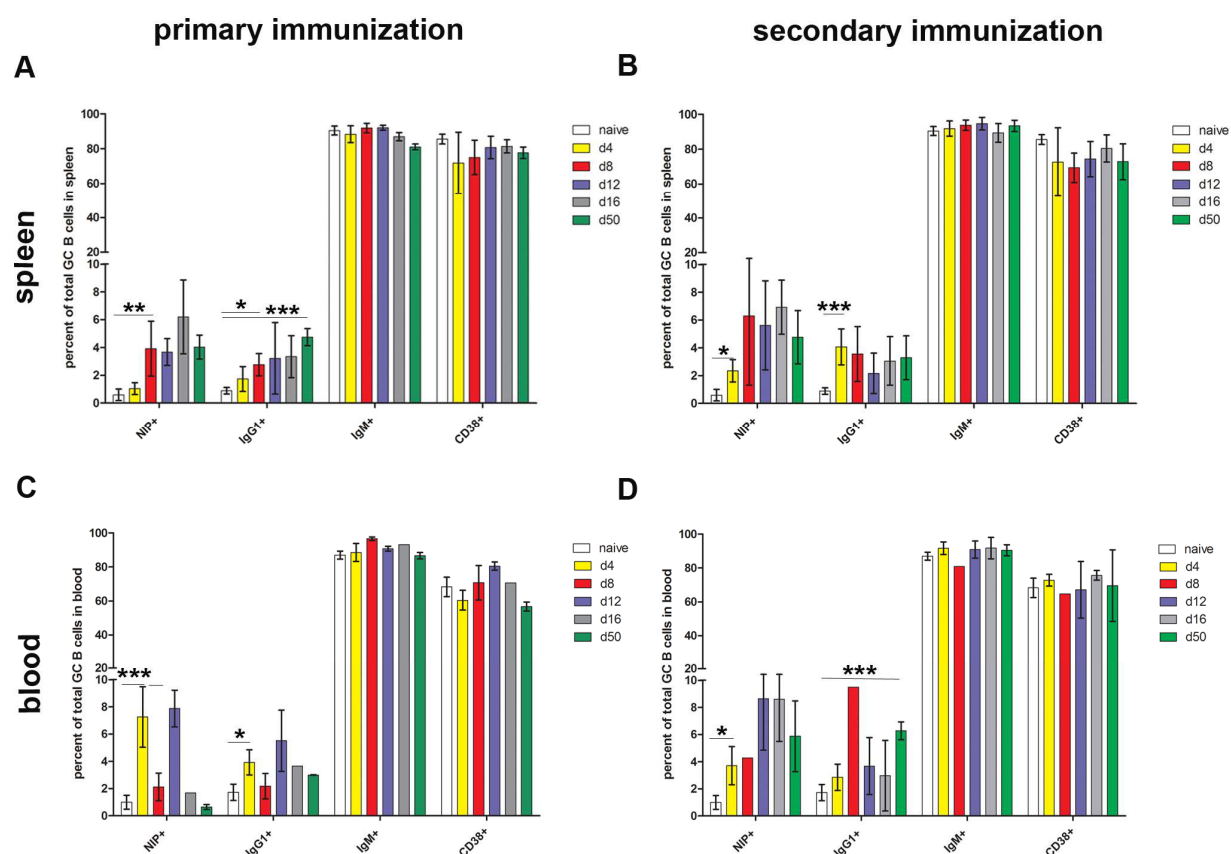


Figure 11: Kinetics and maturation of GC response in C57BL/6 mice. Splenocytes and blood of NP-KLH immunized C57BL/6 mice were harvested at the designated time points post primary (A, C) or secondary (B, D) challenge and compared to naïve animals. Graphs show frequencies of NP specific, IgG1<sup>+</sup>, IgM<sup>+</sup> or CD38<sup>+</sup> cells within splenic (first row) or blood residing (second row) GC B cell populations at days 4, 8, 12, 16 and 50 post challenge. Bar graphs represent means  $\pm$  SD. Data were tested with One-way Anova for significance. 8 mice were analyzed at each time point.

Taken together the evidence above revealed that the blood found B220<sup>+</sup>PNA<sup>hi</sup> cells are mature B cells with follicular origin, thus bona fide GC B cells and display a similar expression profile to splenic GC B cells. Furthermore, the data show widely similar

traits of the primary and secondary GC B cell response in spleen and blood in terms of their cellular composition.

#### **4.1.4 Dynamics of the NP-KLH induced plasmablast and plasma cell response**

An important consequence of the GC response to antigen is the production of plasmablasts and subsequently plasma cells. To obtain a more detailed picture of the regulation of individual responding plasmablast and plasma cell subsets, their phenotype was characterized by investigating the expression and distribution of selected cell markers after induction of the primary and secondary challenges. As described in Figure 12, plasmablasts peaked at day 8 after primary and secondary immunization in spleen. The rapid increase and decline of plasmablasts in spleen was observed within circulating blood in almost the same manner and could be due to migration away from the spleen. Since no rise in bone marrow plasmablasts occurred during the period of sharpest decline in the primary or secondary response until 50 days after immunization (Figure 12), their homing to this compartment is unlikely. In contrast, the decrease of the plasma cells in spleen was accompanied by their enrichment in blood and the rise of plasma cell numbers in bone marrow during primary response. Notably, the bone marrow would be a likely destination for plasma cells emigrants, as it is the major site for the production of serum immunoglobulin (Smith et al., 1996).

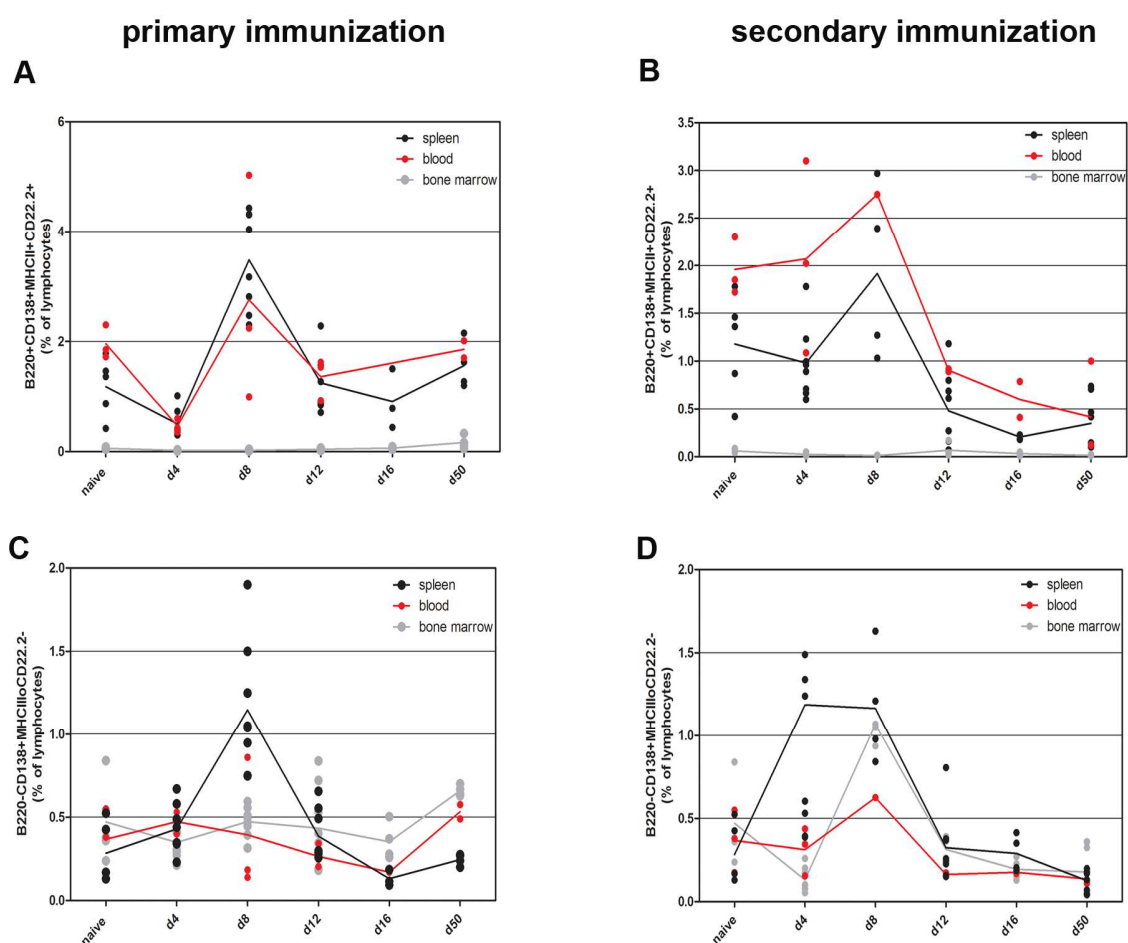


Figure 12: The kinetics of plasmablasts (B220<sup>+</sup>CD138<sup>+</sup>MHCII<sup>+</sup>CD22.2<sup>+</sup>) and plasma cells (B220<sup>+</sup>CD138<sup>+</sup>MHCII<sup>lo</sup>CD22.2<sup>-</sup>) were assessed in spleen (black dots), blood (red dots) and bone marrow (grey dots) during primary (upper row) and secondary (lower row) immune response and compared to naïve animals.

In a next step (Figure 13), frequencies of CD22.2<sup>+</sup>MHCII<sup>+</sup> plasmablasts were enumerated among the B220<sup>+</sup>CD138<sup>+</sup> cell population in spleen and blood. Because of insufficient numbers and the lack of a distinct plasmablast population, the bone marrow compartment was excluded from this analysis (Figure 12). The results showed that CD22.2 and MHCII were uniformly expressed by plasmablasts on all days examined, thus discrete plasmablast subpopulations defined by the presence or absence of these surface markers were not evident. Furthermore, induction of a secondary immune response did not affect the composition of analyzed subsets. The data obtained here suggest a robust pre-defined program for plasmablast development in the NP-KLH immunization model.

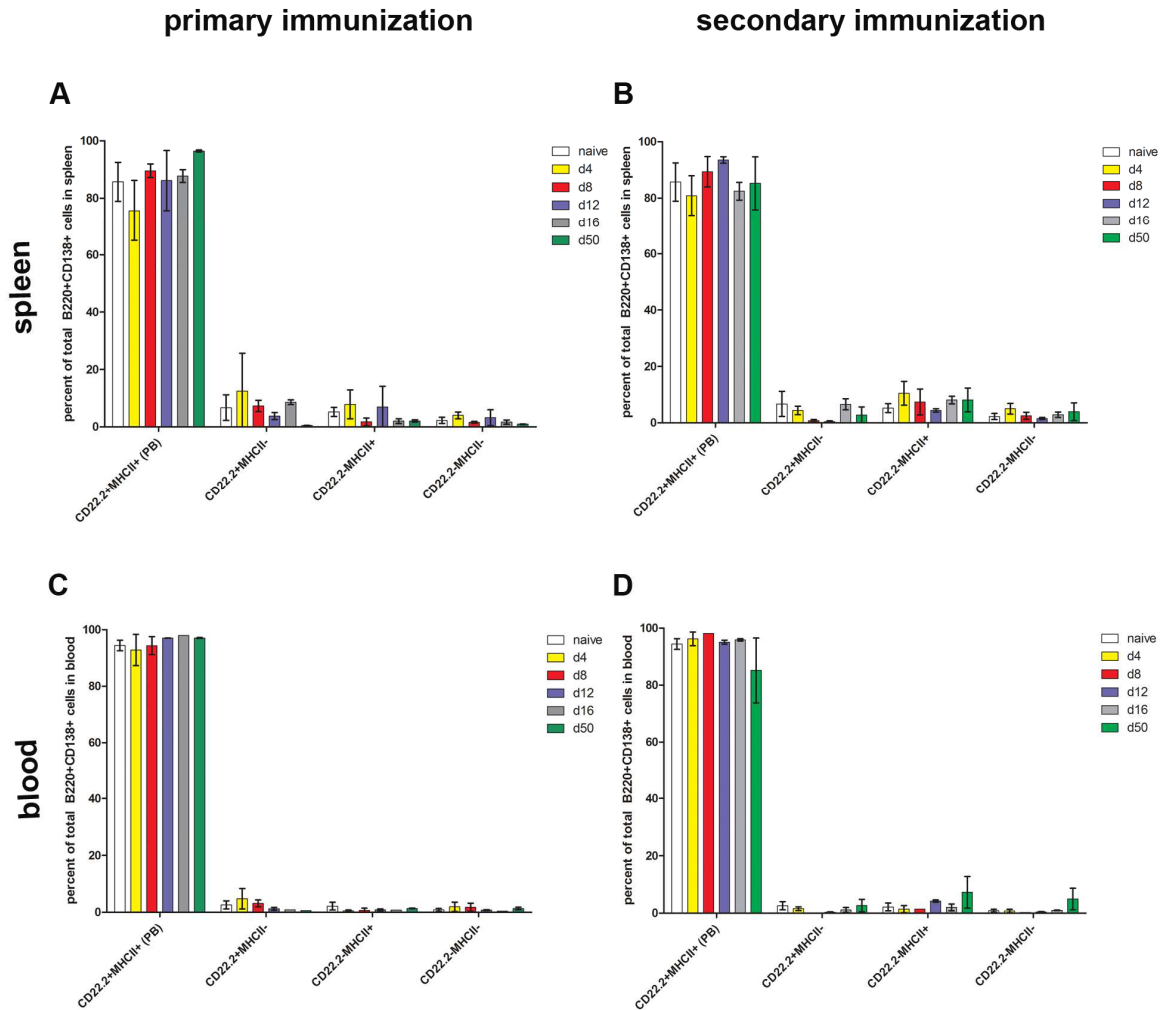


Figure 13: Kinetic and maturation of plasmablasts in course of primary and secondary immunization with NP-KLH. Spleen and blood from C57BL/6 mice were isolated at given time points after primary (A, C) or secondary (B, D) immunization. Among B220<sup>+</sup> CD138<sup>+</sup> cells the expression of CD22.2 and MHCII was examined. Relative frequencies of all detected subsets are shown at day 4, 8, 12, 16 and 50 p.i. and compared to naïve animals. Bar graphs represent means  $\pm$  SD. Four mice were analyzed at each time point. In each experiment pooled blood from 5 mice were subjected to flow cytometric analysis. Experiments were repeated 2 times.

In addition to examining the plasmablast response in C57BL/6 mice, the dynamic of plasma cell development was assessed in the course of primary and secondary response. In particular, the expression of surface CD22.2 and MHCII within the splenic, blood-derived and bone marrow B220<sup>-</sup> CD138<sup>+</sup> subset was examined on various time points after primary and secondary challenge with NP-KLH. In all analyzed organs, the majority of B220<sup>-</sup> CD138<sup>+</sup> cells did not express surface CD22.2 and had down-regulated MHCII, thus clearly belonging to the plasma cell pool. The frequency of antigen induced plasma cells slightly increased as the reaction matured until day 16 p.i. (Figure

14). However, an additional, to our knowledge previously undefined B220<sup>-</sup> CD138<sup>+</sup> CD22.2<sup>-</sup> MHCII<sup>+</sup> population was detected from the very beginning of immune response in spleen and blood and persisted throughout all the analyzed time points. The B220<sup>-</sup> CD138<sup>+</sup> CD22.2<sup>-</sup> MHCII<sup>+</sup> subset was present at a frequency of up to 20% of the B220<sup>-</sup> CD138<sup>+</sup> compartment in spleen and blood, but could only be detected at very low numbers in bone marrow after immunization. In addition, whereas the expression of MHCII was heterogeneous on the B220<sup>-</sup> CD138<sup>+</sup> subset, at none of the analyzed time points was a distinct population expressing surface CD22.2 observed in the bone the marrow.

Taken together, these data suggest MHCII and CD22.2 to be checkpoints for entering the bone marrow compartment and the latter as a stricter marker than MHCII for distinction of plasmablasts and plasma cells.

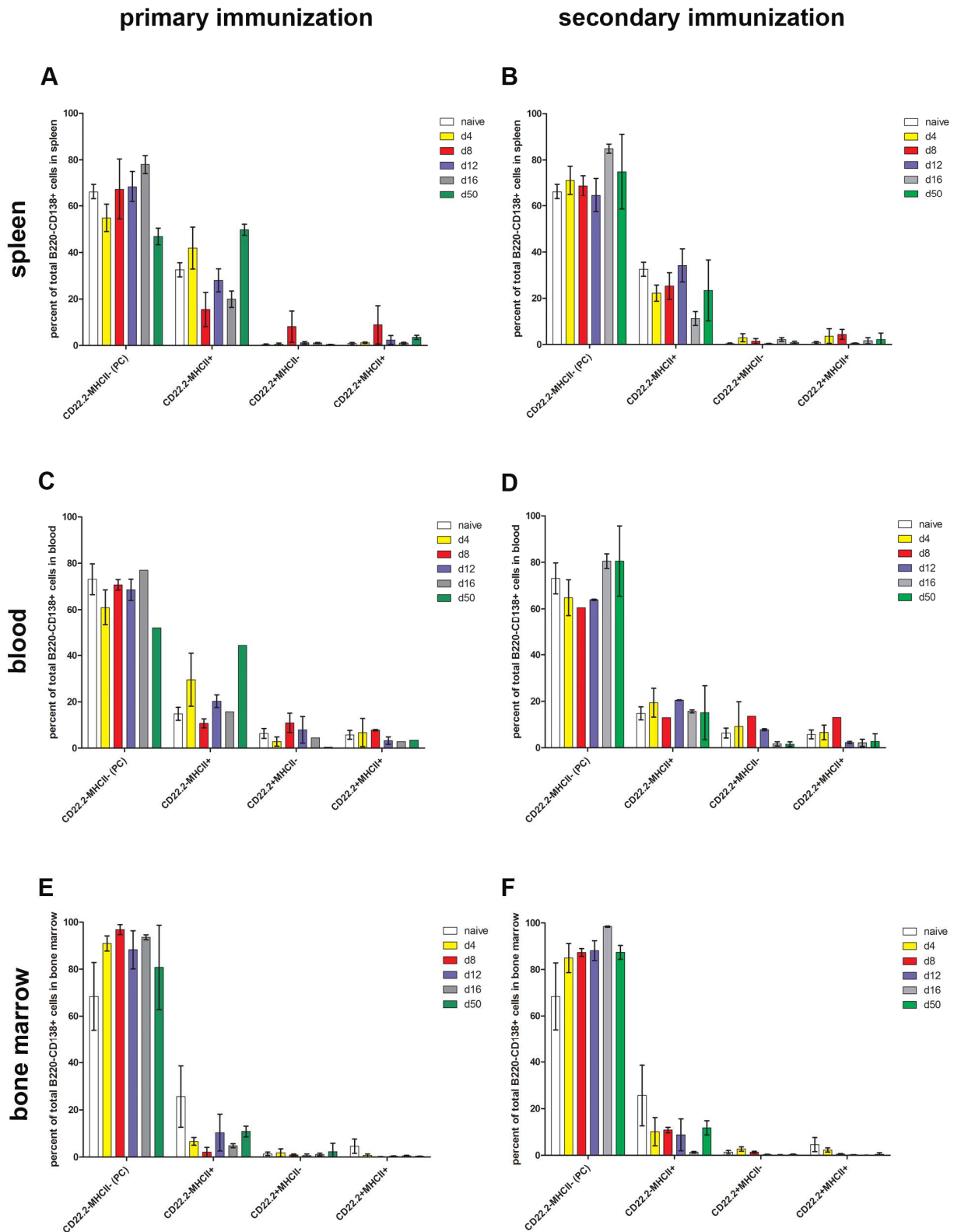


Figure 14: Kinetics and maturation of plasma cell response after primary and secondary immune response to NP-KLH. Spleen (A, B), blood (C, D) and bone marrow (E, F) from C57BL/6 mice were isolated at given time points after primary (A, C, E) or secondary (B, D, F) immunization. Among B220<sup>+</sup> CD138<sup>+</sup> cells the expression of CD22.2 and MHCII was examined. Relative frequencies of all detected subsets are



shown at day 4, 8, 12, 16 and 50 p.i. and compared to naïve animals. Bar graphs represent means +/- SD. Four mice were analyzed at each time point. In each experiment pooled blood from 5 mice was subjected to flow cytometric analysis. Experiments were repeated 2 times.

## 4.2 Migratory behavior of blood-derived B cell subsets after transfer into at an earlier time point after immunization

Following up on the kinetic studies, the next important question to address was if the GC B cell subset detected in blood (4.1) is capable of entering into secondary lymphoid organs and taking part in the ongoing GC reaction of the host. More precisely, (i) is there recruitment into existing GCs of the host, (ii) subsequent proliferation and selection followed by (iii) a further differentiation into plasma cells or memory B cells? Therefore, a detailed analysis of the interrelationship of migration, differentiation, proliferation and microenvironmental locale of 3 populations of blood-derived B cell subsets during the early stages of a T cell dependent immune response was performed by adoptive transfer experiments. In particular, blood-derived  $\text{PNA}^{\text{hi}}\text{CD38}^{\text{lo}}\text{B220}^+$ ,  $\text{IgM}^+\text{PNA}^{\text{lo}}\text{CD38}^{\text{hi}}\text{B220}^+$  or  $\text{IgG1}^+\text{PNA}^{\text{lo}}\text{CD38}^{\text{hi}}\text{B220}^+$  cells were FACS sorted from C57BL/6 mice immunized 8 days before with 100  $\mu\text{l}$  NP-KLH in alum and transferred into recipients 4 days after their immunization. Spleen, bone marrow and mesenteric lymph nodes from recipient mice were subjected to a detailed immunohistological and flow cytometric analyses at 4 different time points after transfer (Figure 15).

Previous studies have shown that at day 4 after i.p. immunization with NP-KLH antigen is available on FDCs and T cells are activated and able to support the B cell response, however, GCs are only fragmentary formed (own data, not shown). Thus, we hypothesized that at such an early time after challenge, antigen experienced donor B cells entering secondary lymphoid organs have a survival advantage compared to the corresponding donor cell subsets due to easier access to presented antigen on FDCs and a better T cell help since competing antigen specific recipient B cells are not formed in great quantities yet (Section 4.1.2.)

The small extractable volume of murine blood (1ml), low lymphocyte frequencies within the blood circulation and the lack of suitable commercially available enrichment methods for isolation of murine B cells from this organ were obstacles which necessitated the development of a new strategy for highly efficient isolation of small cell numbers. Applying this optimized enrichment procedure allowed the recovery of

sufficient cell numbers from pooled murine blood. Thus, in each experiment  $\sim 6,000$  GC ( $\text{PNA}^{\text{hi}}\text{CD38}^{\text{lo}}\text{B220}^{\text{+}}$ ) B cells,  $\sim 3,000$   $\text{IgG1}^{\text{+}}$  ( $\text{IgG1}^{\text{+}}\text{PNA}^{\text{lo}}\text{CD38}^{\text{hi}}\text{B220}^{\text{+}}$ ) and  $\sim 9,000$   $\text{IgM}^{\text{+}}$  ( $\text{IgM}^{\text{+}}\text{PNA}^{\text{lo}}\text{CD38}^{\text{hi}}\text{B220}^{\text{+}}$ ) B cells were transferred respectively.

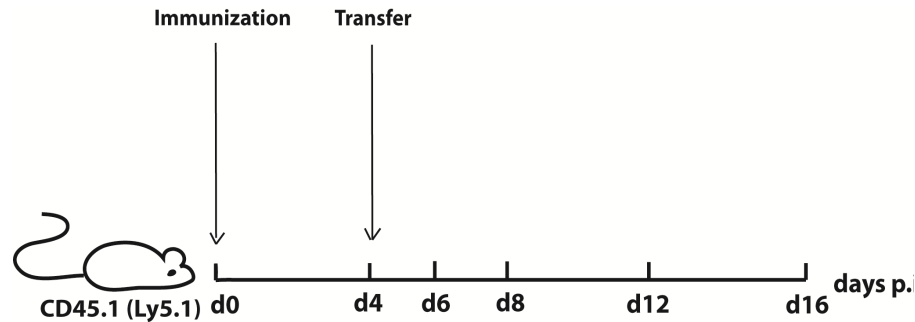


Figure 15: Experimental setup for the used transfer system. GC<sup>+</sup>B cells,  $\text{IgM}^{\text{+}}$  or  $\text{IgG1}^{\text{+}}$   $\text{CD38}^{\text{+}}$  blood-derived potential memory B cells were FACS-sorted from  $\text{CD45.2}^{\text{+}}$  mice 8 d p.i. with NP-KLH in alum and adoptively transferred into  $\text{CD45.1}^{\text{+}}$  recipients at day 4 d after their immunization. Spleen, bone marrow and mesenteric lymph nodes were harvested at days 2, 4, 8 and 12 days after transfer and prepared for either FACS analysis or histology.

#### 4.2.1 Transferred B cells numbers increase as early as 2 days after transfer and do not vary in frequencies until day eight

Two days after transfer approximately 0.02 % of detected lymphocytes in spleen and 0.08% in bone marrow were donor specific (Figure 16). Taking into account that the spleen and bone marrow compartment of a C57BL/6 mouse each contain  $\sim 5.6 \times 10^7$  -  $6.16 \times 10^7$  lymphocytes (section 4.1.1), the detected frequencies equaled about 15,000 cells. Thus, transferred cells must have proliferated at least once during the 2 days after transfer. The observed frequencies after GC and  $\text{IgM}^{\text{+}}$  B cell transfer did not alter significantly at the next two measured time points (Figure 16A, C), 8 days after transfer of  $\text{IgG1}^{\text{+}}$  B cells; however, nearly no donor cells could be detected in samples of  $6 \times 10^7$  cells from spleen and bone marrow of recipients respectively (Figure 16C). 12 days after transfer, the detected donor B cell numbers in spleen had increased in all transfer systems, particularly if  $\text{IgM}^{\text{+}}$  B cells were transferred (Figure 16A, B, C).

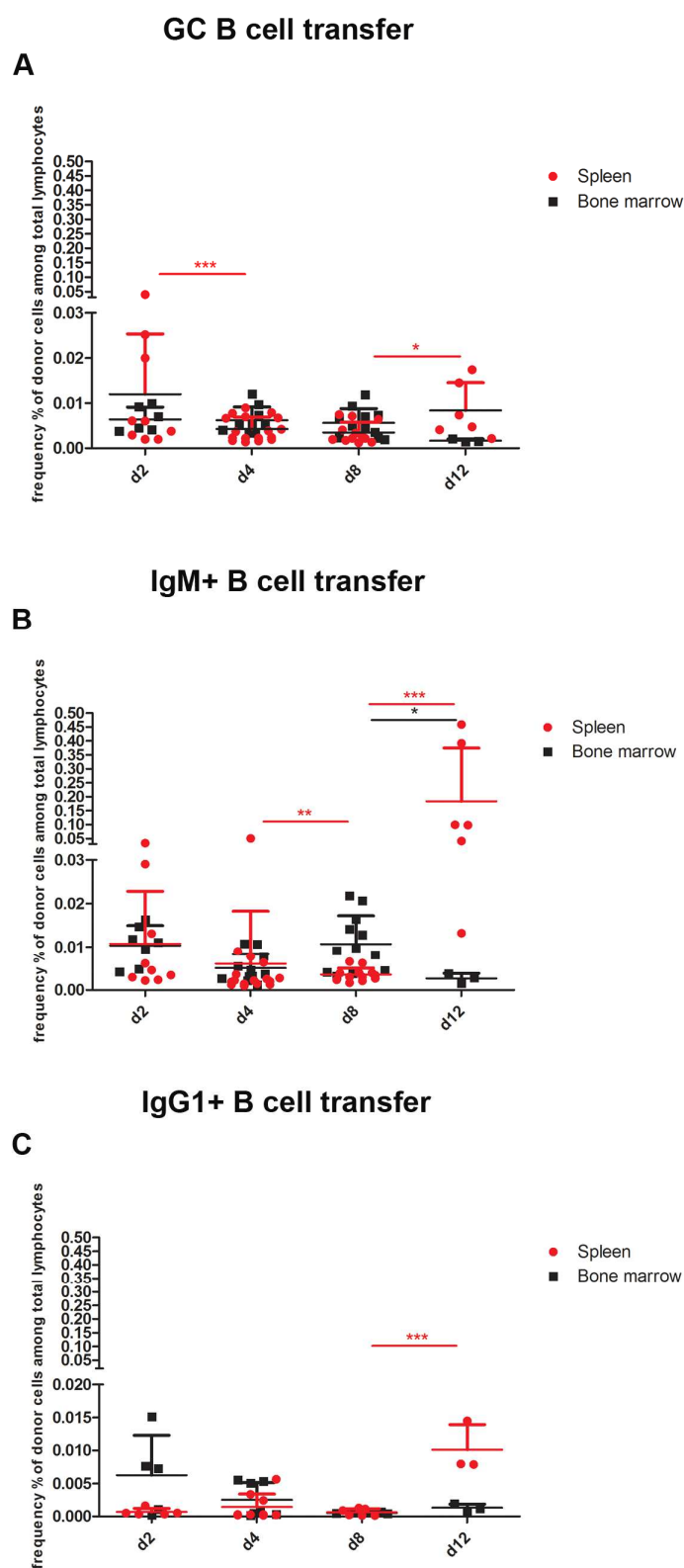


Figure 16: Frequencies of detected donor cells among total gated lymphocytes in spleen (red dots) or bone marrow (black squares) after GC (A), IgM (B) or IgG1 B cell transfer (C) at 4 time points after transfer are shown. Spleen and bone marrow of recipients were harvested, prepared for FACS analysis

and frequencies of CD45.2<sup>+</sup>CD45.1<sup>-</sup> cells among  $6 \times 10^6$  cells within the lymphocyte FSC/SSC gate were determined

#### **4.2.2 Transferred GC B cells home to secondary lymphoid organs, partially keep their phenotype but mainly develop further into post GC B cells and plasma cells**

To gain more insight into the fate of blood residing GC B cells, frequencies of different donor derived B cell subsets were assessed by multi color flow cytometric analysis from spleen and bone marrow of recipients after 2, 4, 8 and 12 days after transfer (Figure 17). As shown in Figure 18, the obtained data revealed that approx. 5% of detected donor cells in the spleen have the GC surface marker phenotype during the first week after transfer. After 12 days this number dropped to 1.5% (Figure 18 G), possibly pointing out the weaning donor and recipient specific GC response, since this time point corresponds to day 16 after immunization of recipient and goes along with the decreasing GC response as previously shown by kinetic data.

However, other donor cell derived B cell subsets displayed a rather varying kinetic. By day 2 after transfer, 5% of donor cells in spleen and 20% of the bone marrow residing donor cells belonged to the isotype-switched post GC B cell pool as proven by binding low amounts of PNA and expression of IgG1 (Figure 18 A, B). Strikingly, whereas the frequency of this subset in the spleen increased during time as shown by a peak at day 12 after transfer, nearly no switched donor B cells could be detected in bone marrow after 4 days (Figure 18 C, D). However, 4 days later a small population of IgG1<sup>+</sup> B cells re-appeared in bone marrow and increased to 15% at day 12 post transfer (Figure 18 F, H). Donor specific plasma cells appeared as early as 2 days after transfer in the spleen, increased their numbers and peaked at day 12 but were mainly absent in the bone marrow compartment except day 8 after transfer.

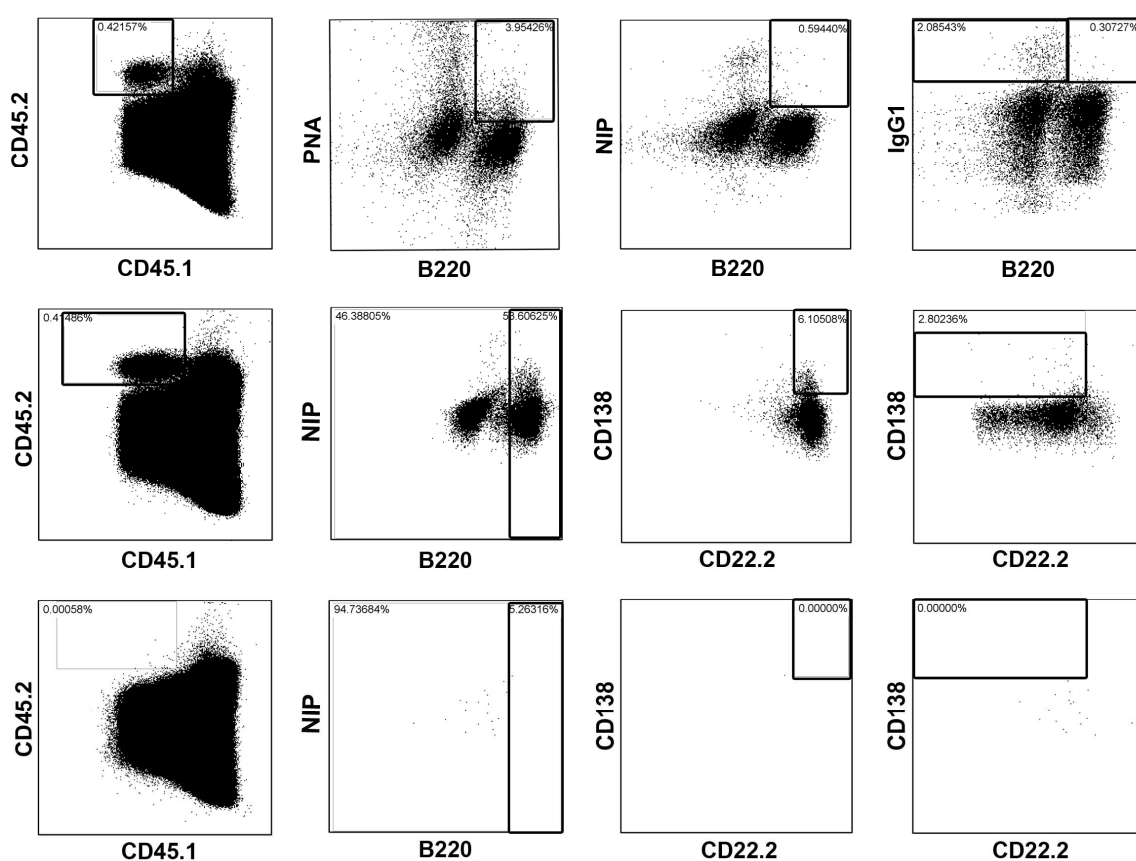


Figure 17: Analysis of the surface expression marker profile of detected donor B cells in spleen and bone marrow. Organs were harvested and prepared for FACS analysis. Single cell suspensions from whole spleen and bone marrow were stained with different antibodies. Donor cells were detected among the lymphocytes and analyzed for the expression of B220, PNA, NIP, IgG1, CD22.2 and CD138. Representative plots of the applied gating strategy for detected donor cells in spleen after GC B cell transfer (two top lines) and IgD B cell transfer (bottom line) after 12 days are shown

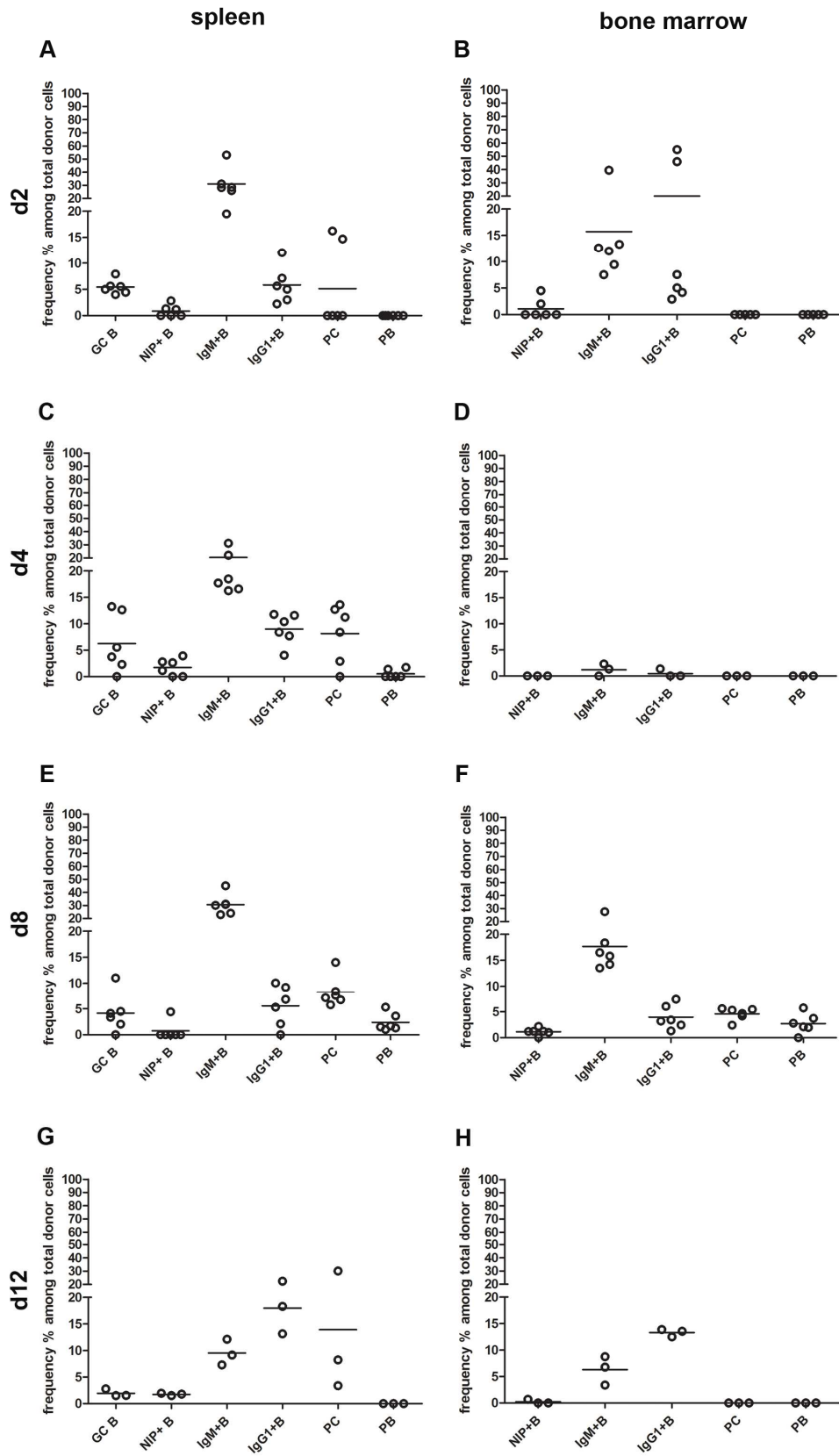


Figure 18: Kinetic and differentiation of donor GC B cells. Whole spleen, femur and tibia of recipients were isolated 2, 4, 8 and 12 days after transfer, harvested and stained with anti CD45.1, CD45.2, B220,

PNA, NIP, IgG1, CD22.2, CD138, Lambda and Kappa antibodies. Relative frequencies of GC, IgM<sup>+</sup>, IgG1<sup>+</sup> B cells and plasma cells as well as plasmablasts within donor cells detected in samples of  $6 \times 10^6$  cells from spleen (left) and bone marrow (right) 2 days (Figure A, B), 4 days (Figure C, D), 8 days (Figure E, F) or 12 days (Figure G, H) after transfer are shown. At least three mice were analyzed for each transfer at each time point

Taken together, these data show that blood-derived GC B cells migrate to secondary lymphoid organs and expand in numbers. However, only a fraction (5%) keeps the original phenotype while the vast majority differentiates further into post GC B cells and plasma cells.

### **4.2.3 Transferred IgM<sup>+</sup> CD38<sup>+</sup> PNA<sup>lo</sup> B cells home to secondary lymphoid organs, switch their isotype and induce a strong but rather short lived plasma cell response**

To further investigate the migration and differentiation properties of the transferred post GC IgM<sup>+</sup>CD38<sup>hi</sup>PNA<sup>lo</sup> B cells, their surface expression marker profile was monitored by a combination of differentiation-associated antibodies at 4 consecutive time points after transfer. Although the transferred IgM B cell population expressed high amounts of CD38 on their surface and bound low amounts of PNA, thus clearly belonging to the post GC B cell pool, 2 days after transfer 7% of the detected donor cells had regained the GC phenotype (Figure 19 A). At the same time a fraction of 20% of the donor cells clearly partitioned to the PC compartment. Further analysis revealed that a distinct proportion of donor cells ranging from 10-15% in spleen and bone marrow switched their isotype to IgG1 suggesting a so far unexpected plasticity of this cell subset (Figure 19 A, B). Although by day 4, the number of switched donor B cells to IgG1 increased to 20% of total CD45.2<sup>+</sup> cells in spleen (Figure 19 C, D), 8 days later this population vanished from the spleen and bone marrow compartment. The strong donor specific plasma cell response observed at day 2 after transfer was clearly restricted to the spleen and of a rather short live span, as by day 12 after transfer this organ was cleared of plasma cells and plasmablasts (Figure 19 G).

Parallel analysis of the bone marrow confirmed the observations in spleen, since this compartment could only contribute to the plasma cell response until day 8 and 12 days after transfer no plasma cells were scored in samples of  $6 \times 10^6$  lymphocytes (Figure 19 H). Interestingly, at this time point the absolute numbers of donor cells strongly increased, but these cells mainly belonged to the unswitched IgM<sup>+</sup> B cell population

(Figure 19 G, H) and intermediates which, based on their surface marker profile did not belong to the predefined plasma cell and blast pool (Figure 17).



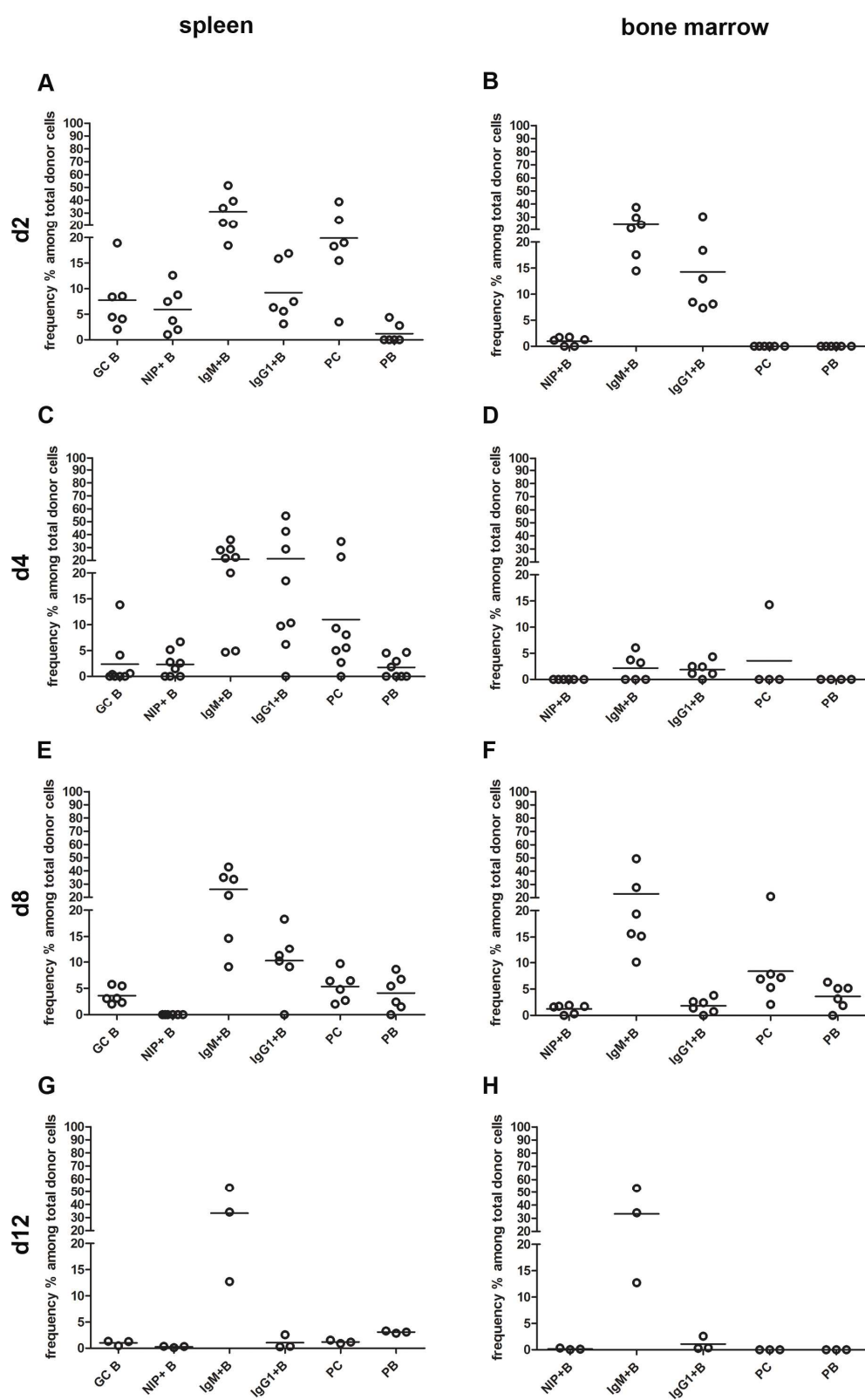


Figure 19: Kinetic and differentiation of transferred  $\text{IgM}^+$  B cells. To quantify the composition of donor B cell subsets whole spleen, femur and tibia of recipients were isolated 2, 4, 8 and 12 days after transfer,

harvested and stained with anti CD45.1, CD45.2, B220, PNA, NIP, IgG1, CD22.2, CD138, Lambda and Kappa antibodies. Relative frequencies of GC, IgM<sup>+</sup>, IgG1<sup>+</sup> B cells and plasma cells as well as plasmablasts within donor cells detected in samples of  $6 \times 10^6$  cells from spleen (left) and bone marrow (right) 2 days (A, B), 4 days (C, D), 8 days (E, F) or 12 days (G, H) after transfer are shown. Each data point represents one mouse.

Thus, blood-derived IgM<sup>+</sup> B cells home to secondary lymphoid organs and proliferate as indirectly shown by increasing cell numbers. Having entered the spleen, these cells are able to regain the GC B cell phenotype; however, a stable fraction of 30% keeps the original phenotype throughout 12 days or differentiates into short lived plasma cells.

#### **4.2.4 Transferred IgG1 B cells home to spleen and bone marrow and down-regulate surface B220 at later time points**

Previous data showed that transferred GC B cells and IgM B cells partitioned, respectively into different B cell compartments and switched their isotype to IgG1 as soon as 2 days after transfer. These processes are the logical consequence of the T cell dependent immune response and mirror the classical steps a B cell undergoes during the GC response. IgG1<sup>+</sup> B cells however, do not display such heterogeneity of known surface marker expression and are a late product of GC specific immune response per se. Therefore, it was not predictable to which compartment these cells are dedicated and which differentiation steps would precede their subsequent accumulation in the particular organ. A major finding of this study was that IgG1<sup>+</sup> B cells first appeared in the bone marrow compartment, as early as 2 days after transfer (Figure 20 B). By this time point, up to 60% of these cells had down-regulated B220 on their surface. The B220<sup>+</sup>/B220<sup>-</sup> ratio of detected donor cells in bone marrow consecutively changed in favor of B220<sup>lo</sup> IgG1<sup>+</sup> B cells until the last time point of analysis. This observation combined with the decrease of the absolute numbers of detected donor B cells in this compartment indicates a rapid turnover of B220<sup>+</sup>IgG1<sup>+</sup> cells either due to cell death or as a result of further cell differentiation into B220<sup>lo</sup>IgG1<sup>+</sup> cells. Although the number of IgG1<sup>+</sup> donor cells in spleen increased over time (Figure 16), the changes of B220<sup>+</sup>/B220<sup>-</sup> ratio within this organ reflected the observations in bone marrow (Figure 20 A, B). Consequently, 12 days after transfer, the majority of detected IgG1<sup>+</sup> CD45.2<sup>+</sup> cells in spleen were B220<sup>lo/-</sup>. Hapten-specific cells, however, were only detected in the recipients' spleen.

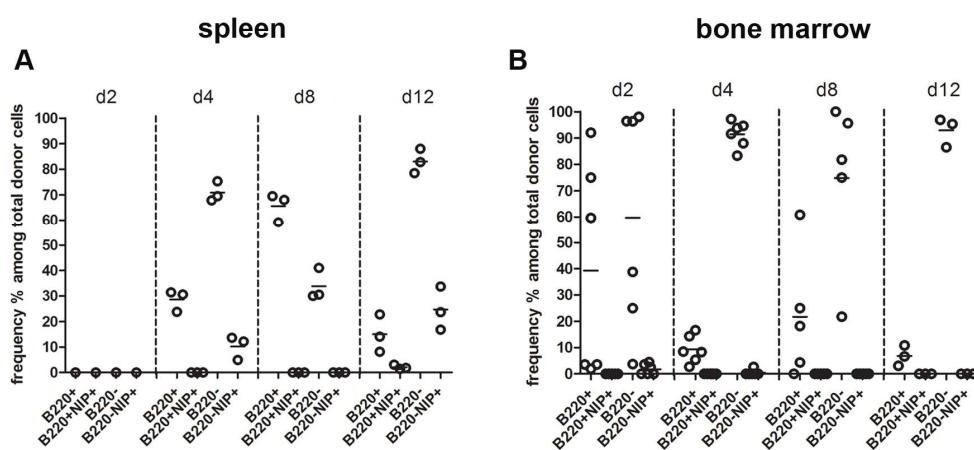


Figure 20: Kinetic and differentiation of transferred IgG1<sup>+</sup> B cells in spleen and bone marrow. Spleen, femur and tibia of recipients were isolated at different time points after transfer, harvested and stained with anti CD45.1, CD45.2, B220, NIP and IgG1 antibodies. Relative frequencies of B220<sup>+</sup>, B220<sup>-</sup>, hapten-specific or carrier-specific IgG1<sup>+</sup> donor cells in samples of 6x10<sup>6</sup> cells from spleen (A) bone marrow (B) after 2, 4, 8 and 12 days after transfer are shown. Each data point represents one mouse.

IgG1 was not uniformly expressed on the detected CD45.2<sup>+</sup>CD45.1<sup>-</sup> cell subset (Figure 21). Strikingly, until 8 days after transfer the majority of detected donor cells did not express surface IgG1. Since the origin of the CD45.2<sup>+</sup>CD45.1<sup>-</sup> IgG1<sup>-</sup> subset was not clear, these cells were excluded from the analysis. Nevertheless, it should be taken into consideration that these cells may not only be an artifact due to an inefficient sort procedure with purity less than 100%, but also contain further switched donor cells. By day 12 after transfer, however, the donor cell subset was homogenously expressing surface IgG1.

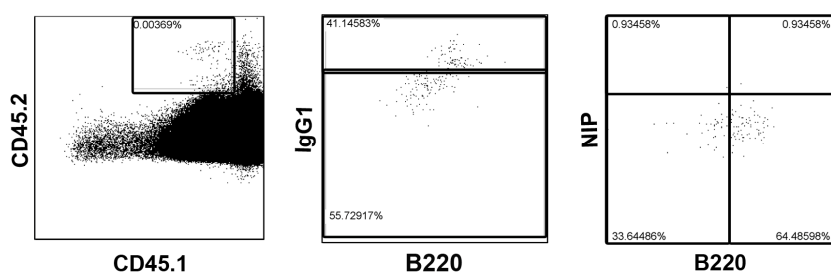


Figure 21: Flow cytometric analysis of the CD45.2<sup>+</sup>CD45.1<sup>-</sup>IgG1<sup>-</sup> donor cell population. Representative dot plots of single cell suspensions of recipient's spleen, tested for the expression of CD45.1, CD45.2, B220, PNA, NIP and IgG1 at day 8 after transfer.

#### **4.2.5 Transferred GC B cells are initially located along the T cell border and partially proliferate within the B cell zone and interfollicular zone whereas another fraction enters the dark zone and subsequently accumulates in the GC light zone**

To further substantiate the migration route of blood-derived GC B cells and investigate their differentiation within secondary lymphoid organs, mesenteric lymph nodes of recipients were harvested 2, 4 and 8 days after transfer and prepared for histological sectioning. Localization of CD45.2<sup>+</sup> cells was determined with respect of the different areas of the organ. In particular, extensive series of consecutive sections of whole lymph nodes were conducted and stained with different antibody combinations. By using a multiple signal amplification system, absolute numbers of migrated cells into mesenteric lymph nodes were sustained and allocated to different identified regions based on follicular borders and the capsule (Figure 23). To determine whether blood-derived GC B cells proliferate and progress along the GC B cell pathway, expression levels of Ki67 (Scholzen and Gerdes, 2000) and Bcl-6 (Crotty et al., 2010) were assessed, respectively. For this purpose, a specific protocol was established which permitted a staining without the usual antigen recovery method and hence kept all other used antigens and markers intact. Additionally, combined Bcl-6 staining with CD3 was used to score the number of associated donor cells with T cells and to address the question whether the observations correlate with T cell contact.

Localization of donor B cells 2 days after transfer within recipient lymph nodes revealed their evenly distribution within B and T cell areas but their absence from the light zone. Many of these cells were in direct contact with T cells and were Ki67<sup>+</sup> which is an indicator of proliferation (Figure 23 A). Plasma cells were found rarely but mostly accumulated in the areas close to the subcapsular sinus (SCS) (Figure 23 B). At day 4 after transfer, detected donor cells had increased in absolute numbers, were less frequently Ki67<sup>+</sup> and had almost no T cell contact. A proportion of the cells had moved to the interfollicular (IF) zones (Figure 23 C). Also plasma cells were numerous within lymph nodes but accumulated mainly in the B cell zone (BCZ), reflecting their origin of production, which are the GCs. 8 days after transfer, donor B cells had increased their numbers 5 times within the BCZ and detected in the light zone for the first time. Unlike day 4 after transfer, 10-30% of detected donor cells in BCZ and IF zone were directly associated with Bcl-6<sup>+</sup> T helper cells. Parallel staining of serial sections showed that the

Bcl-6 expression in donor B cells underlies their localization within the GC, since Bcl-6 expression by donor cells was not evident in any other compartment of mesenteric lymph nodes. Therefore, obtained data confirm the participation of GC residing donor B cells in the ongoing germinal center reaction of recipients. In contrast to the invasion of BCZ by donor B cells, plasma cells disappeared from the follicles 8 days after transfer and mainly accumulated within the T cell zone (TCZ) and the medullar cords.

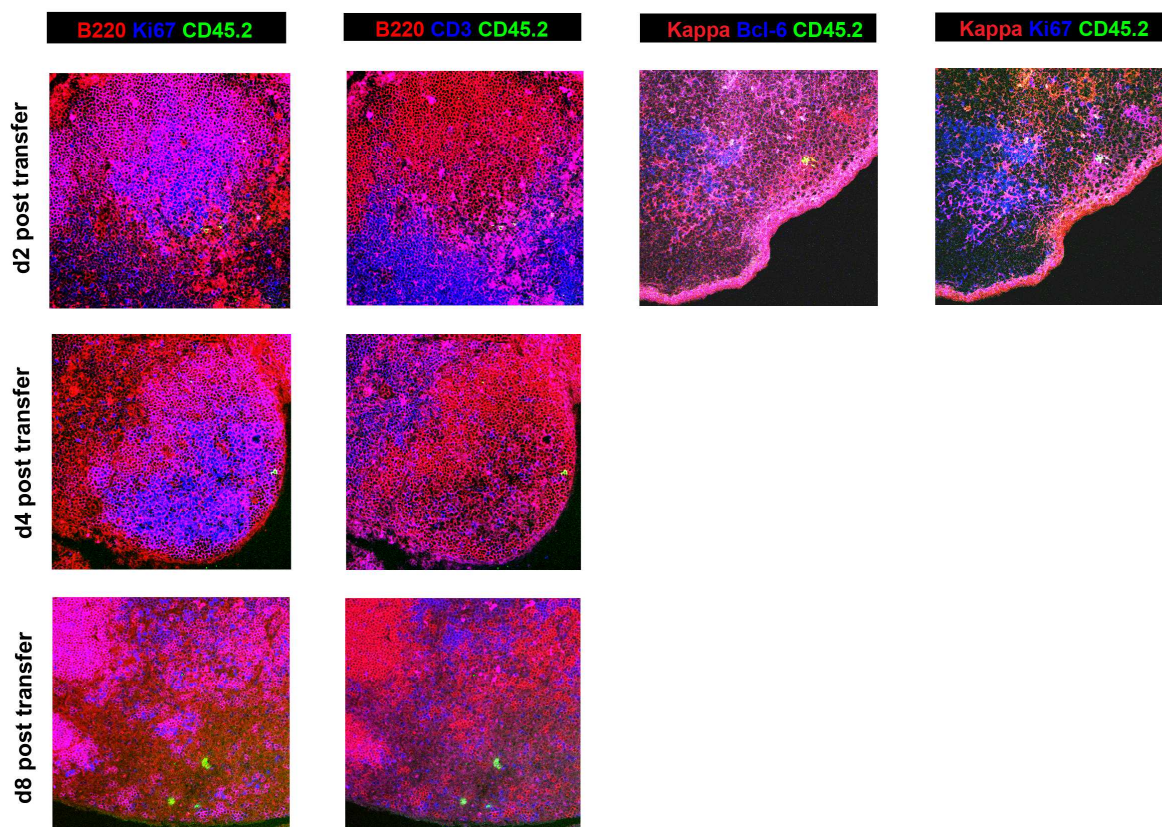


Figure 22: Localization and proliferation of  $B220^{+}PNA^{hi}CD38^{lo}$  donor cells within different areas of mesenteric lymph nodes at early time points of immune response.  $B220^{+}PNA^{hi}CD38^{lo}$  blood B cells were transferred as previously described. Mesenteric lymph nodes were harvested, consecutively sectioned and stained with 2 different antibody cocktails to visualize different areas of lymph nodes based on follicular borders and the SCS. The first two panels from left illustrate the location of donor cells (CD3, green) with respect of B cell zone (B220, red) and GCs (Ki67, blue) or the B cell zone (red) and the T cell zone (blue) at day 2, 4 and 8 after transfer. Panels on the 2 right columns of images show the result of staining of adjacent sections for the Ki67 proliferation or Bcl-6 expression (both in blue) of Kappa (red) donor (green) plasma cells and B cells. Images are shown in 20x magnification. The data shown are representative of those obtained from at least three mice from each time point.

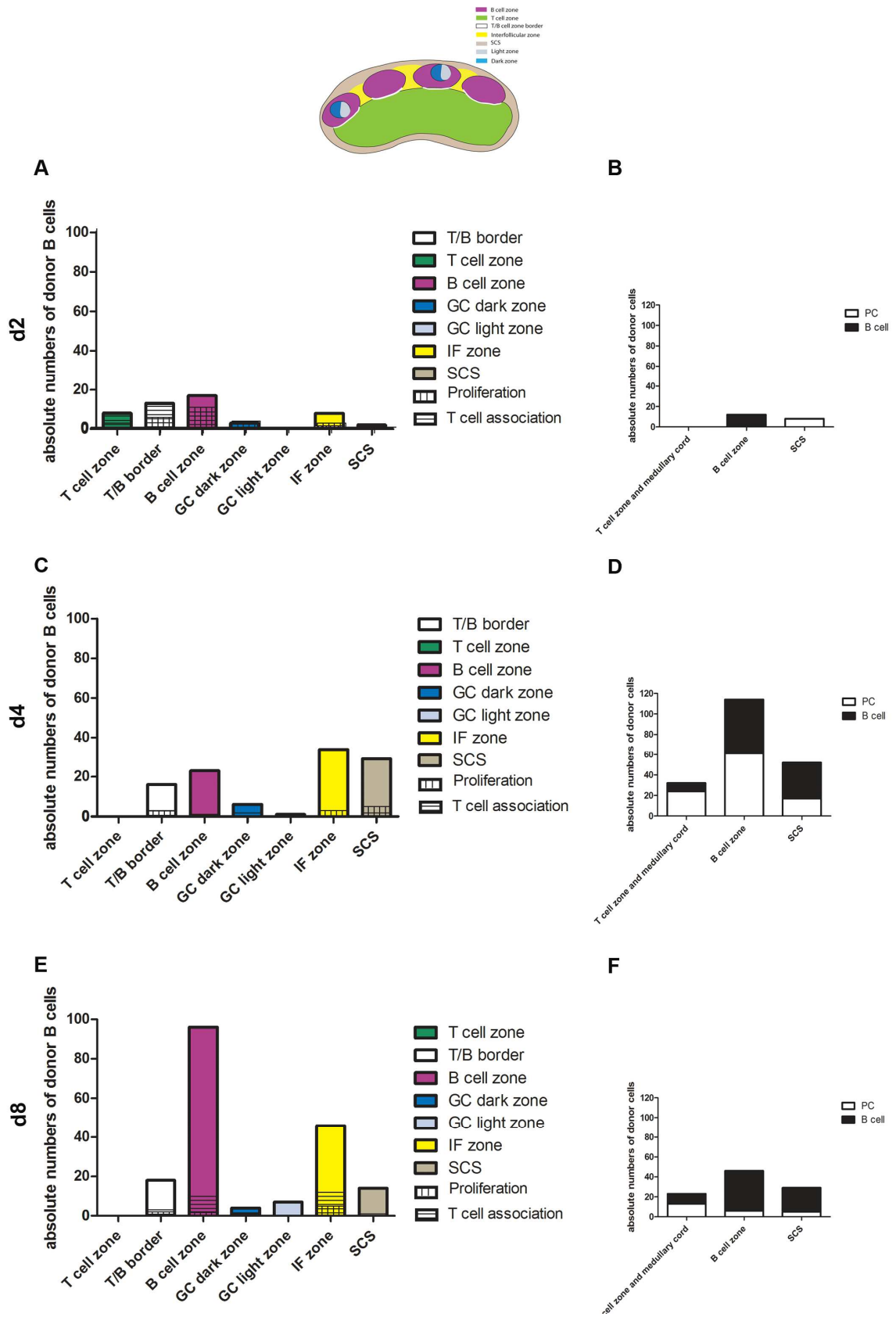


Figure 23: Localization of transferred GC B cells through mesenteric lymph node microenvironments at different time points of immune response. Consecutive sections were stained with anti B220, CD3, Ki67,

Bcl-6, CD21, Kappa, Lambda and CD45.2 antibodies to identify different areas of lymph node based on their borders. The adjacent area to SCS was defined as the contiguous 100  $\mu\text{m}$  of the outer face of lymph nodes. An area of 50  $\mu\text{m}$  width between B and T cell zone was determined as the B/T zone border. Homing of CD45.2<sup>+</sup> donor cells was quantified within the different pre-defined lymph node microenvironments. Donor B cells and plasma cells in each zone were counted in complete lymph nodes. Data show absolute numbers of counted donor B cells within different areas of 5 isolated mesenteric lymph nodes from 3 animals at 2 (A), 4 (C) and 8 days (E) after transfer. The right panel shows the calculated numbers of detected donor B cells versus plasma cells in medullar cord, B cell zone and the area close to SCS 2 days (B), 4 days (D) and 8 days after transfer (F).

To get a deeper understanding of the homing behavior of donor B cells within the different microenvironments of mesenteric lymph nodes as a function of time, relative accumulation of detected donor cells in each predefined region of lymph node were calculated (Figure 24). The obtained results affirmed the previously described observations and displayed a clear migration route of donor B cells. Two days after transfer donor B cells accumulated along the B/T cell zone border, within the B cell zone, the IF zone possibly reflecting their entrance path from peripheral blood through the mesenteric lymph nodes. By this time they had already entered the dark zones of recipient GCs. By day 4, a fraction of donor cells which probably acquired T cell help moves away from the B/T border and the BCZ to the IF and the area close to the SCS. However, the fraction of dark zone residing B cells remains at stable frequencies. By day 8, more cells accumulate within the BCZ and for the first time, donor cells left the dark zones and accumulated within the light zones of recipient GCs.

Taken together, these data strongly suggest that transferred GC B cells migrate from peripheral blood along the T/B border probably to acquire T cell help, a fraction enters the BCZ and IF zone and proliferates outside the GCs end differentiates into plasma cells whereas another distinct fraction first moves to the dark zone and enters the light zone as soon as 8 days after transfer.

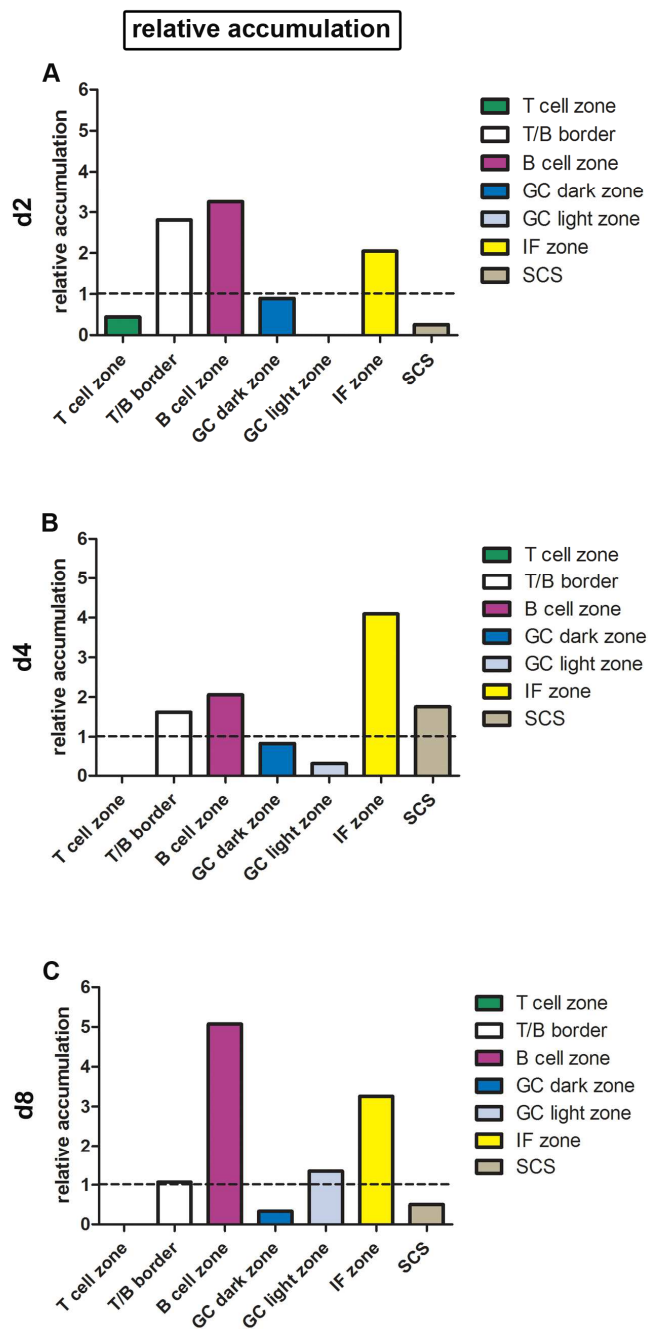


Figure 24: Relative accumulation of donor B cells within lymph node microenvironments at 2 (A), 4 (B) and 8 days (C) after transfer. To quantify cell homing of detected donor cells within lymph node compartments, counted cells in each zone in images from complete lymph node sections were fractioned and divided by the fraction of the area. Thereby, a value  $>1$  is regarded as enrichment.  $n=3$  for each time point.



#### **4.2.6 Transferred B220<sup>+</sup>PNA<sup>lo</sup>CD38<sup>hi</sup>IgM<sup>+</sup> cells accumulate along the B/T border and within the IF zone prior to entering the GC dark and light zones**

The data explained above confirmed a selective accumulation of blood-derived GC B cell subsets in distinct compartments of mesenteric lymph nodes. This finding raised the possibility of a purposive migration of GC derived B cells, depending on their state within GC B cell ontogeny. Thus, to verify the relative role of the developmental stage of GC derived B cells in their migration pattern, the localization of transferred B220<sup>+</sup>PNA<sup>lo</sup>CD38<sup>hi</sup>IgM<sup>+</sup> cells within different regions of mesenteric lymph nodes over the course of the first seven days of NP-KLH immune response was assessed and the number of Ki67<sup>+</sup> cells and direct T cell contacts were scored (as described in section 4.2.5). B220<sup>+</sup>PNA<sup>lo</sup>CD38<sup>hi</sup>IgM<sup>+</sup> cells accumulated within the interfollicular zone, at the B/T cell zone borders and less frequently within the T cell zone after two days (Figure 25, Figure 26). As expected, a large fraction of detected donor cells within the T cell zone and at the borders were in direct contact with T cells, whereas the largely Ki67<sup>+</sup>, IF zone residing donor cells were rarely found to be associated with T cells. By this time, analyzed mesenteric lymph nodes were almost empty of CD45.2<sup>+</sup> plasma cells. By day 4, donor cells were absent from the TCZ and the T/B border but had accumulated within the BCZ (Figure 26C). Further analysis showed that the BCZ residing donor cells were numerous in the locale of the border to GCs and within the GC dark zones. Additionally, a population of donor derived plasma cells was recruited for the first time into the analyzed lymph nodes. In contrast to the occupation of the BCZ by donor B cells, CD45.2<sup>+</sup> plasma cells were found to accumulate almost exclusively within the area close to the SCS. At day 8 after transfer, absolute numbers of detected CD45.2<sup>+</sup> cells within lymph nodes had increased 2-3 times, as reflected by invasion of the T/B borders, the IF zone and the areas close to the SCS by higher numbers of T cell associated donor B cells (Figure 26E). A minor fraction of such cells also appeared within the GC light zones. Analogous to obtained results from B cells, absolute numbers of detected donor plasma cells increased to a similar extend. Figure 26F illustrates their recruitment to the BCZ and the medullary chords for the first time in this study.

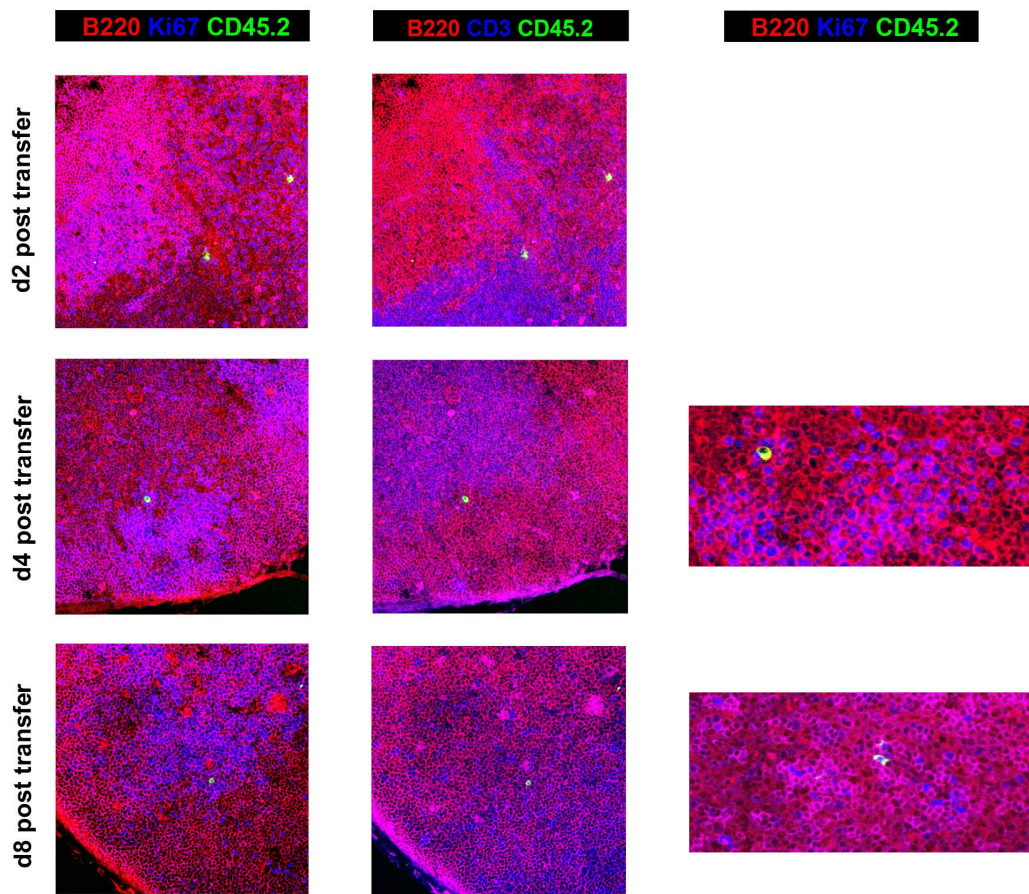


Figure 25: Localization and proliferation of B220<sup>+</sup>PNA<sup>lo</sup>CD38<sup>+</sup>IgM<sup>+</sup> donor cells within different areas of mesenteric lymph nodes at early time points of immune response. B220<sup>+</sup>PNA<sup>lo</sup>CD38<sup>+</sup>IgM<sup>+</sup> blood B cells were transferred as previously described. Mesenteric lymph nodes were harvested, consecutively sectioned and stained with 2 different antibody cocktails to visualize different areas of lymph nodes based on follicular borders and the SCS. The first two panels from left illustrate the location of donor cells (CD45.2, green) with respect of B cell zone (B220, red) and GCs (Ki67, blue) or the B cell zone (red) and the T cell zone (blue) at day 2, 4 and 8 after transfer. Images are shown in 20x magnification. The panel on the right column of images is representative of staining of the adjacent sections for the Ki67 proliferation (blue) of B220 (red) donor (green) cells, taken with a 40x magnification. The data shown are representative of those obtained from at least three mice from each time point.

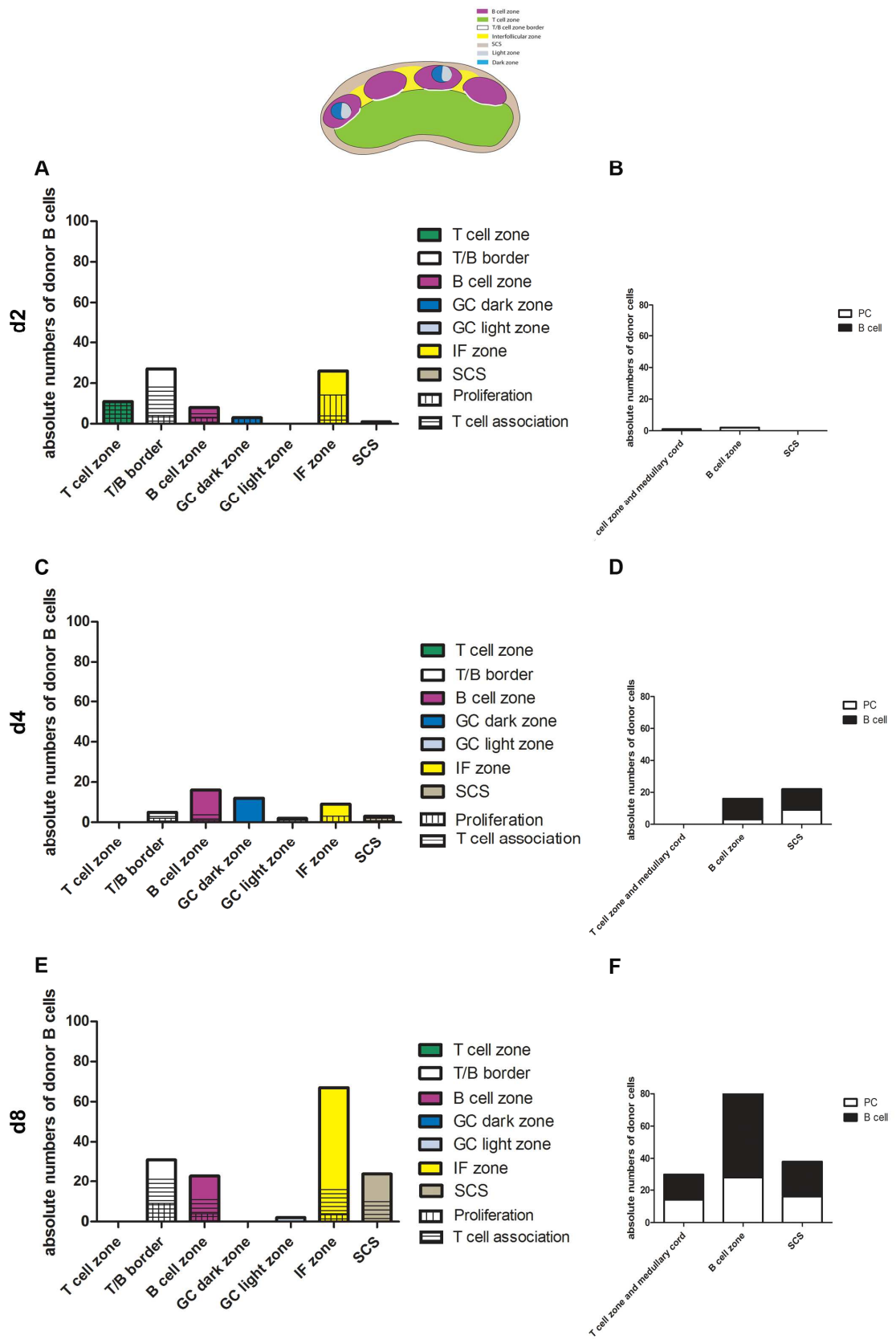


Figure 26: Migration of transferred  $\text{IgM}^+$  B cells through mesenteric lymph node microenvironments at different time points of immune response. Consecutive sections were stained with anti B220, CD3, Ki67,

Bcl-6, CD21, Kappa, Lambda and CD45.2 antibodies to identify different areas of lymph node based on their borders. The adjacent area to SCS was defined as the contiguous 100  $\mu\text{m}$  of the outer face of lymph nodes. An area of 50  $\mu\text{m}$  width between B and T cell zone was determined as the B/T zone border. Homing of CD45.2<sup>+</sup> donor cells was quantified within the different pre-defined lymph node microenvironments. Donor B cells and plasma cells in each zone were counted in complete lymph nodes. Data show absolute numbers of counted donor B cells within different areas of 5 isolated mesenteric lymph nodes from 3 animals at 2 (A), 4 (C) and 8 days (E) after transfer. The left panel shows the calculated numbers of detected donor B cells versus plasma cells in medullar cord, B cell zone and the area close to SCS 2 days (B), 4 days (D) and 8 days after transfer (F).

To further emphasize the migration path of transferred cells during the proceeding primary NP-KLH response with respect to different regions of the lymph node, relative accumulation of donor B cells within predefined microenvironments of mesenteric lymph nodes were calculated (as described in 4.2.5). The obtained data revealed that by day 2 after transfer donor B cells accumulated along the B/T border, within the IF zone, and to some extent inside the B cell follicle. Two days later, the distribution of donor cells changed as shown in Figure 27B. Instead of concentrating at the border between the follicle and the T cell zone, donor cells accumulated within the BCZ and predominantly clustered in the GC dark and light zones. These observations suggest an overall migration of donor cells from the B/T border into the follicle and their recruitment into GCs during the first 4 days after transfer. At day 8 after transfer, the distribution pattern of donor cells had changed once more. The vast majority of cells were confined to the IF zone, but the number of donor cells along the B/T border increased with some having entered the area adjacent to SCS: Remarkably, the accumulation pattern of donor cells at day 8 resembled the observations at day 2 after transfer.

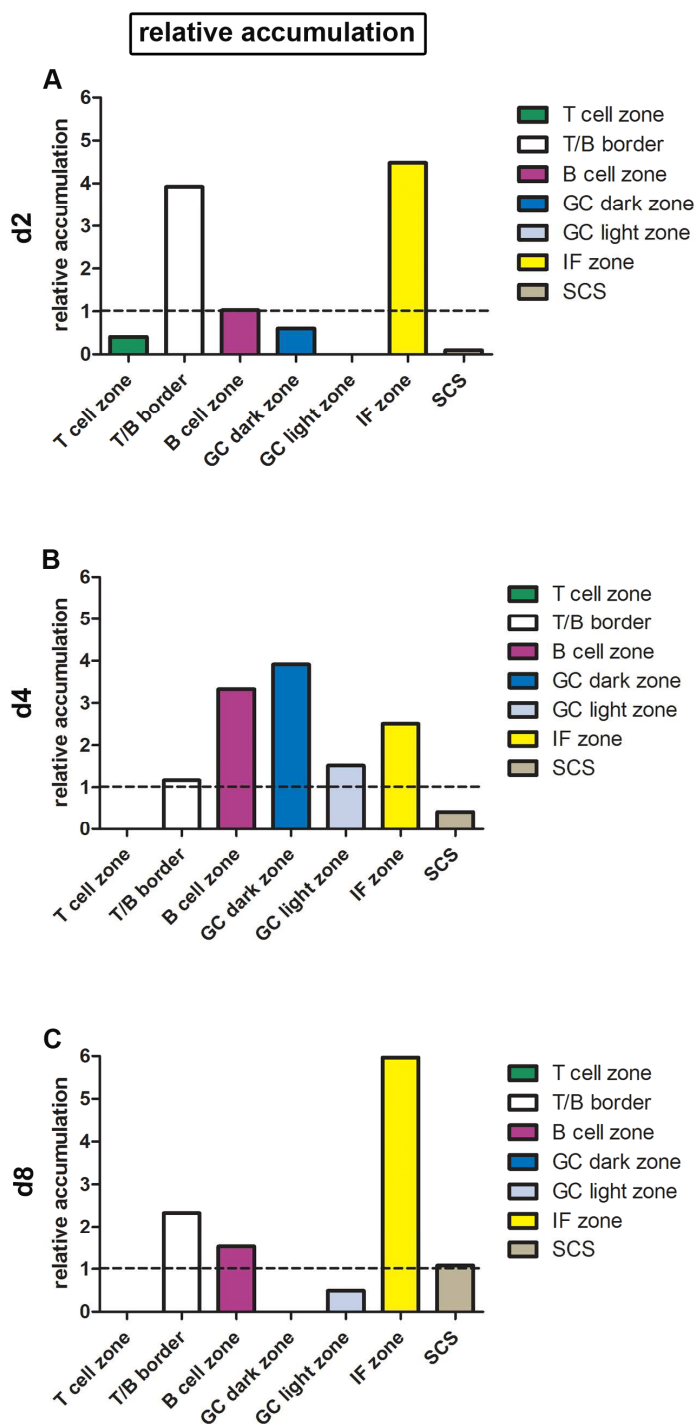


Figure 27: Relative accumulation of donor B cells within lymph node microenvironments at day 2 (A), 4 (B) and 8 (C) after transfer. To quantify cell homing of detected donor cells within lymph node compartments, counted cells in each zone in images from complete lymph node sections were fractioned and divided by the fraction of the area. Thereby, a value  $>1$  is regarded as enrichment.  $n=3$  for each time point.

Taken together, the evidence presented above suggests that within this transfer system the IF zone and the border between the follicle and T cell zone are the main sites of

accumulation of  $B220^+PNA^{lo}CD38^{hi}IgM^+$  cells throughout the first week. After 4 days a fraction of these cells enter the B cell follicle and get recruited to GC dark zone and light zone. However, the bulk of accumulation and proliferation within IF zone and along the B/T border precedes that of entering the GCs by approximately 2 days.

### 4.3 Migratory behavior of blood-derived B cell subsets after transfer into recipients at the time point after immunization

Introduction of different B cell subsets from mice with a fully established immune response into recipients with a beginning response clearly does not directly mimic conditions at the onset of a conventional immune response. As such, a second experiment was conducted to monitor the migratory behavior of GC derived B cell subsets with no obvious advantage in terms of their immunological state and antigen specificity. To mimic conditions at the onset of a conventional immune response transferred cells were retrieved from donor wild type animals challenged at the same time point as their corresponding recipients. This enrichment procedure allowed us to transfer in each experiment  $\sim 6,000$  GC B cells,  $3,000$   $IgG1^+$  and  $9,000$   $IgM^+$  B cells respectively.

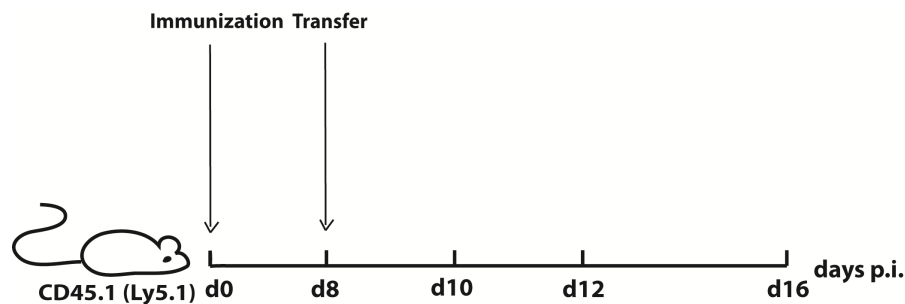


Figure 28: Experimental setup for the used transfer system.  $GC^+B$  cells,  $IgM^+$  or  $IgG1^+CD38^+$  blood-derived potential memory B cells were FACS-sorted from  $CD45.2^+$  mice 8 d p.i. with NP-KLH in alum and adoptively transferred into  $CD45.1^+$  recipients, 8 d after immunization, respectively. Spleen, bone marrow and mesenteric lymph nodes were harvested 2, 4 and 8 days later and prepared for FACS analysis or histology.

---

### **4.3.1 Transferred GC B cells and IgM<sup>+</sup> B cells proliferate 2 days after transfer in spleen and bone marrow but decrease in numbers afterwards, whereas IgG1<sup>+</sup> B cells are only detected in bone marrow and remain there at stable frequencies**

We sought to gain a comprehensive view of the migration and potential proliferation of different GC derived B cell subsets by transferring them and tracing their fate in terms of their localization and expression of different markers in secondary lymphoid organs throughout the primary immune response. Adoptive transfer of GC or IgM B cells revealed that 2 days after transfer approx. 0.06% of total gated lymphocytes in spleen belonged to the donor population (Figure 29). This frequency dropped at later time points, as finally after 8 days 0.002% of detected lymphocytes were donor specific. In contrast, the frequencies of CD45.2<sup>+</sup> cells located in bone marrow were rather stable until 8 days after transfer.

Isotype-switched CD45.2<sup>+</sup> cells were undetectable in  $6 \times 10^6$ -cell samples from  $10^8$  splenic lymphocytes of recipients which had received IgG1<sup>+</sup> B cells. However, these cells were found in the bone marrow as soon as 4 days after transfer and their frequencies did not decline.

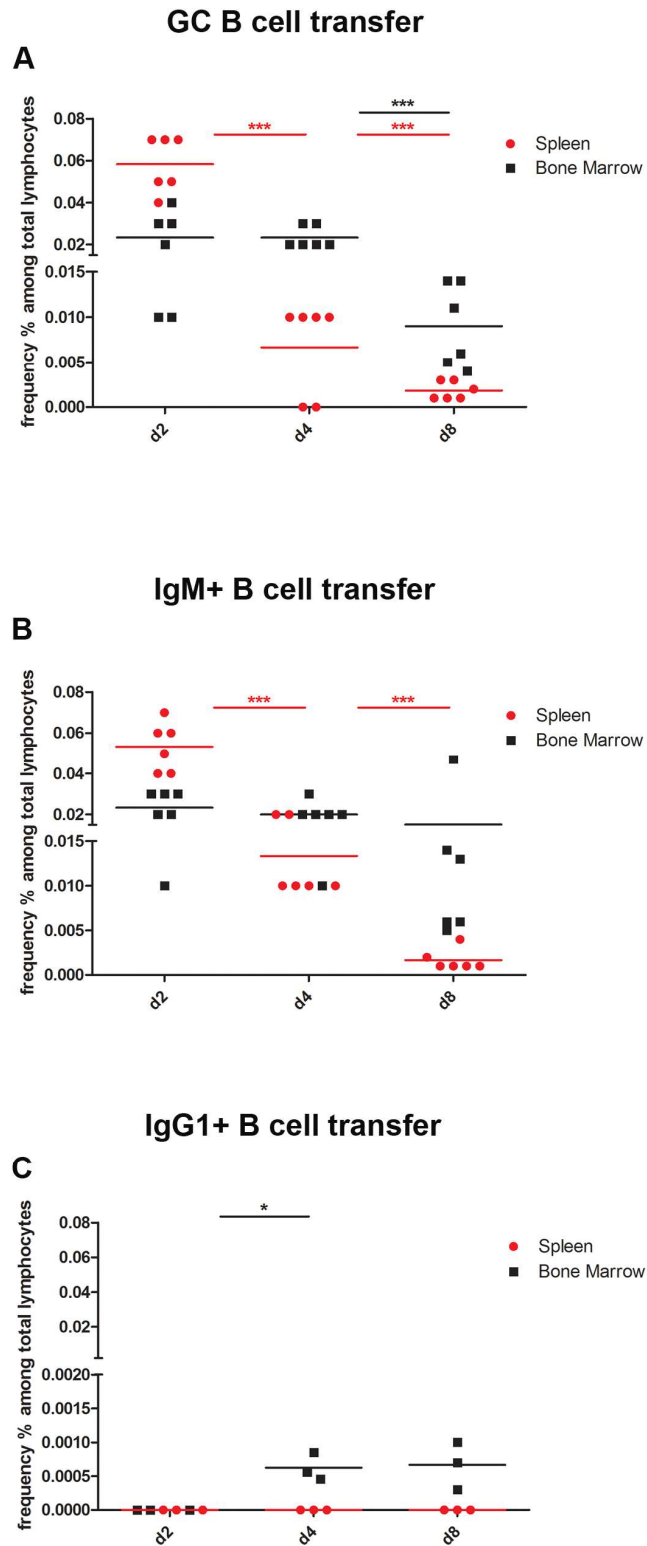


Figure 29: Frequencies of detected donor cells among gated lymphocytes in spleen (red dots) or bone marrow (black squares) after GC (A), IgM (B) or IgG1 B cell transfer (C) at 3 time points after transfer are shown. Spleen and bone marrow of recipients were harvested, prepared for FACS analysis and frequencies of  $CD45.2^+CD45.1^-$  cells among  $6 \times 10^6$  cells within the lymphocyte FSC/SSC gate were determined.



To get a better insight into the dynamics of the migration of transferred B cell subsets in terms of their survival and proliferation, absolute numbers of detected donor cells within the spleen and bone marrow were estimated. Retrieved data from the NP-KLH specific kinetic and previous observations indicate that lymphocyte numbers in secondary lymphoid organs do not depend on the state of immune response, but rather vary with the size and age of animals (Cesta, 2006 and own data not shown). Therefore, absolute numbers of donor cells were calculated by using the mean of all measured animals at all analyzed time points after primary immunization. For estimation of donor cell numbers within the bone marrow compartment, the mean of measured lymphocyte numbers of femur, tibia, hip, breastbone, cranium, shoulder and spine were used.

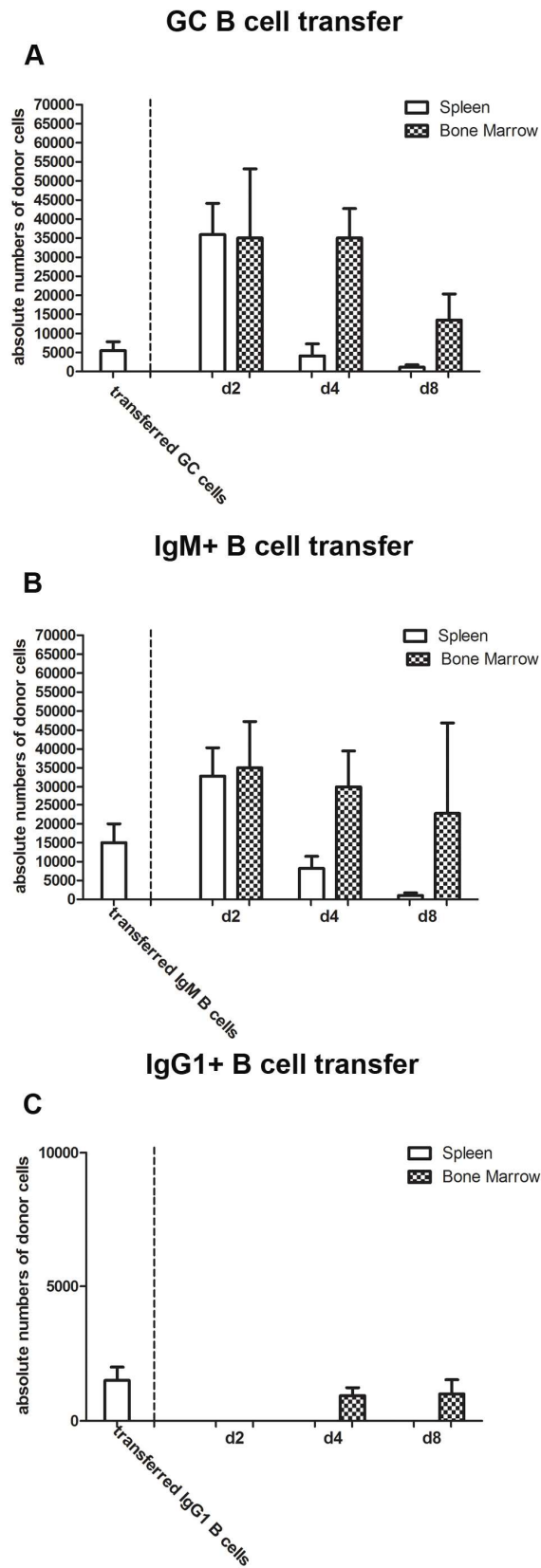


Figure 30: Estimation of absolute donor cell numbers in spleen and bone marrow after GC (A), IgM<sup>+</sup> (B) or IgG1<sup>+</sup> (C) B cell transfer. Combined data from multiple experiments show the estimated absolute

numbers of transferred donor B cell subsets in each experiment (first bar from left) compared to detected donor cell numbers in spleen and bone marrow during 8 days. The mean and SD are shown for each time point (n=3).

The number of detected donor cells in spleen and bone marrow increased 11-fold compared to the originally transferred level as soon as 2 days after the GC and IgM<sup>+</sup> B cell transfer (Figure 30). In contrast to the 8-fold decrease of numbers in spleen, the located donor cell population in bone marrow did not alter significantly after 4 days. However, after 8 days the donor cell population in this compartment was declined to 50%, even though to a lesser extent compared to the IgM B cell transfer. However, even at the latest time point of analysis in both transfers ultimately more cells were detected than originally transferred (Figure 29, Figure 30). Contrary to the previously described transfer systems, IgG1<sup>+</sup> donor B cells were detectable only within the bone marrow compartment after 4 days and did not substantially change in numbers after 8 days.

Taken together, these data show that B cells bearing GC phenotype and IgM<sup>+</sup>CD38<sup>+/high</sup> from blood are capable of immigration into spleen and bone marrow. Once arrived within the secondary lymphoid organs, they proliferate up to 11-fold numbers within 2 days, followed by a strong decrease in numbers within the spleen but less in the bone marrow at the following 6 days. Transferred IgG1<sup>+</sup> B cells only appear at a detectable level within the bone marrow compartment as early as 4 days after transfer and remain at unchanged numbers at least until day 8.

#### **4.3.2 Transferred blood GC B cells home to secondary lymphoid organs, partially keep their phenotype but mainly differentiate further and induce a short lived plasma cell response**

To gain an extensive view on the migration and differentiation pattern of transferred GC B cells their phenotype was analyzed by investigating the expression and distribution of selected cell surface markers within the CD45.2<sup>+</sup>CD45.1<sup>-</sup> cell compartment (Figure 31) at consecutive time points following transfer.

As shown in Figure 32 after 2 days, approximately 5% of donor cells in spleen were found to express a GC phenotype. In addition, transferred GC B cells gave rise to a population of IgG1<sup>+</sup> B cells located in spleen and bone marrow. Nonetheless, the majority of detected cells expressed IgM and bound low amounts of PNA. Despite the expansion of GC derived B cell subsets a discrete population of plasmablasts, defined

by the expression of CD138, CD22.2, Kappa or Lambda and B220 was detected with a frequency of 5-10% in spleen and bone marrow.

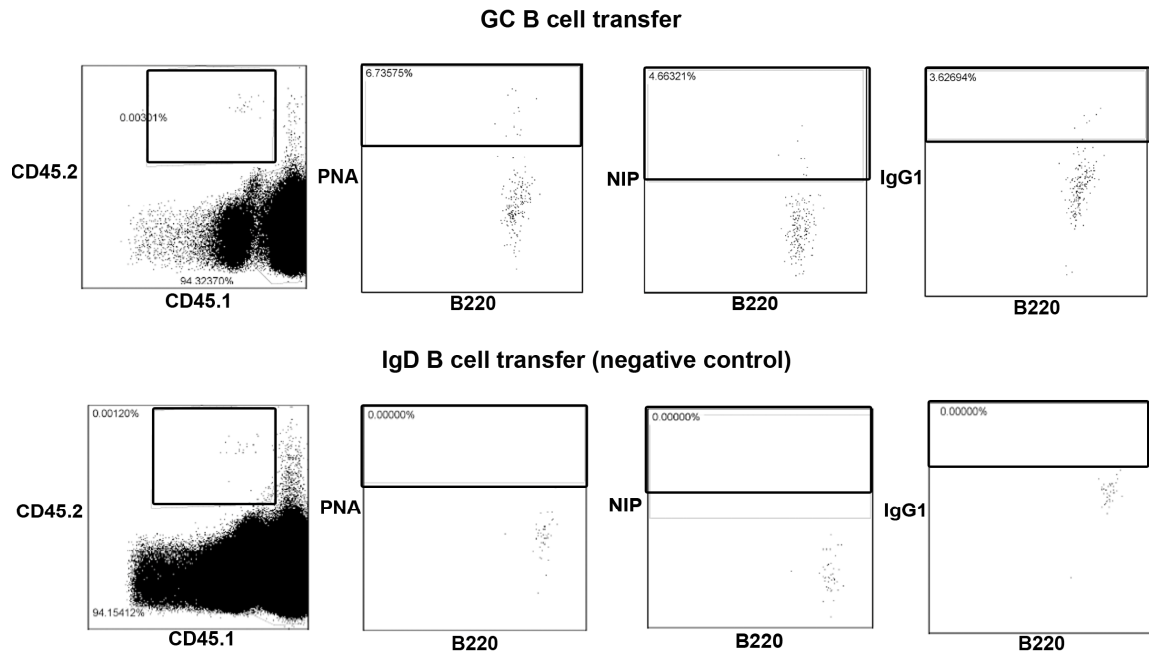


Figure 31: Analysis of the expression of detected donor B cells in spleen and bone marrow. Organs were harvested and prepared for FACS analysis. Single cell suspensions from whole spleen and bone marrow were stained with different antibodies. Donor cells were detected among the lymphocytes and analyzed for the expression of B220, PNA, NIP and IgG1. Representative plots of the applied gating strategy for detected donor cells in spleen after IgD B cell transfer as a negative control and GC B cell transfer after 4 days are shown.

After 4 days the composition of donor B cell subsets underwent substantial changes. While the frequency of GC B cells remained rather stable, the plasmablasts had almost disappeared in favor of a newly-observed population of plasma cells in spleen and bone marrow which represented up to 20% of total donor cells. Taking into account that the absolute numbers of donor cells in bone marrow remained constant until day 4 (Figure 30), we concluded that the arisen plasma cells likely had differentiated from previously detected plasmablasts. 8 days after transfer a slightly smaller fraction of donor cells still displayed a GC B cell phenotype; however, for the first time switched GC B cells could be assessed at detectable numbers. Consistent with this observation, also the B220<sup>+</sup>IgG1<sup>+</sup> subset reached a maximum of 10% among the donor B cell populations in spleen and bone marrow 8 days after transfer. Notably, by this time, the donor B cell fraction was determined to consist of only a minority of plasmablasts and plasma cells in spleen. Correspondingly, thorough characterization of resident donor cells in bone

marrow revealed a diminishing plasma cell response after 8 days, suggesting a rather short term plasma cell response (Figure 32).

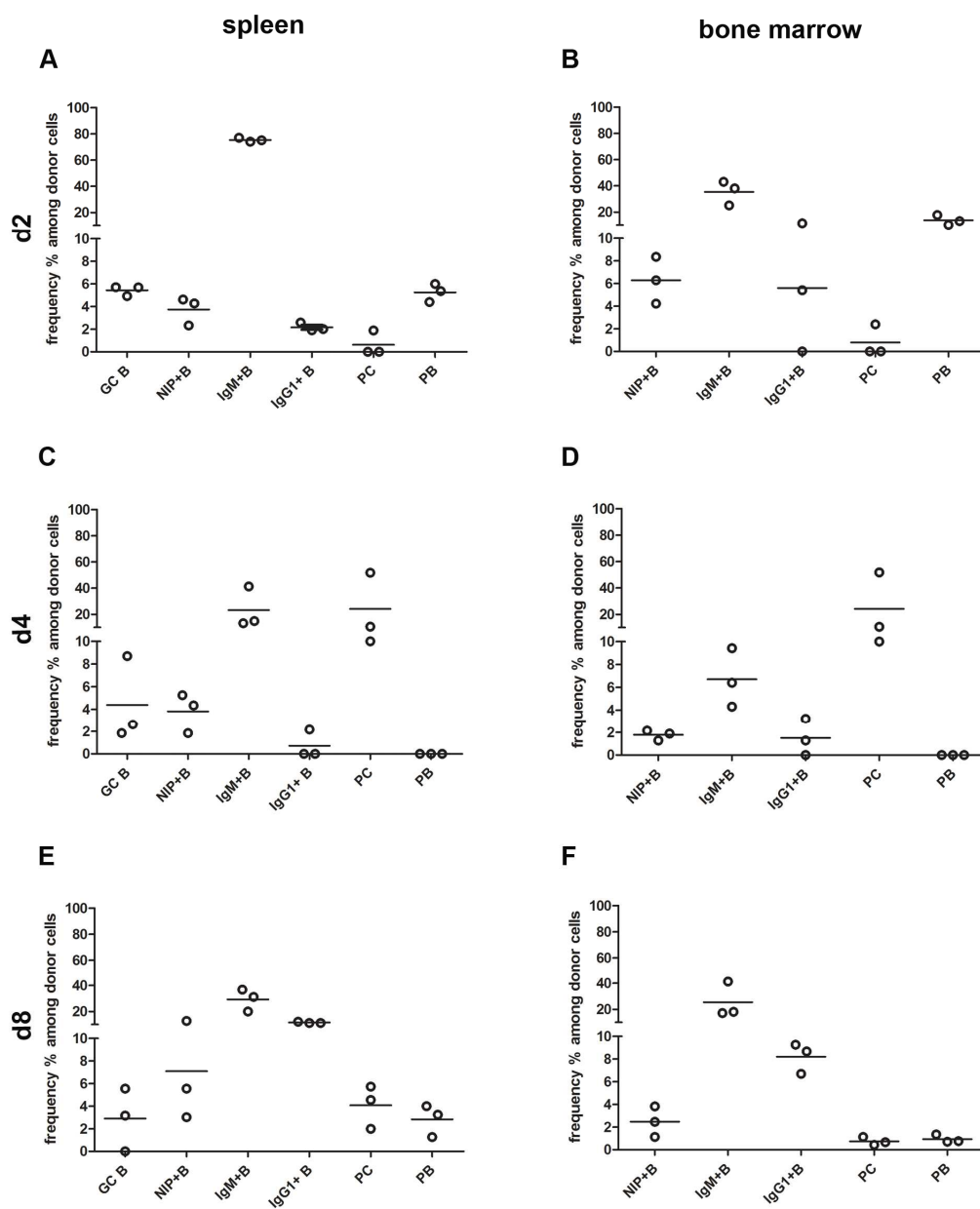


Figure 32: Kinetic and differentiation of transferred GC B cells. Whole spleen, femur and tibia of recipients were isolated 2-8 days after transfer, harvested and stained with CD45.1, CD45.2, B220, PNA, NIP, IgG1, CD22.2, CD138, Lambda and Kappa antibodies. Relative frequencies of GC, IgM<sup>+</sup>, IgG1<sup>+</sup> B cells and plasma cells as well as plasmablasts within donor cells detected in samples of  $6 \times 10^6$  cells from spleen (left) and bone marrow (right) 2 days (Figure A, B), 4 days (Figure C, D) or 8 days (Figure E, F) after transfer are shown. Three mice were analyzed for each transfer at each time point.

### 4.3.3 Transferred blood residing IgM<sup>+</sup>CD38<sup>+</sup> B cells can regain a GC phenotype for a few days and induce a strong short lived plasma cell response

To further substantiate the characteristics and capabilities of blood-derived IgM<sup>+</sup>CD38<sup>+</sup>PNA<sup>lo-neg</sup> B cells, a kinetic of their surface marker expression profile after transfer was assessed during multiple time points at the early phase of primary immune response. More than 70% of detected donor B cells in the spleen had not changed their isotypes at the two following days after transfer (Figure 33). However, about 5% of the CD45.2<sup>+</sup>CD45.1<sup>-</sup> fraction displayed a GC B cell phenotype. This subset originated from a high-purity previously injected IgM<sup>+</sup>CD38<sup>+</sup>PNA<sup>-</sup> population which apparently regained the GC B cell phenotype in spleen. As expected, this population was absent in the bone marrow compartment at all analyzed time points. In contrast to transferred GC B cells, the IgM<sup>+</sup> B cell derived GC B cell population vanished by day 8 after transfer (Figure 33), suggesting these cells to have a rather short term capability to acquire a GC phenotype. Despite the early diminution of the donor GC compartment, transfer of IgM<sup>+</sup> B cells resulted in a strong plasma cell response, with respect to the frequencies of other subsets, particularly among the spleen residing donor cells. Four days after transfer, more than half of the detected donor cells in the spleen displayed a plasma cell phenotype (Figure 33). The subtle variance of absolute cell numbers during 4 days after transfer implies their development from the previously detected plasmablast subset. Another difference between the two transfer systems was the kinetic of IgG1 B cells; unlike transferred GC B cells switched donor cells to IgG1 were not detected in the spleen before day 8 after IgM B cell transfer. However, irrespective of slightly lower frequencies, the kinetic of bone marrow residing donor IgG1 B cells was comparable to the GC B cell transfer data (Figure 32, Figure 33).

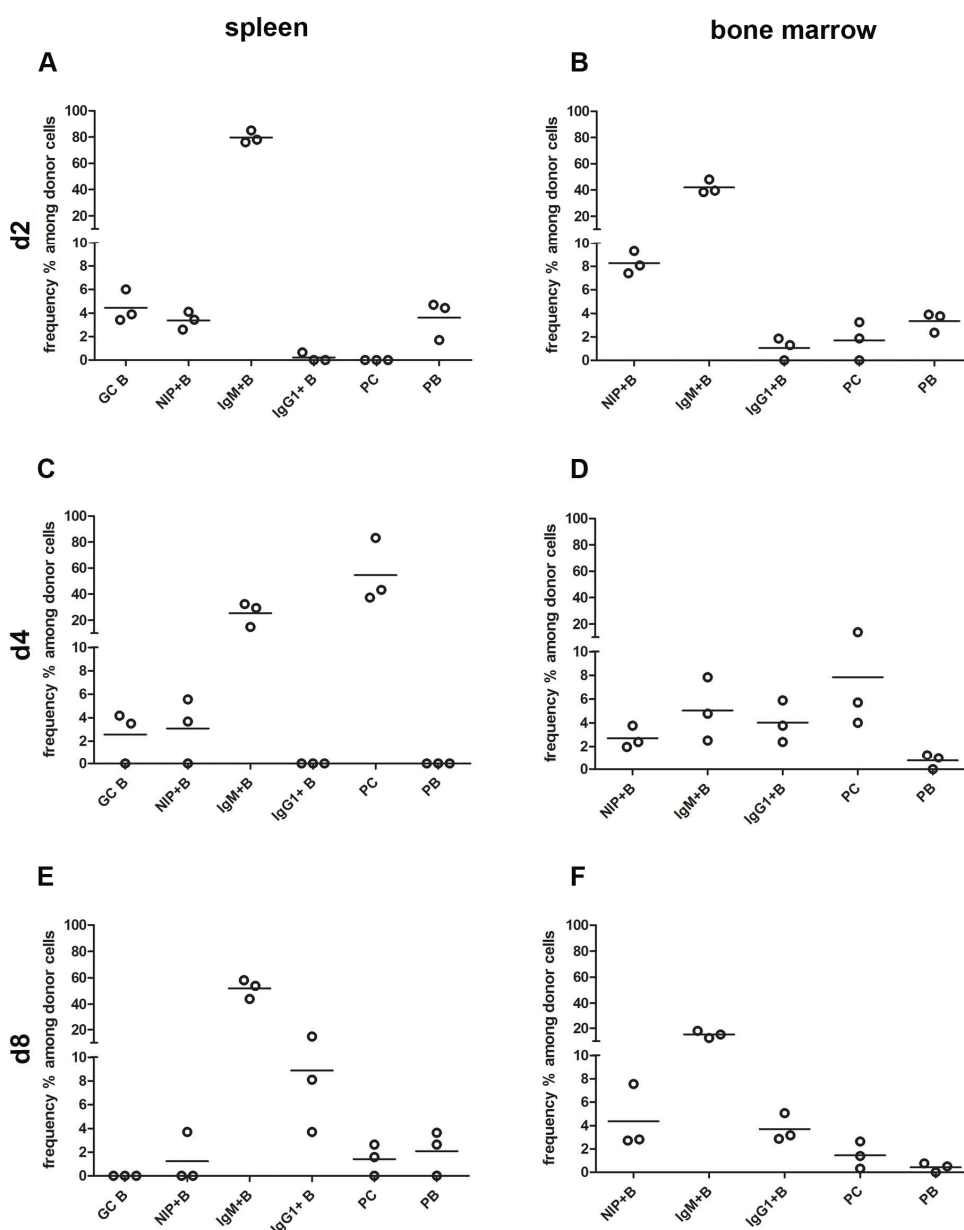


Figure 33: Kinetic and differentiation of transferred  $\text{IgM}^+$  B cells. To quantify the composition of donor B cell subsets whole spleen, femur and tibia of recipients were isolated 2, 4 and 8 days after transfer, harvested and stained with CD45.1, CD45.2, B220, PNA, NIP, IgG1, CD22.2, CD138, Lambda and Kappa antibodies. Relative frequencies of GC,  $\text{IgM}^+$ ,  $\text{IgG1}^+$  B cells and plasma cells as well as plasmablasts within donor cells detected in samples of  $6 \times 10^6$  cells from spleen (left) and bone marrow (right) 2 days (A, B), 4 days (C, D) or 8 days (E, F) after transfer are shown. Each data point represents one mouse. Three mice were analyzed in each group at each time point.

#### 4.3.4 Blood-derived IgG1<sup>+</sup> CD38<sup>+</sup> B cells accumulate in the bone marrow and change their surface expression of B220 at early time points of immune response

An interesting element of the NP-specific immune response is the isotype switch of post-GC B cells to IgG1 and their subsequent release in blood at early time points of the immune response (Blink, 2005). To address the question whether these cells display the same homing features as previously examined B cell subsets, IgG1<sup>+</sup>CD38<sup>hi</sup> B cells were enriched from blood of NP-KLH immunized mice (materials and methods) and transferred into recipients who were immunized synchronous with the donors. Spleen, bone marrow and mesenteric lymph nodes of recipients were harvested at consecutive time points after transfer and prepared for flow cytometry or histological sectioning. CD45.2<sup>+</sup> CD45.1<sup>-</sup> IgG1<sup>+</sup> B cells were detected among spleen and bone marrow samples and thoroughly analyzed for the expression of B220 and binding of NIP within 1 week after transfer (Figure 34). At none of the analyzed time points IgG1<sup>+</sup> donor B cells could be detected in spleen. Instead, a population of CD45.2<sup>+</sup> CD45.1<sup>-</sup> IgG1<sup>+</sup> donor cells was observed in the bone marrow as soon as 4 days after transfer. About 80% of these expressed B220 on their surface thus were clearly B cells. Within this population a fraction, comprising 20% of total donor cells were hapten-specific (Figure 34). The populations differed, however at day 8, in that IgG1<sup>+</sup> cells expressed lower amounts of B cell markers and failed to bind NIP, resulting in a ratio 3:2 of B220<sup>+</sup>:B220<sup>-</sup> cells. Taking into account the stable absolute numbers of donor cells in bone marrow and their absence in the spleen, it is reasonable to assume that indeed some cells including the NP-specific compartment disappeared as a result of apoptosis and a proportion of surviving IgG1<sup>+</sup> B cells further differentiated into a B220<sup>low/neg</sup> subset probably representing plasma cells.

Furthermore, an IgG1<sup>-</sup> donor B cell population appeared in spleen and bone marrow as early as day 2 after transfer (Data not shown). These cells were found within the lymphocyte gate on the forward and sideward scatter and partially expressed surface CD22.2. They did not display a GC phenotype at any analyzed time point and failed to bind NIP. Nevertheless, a fraction bound surface CD138 and down-regulated CD22.2 as early as 2d after transfer, suggesting them to be plasma cells. The frequency of these



IgG1<sup>-</sup> plasma cells increased by day 4 after transfer to 40% of the IgG1<sup>-</sup> donor B cell population but decreased to approx. 10% by day 8 after transfer.

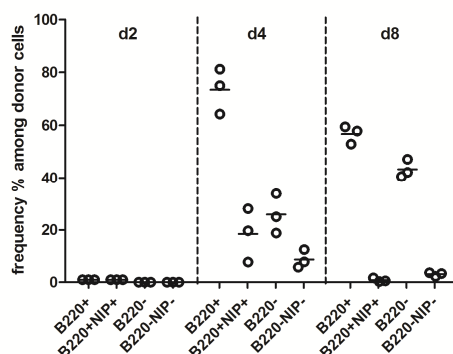


Figure 34: Kinetic and differentiation of transferred IgG1<sup>+</sup> B cells in bone marrow. Femur and tibia of recipients were isolated after 2, 4 and 8 days after transfer, harvested and stained with CD45.1, CD45.2, B220, NIP and IgG1 antibodies. Relative frequencies of B220<sup>+</sup>, B220<sup>-</sup>, hapten-specific or carrier-specific IgG1<sup>+</sup> donor cells in samples of  $6 \times 10^6$  cells from bone marrow after 2, 4 or 8 days after transfer are shown. Each data point represents one mouse.

Taken together, these data suggest the preferential migration of blood-derived B220<sup>+</sup>IgG1<sup>+</sup>CD38<sup>hi</sup> cells to the bone marrow compartment and their ability to differentiate into plasma cells over time.

#### 4.3.5 T cell associated proliferation of blood-derived GC B cells within the follicle precedes their migration to the GC dark zone followed by their recruitment to GC light zone

To monitor the migration of blood-derived GC B cells within secondary lymphoid organs mesenteric lymph nodes of recipients were harvested 2, 4 and 8 days after transfer, prepared for histological sectioning and localization of CD45.2<sup>+</sup> cells was determined with respect of the different areas of the organ. In particular, extensive series of consecutive sections of whole lymph nodes were conducted and stained with different antibody combinations. This procedure allowed us to obtain absolute numbers of migrated cells in mesenteric lymph nodes and allocate them to different identified regions based on follicular borders and the capsule (Figure 36), (Kerfoot et al., 2011). At day 2 after transfer, donor cells were dispersed as single or small aggregates of 2-3 cells within different regions of the B cell follicle but more in the area close to the SCS (Figure 35, Figure 36 A). Many of these were in direct contact with T cells and had undergone proliferation. Analysis of CD45.2<sup>+</sup> B220<sup>lo/neg</sup> Kappa<sup>+</sup> or Lambda<sup>+</sup> plasma

cells displayed their main localization at the outer borders of B cell follicle and within the medullar cords (Figure 36 B). By day 4, two major changes occurred. First, donor B cells were predominantly located within the B cell zone and the IF zone, built clusters with up to 30 cells (Figure 36 C, Figure 35). Notably, at this time point they had increased their absolute numbers up to 4 times, but analogous numbers to day 2 were in direct contact with T cells and Ki67<sup>+</sup>. Second, higher numbers of donor B cells were located within the dark zone of recipients, mainly in direct contact to Th cells. However, plasma cells were uniformly distributed between the outer follicle borders; the medullar cord and the border to SCS (Figure 36 D). 8 days after transfer, donor B cells were almost diminished in the dark zone and were also less observed in other areas of the follicle and IF zone, but appeared for the first time within the light zone (Figure 36 E). Parallel staining of serial sections showed that the Bcl-6 expression in donor cells completely underlies their localization within the GC, since Bcl-6 expression by donor cells was not evident in any other compartment of mesenteric lymph nodes. Hence, previous data confirm the participation of GC residing donor B cells in the ongoing germinal center reaction. Concurrent with the invasion of the light zone many donor B cells were detected for the first time at the B/T zone border (Figure 36 E). Although occasional CD45.2<sup>+</sup> cells could be found earlier in this zone, widespread localization of these cells was not evident before day 8 after transfer. Unlike the B cells, however, donor plasma cells disappeared from the B cell follicle at day 8 and were almost exclusively localized in the medullar cord and at the SCS border (Figure 36 F). Notably, at this time point the absolute numbers of donor derived plasma cells had been reduced, confirming the previously retrieved flow cytometric data from spleen (Figure 32).

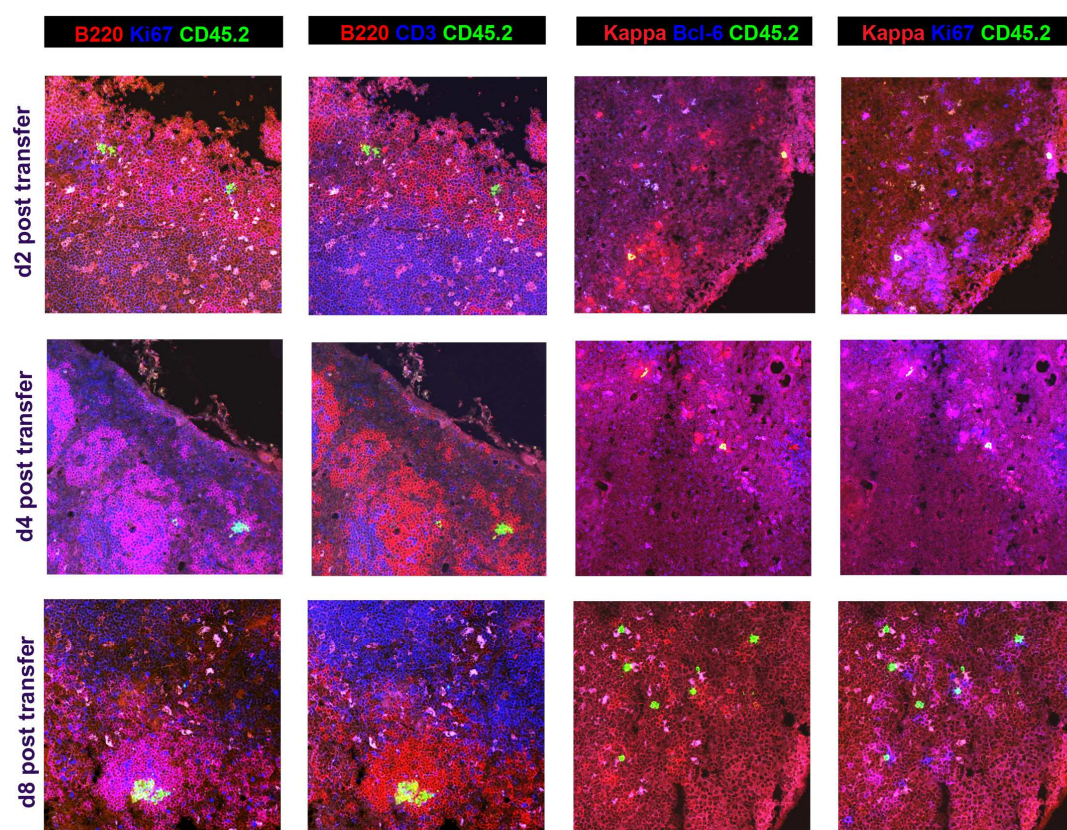


Figure 35: Migration and proliferation of B220<sup>+</sup>PNA<sup>hi</sup>CD38<sup>lo</sup> donor cells within different areas of mesenteric lymph nodes at early time points of immune response. B220<sup>+</sup>PNA<sup>hi</sup>CD38<sup>lo</sup> blood B cells were transferred as previously described. Mesenteric lymph nodes were harvested, consecutively sectioned and stained with 2 different antibody cocktails to visualize different areas of lymph nodes based on follicular borders and the SCS. The first two panels from left illustrate the location of donor cells (CD3, green) with respect of B cell zone (B220, red) and GCs (Ki67, blue) or the B cell zone (red) and the T cell zone (blue) at day 2, 4 and 8 after transfer. Panels on the 2 right columns of images show the result of staining of adjacent sections for the Ki67 proliferation or Bcl-6 expression (both in blue) of Kappa (red) donor plasma cells and B cells. Images are shown in 20x magnification. The data shown are representative of those obtained from at least three mice from each time point.

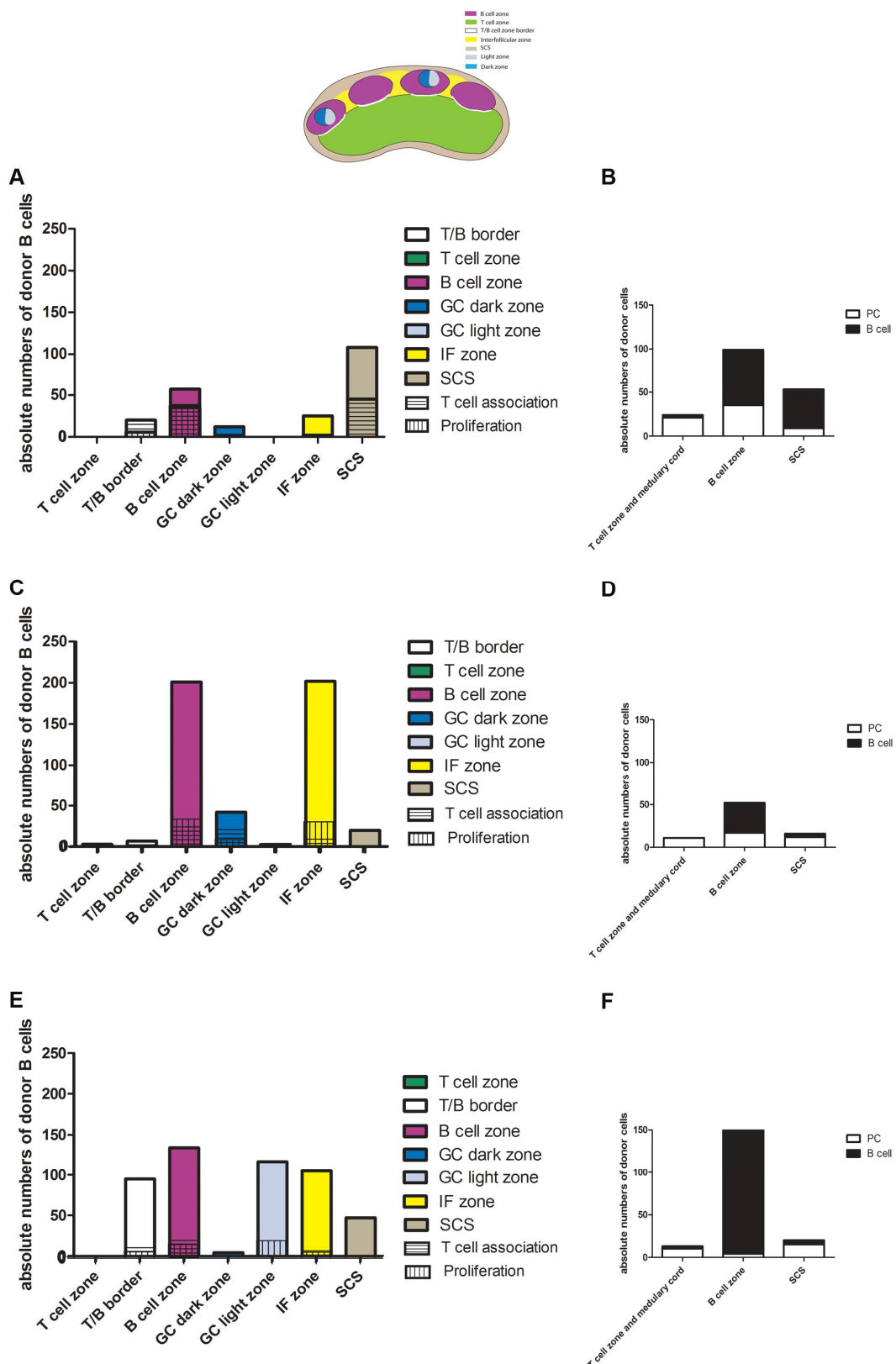


Figure 36: Migration of transferred GC B cells through mesenteric lymph node microenvironments at different time points of immune response. Consecutive sections were stained with B220, CD3, Ki67, Bcl-6, CD21, Kappa, Lambda and CD45.2 to identify different areas of lymph node based on their borders. The adjacent area to SCS was defined as the contiguous 100  $\mu$ m of the outer face of lymph nodes. An

---

area of 50  $\mu\text{m}$  width between B and T cell zone was determined as the B/T zone border. Homing of CD45.2<sup>+</sup> donor cells was quantified within the different pre-defined lymph node microenvironments. Donor B cells and plasma cells in each zone were counted in complete lymph nodes. Data show absolute numbers of counted donor B cells within different areas of 5 isolated mesenteric lymph nodes from 3 animals at 2 (A), 4 (B) and 8 days (C) after transfer. The right panel shows the calculated ratio of detected donor B cells versus plasma cells in medullar cord, B cell zone and the area close to SCS 2 days (B), 4 days (D) and 8 days after transfer (F).

Further quantification of donor B cell homing within lymph node microenvironments displayed a clear migration route of these cells and confirmed the previously described observations. By day 2 after transfer donor B cells clustered within the B cell zone, the IF zone and the adjacent area to the SCS, reflecting their initial entrance path through lymph node (Figure 37 A). 2 days later, a large number of donor B cells concentrated within the B cell zone and IF zone, suggesting an overall migration of the cells to the follicle (Figure 37 B). By this time, donor B cells had entered the GC dark zones for the first time but were absent from the GC light zone. At day 8 after transfer donor cells had left the dark zone and accumulated largely in the GC light zone (Figure 37 C). However, a fraction of donor B cells still accumulated outside the GCs and within the IF zone, although less exclusively than at day 4 after transfer. Additionally, donor B cells were enriched for the first time at the border between B and T cell zone suggesting their search for T cell help (Figure 37 C).

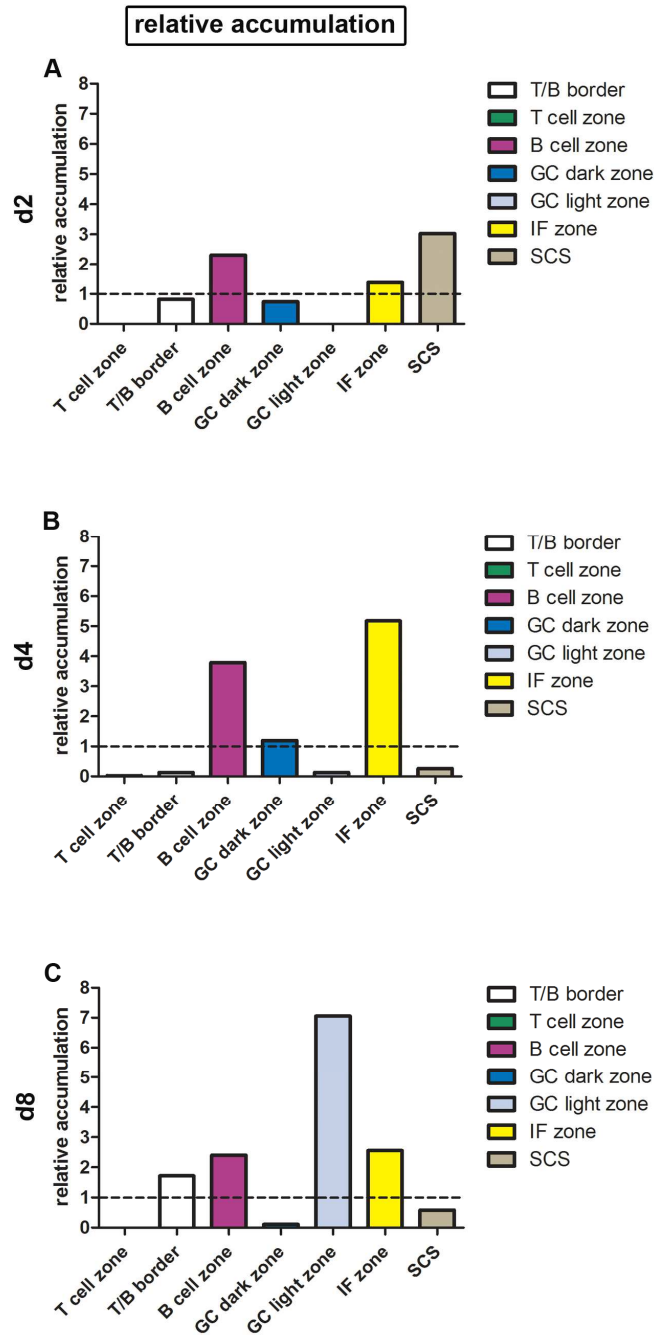


Figure 37: Relative accumulation of donor B cells within lymph node microenvironments at 2 (A), 4 (B) and 8 days (C) after transfer. To quantify cell homing of detected donor cells within lymph node compartments, counted cells in each zone in images from complete lymph node sections were fractioned and divided by the fraction of the area. Thereby, a value >1 is referred as enrichment. n=3 for each time point.

#### 4.3.6 The B cell follicle is the main assembly side of transferred blood-derived PNA<sup>lo</sup>CD38<sup>hi</sup>IgM<sup>+</sup> B cells

The evidence presented above suggested that the B cell follicle and particularly IF zone are sites of accumulation of blood-derived GC B cells prior to their recruitment into

GCs (section 4.3.5). Within this transfer system migration into the B cell follicle and proliferation were clearly associated with direct Th cell contact as proved by Bcl-6 staining. To address the question if the migration path of GC derived B cells underlies their developmental stage, PNA<sup>lo</sup>CD38<sup>hi</sup>IgM<sup>+</sup> B cells were transferred with the same procedure explained above and mesenteric lymph nodes of recipients were isolated and prepared for histology at different time points after transfer. Localization of donor B cells and plasma cells in consecutive sections were determined in different previously defined microenvironments (Figure 39) of lymph nodes. Histology study of transferred IgM<sup>+</sup> B cells 2 days after transfer revealed the B cell follicle as the major entry site of donor cells (Figure 38, Figure 39 A). About 30% of them were associated with T cells and a fraction of them was proliferating. Notably, the absolute numbers of detected donor cells at this time point were comparable to the scored donor cell numbers obtained from the GC B cell transfer. Similar to donor B cells, the largest numbers of plasma cells were observed within the B cell zone (Figure 39 B), although they were mainly assembled closer to the outer border of the follicle. Unexpectedly, after 4 days donor B cells almost had disappeared from the lymph nodes, except a few scattered cells within and around the follicle (Figure 38, Figure 39 C). Consistent with this observation, numbers of plasma cells were strongly reduced and exclusively residing close to the outer B cell follicle border (Figure 38, Figure 39 D). However, by day 8 clusters of Ki67<sup>+</sup> donor B cells appeared along the border to T cell zone, although some were also found within the B cell follicle and adjacent to the SCS. Similarly, numbers of located plasma cells along the SCS and within medullar cords increased, whereas numbers of the follicle residing plasma cell population tended to remain constant (Figure 39 E, F). Within this adoptive transfer system, B cell proliferation and differentiation was largely independent of participation in the ongoing GC reaction, as indicated by the fact that no evidence of GC formation or expansion of the donor B cell population was observed until 8 days after transfer.

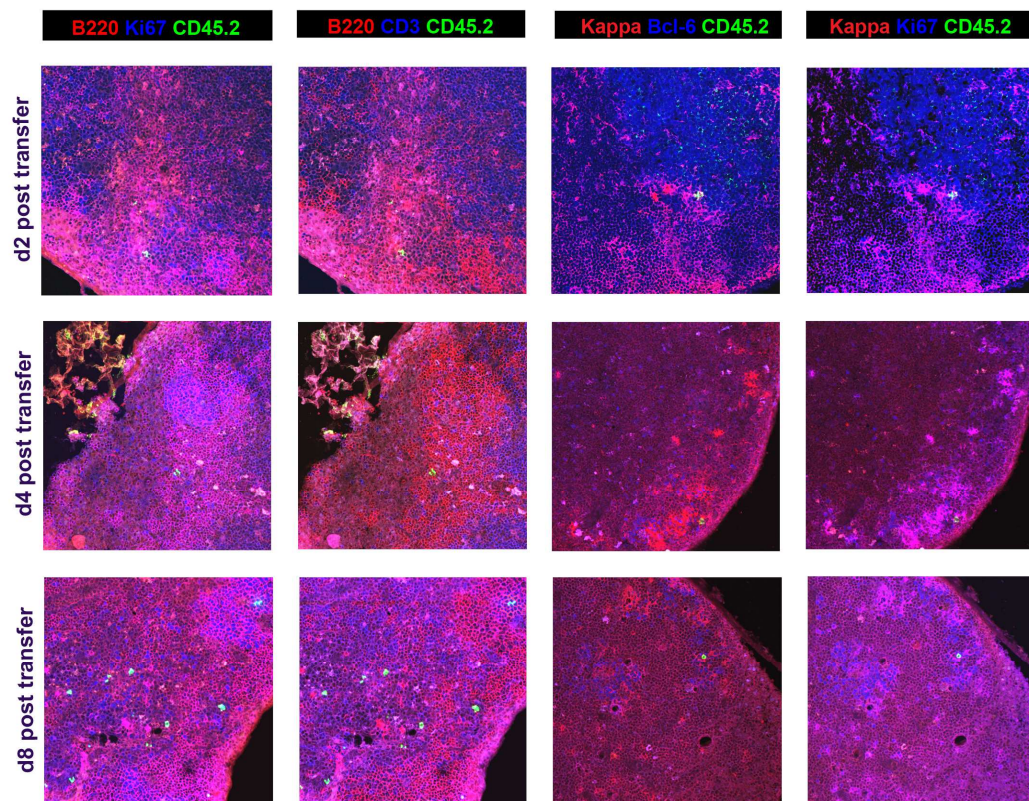


Figure 38: Migration and proliferation of  $B220^{+}PNA^{lo}CD38^{+}IgM^{+}$  donor cells within different areas of mesenteric lymph nodes at early time points of immune response.  $B220^{+}PNA^{lo}CD38^{+}IgM^{+}$  blood B cells were transferred as previously described. Mesenteric lymph nodes were harvested, consecutively sectioned and stained with 2 different antibody cocktails to visualize different areas of lymph nodes based on follicular borders and the SCS. The first two panels from left illustrate the location of donor cells (CD45.2, green) with respect of B cell zone (B220, red) and GCs (Ki67, blue) or the B cell zone (red) and the T cell zone (blue) at day 2, 4 and 8 after transfer. Panels on the 2 right columns of images show the result of staining of adjacent sections for the Ki67 proliferation or Bcl-6 expression (both in blue) of Kappa (red) donor (green) plasma cells and B cells. Images are shown in 20x magnification. The data shown are representative of those obtained from at least three mice from each time point.



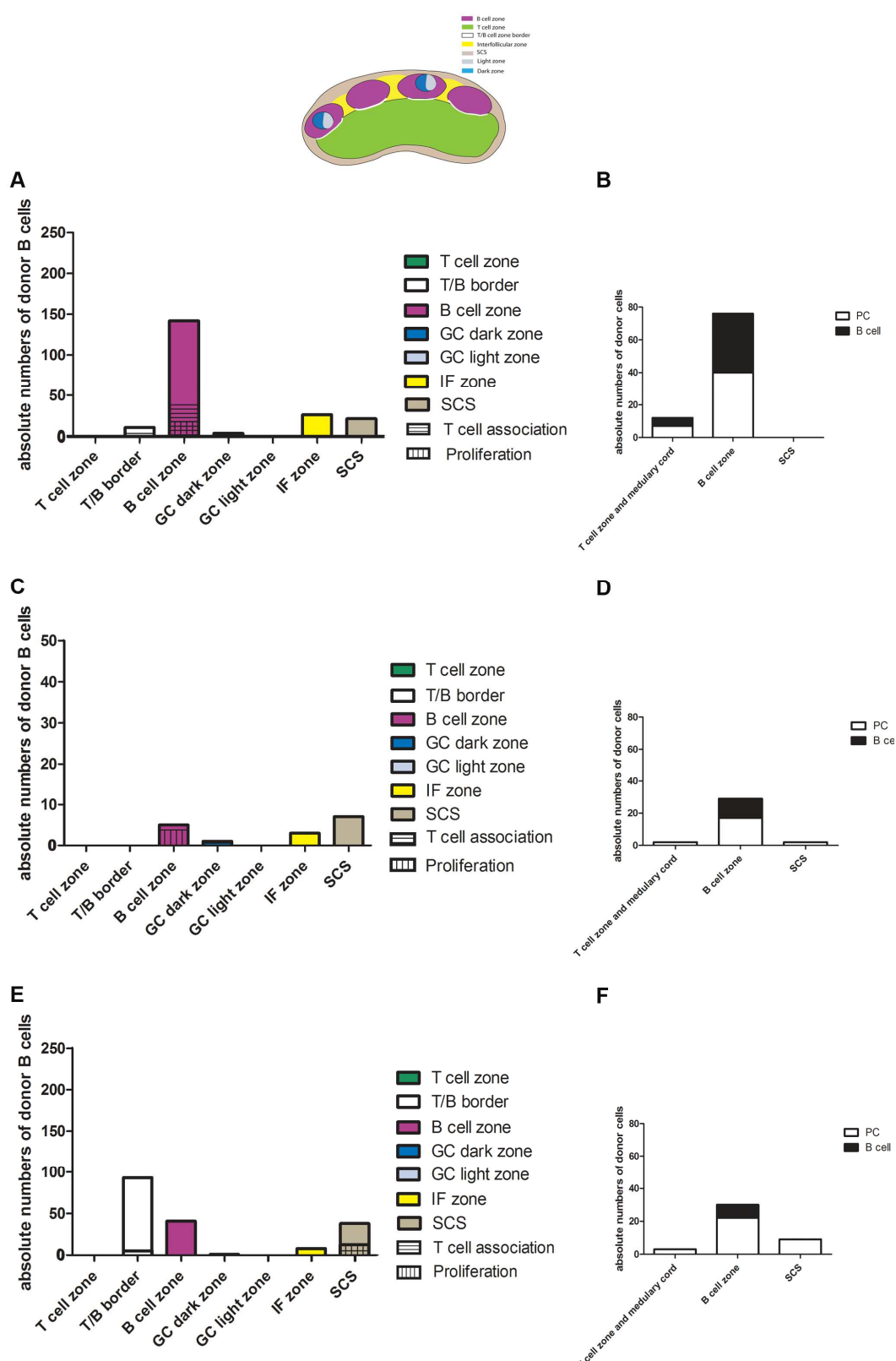


Figure 39: Migration of transferred IgM<sup>+</sup> B cells through mesenteric lymph node microenvironments at different time points of immune response. Consecutive sections were stained with B220, CD3, Ki67, Bcl-6, CD21, Kappa, Lambda and CD45.2 to identify different areas of lymph node based on their borders. The adjacent area to SCS was defined as the contiguous 100  $\mu$ m of the outer face of lymph nodes. An

area of 50  $\mu\text{m}$  width between B and T cell zone was determined as the B/T zone border. Homing of  $\text{CD45.2}^+$  donor cells was quantified within the different pre-defined lymph node microenvironments. Donor B cells and plasma cells in each zone were counted in complete lymph nodes. Data show absolute numbers of counted donor B cells within different areas of 5 isolated mesenteric lymph nodes from 3 animals at 2 (A), 4 (B) and 8 days (C) after transfer. The left panel shows the calculated ratio of detected donor B cells versus plasma cells in medullar cord, B cell zone and the area close to SCS 2 days (B), 4 days (D) and 8 days after transfer (F).

As shown in Figure 40, transferred  $\text{IgM}^+$  B cells displayed a different migratory behavior than GC B cells (Figure 37). Within 2 days, donor  $\text{IgM}^+$  B cells had entered the follicle area and predominantly clustered within the B cell zone and IF zone (Figure 40 A). However, by day 4 after transfer the relative accumulation of donor cells within the B cell zone decreased while they became enriched adjacent to the SCS. This process was accompanied by a diminution of the absolute numbers of detected donor B cells (Figure 40 B). At day 8 after transfer donor B cell numbers had increased 4 fold and in addition to clusters within the B cell zone, a fraction of donor B cells aggregated at the T/B cell border (Figure 40 C).

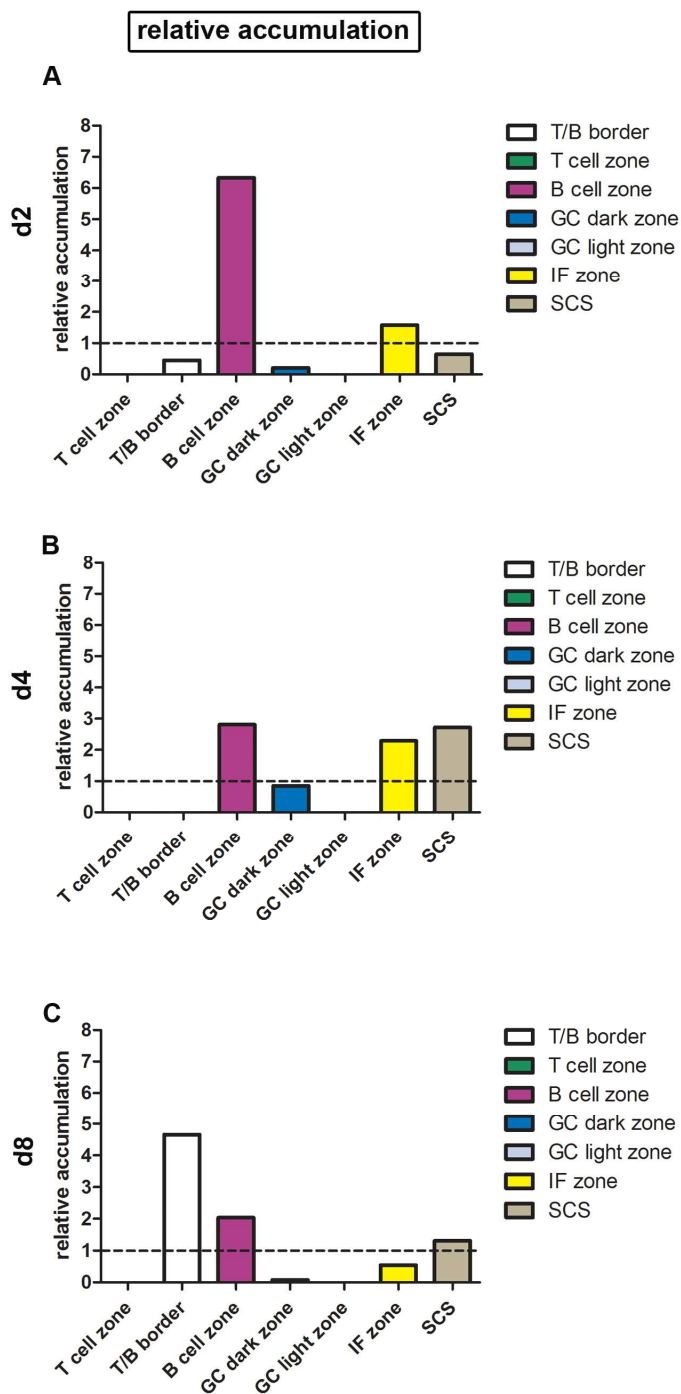


Figure 40: Relative accumulation of donor B cells within lymph node microenvironments at day 2 (A), 4 (B) and 8 (C) after transfer. To quantify cell homing of detected donor cells within lymph node compartments, counted cells in each zone in images from complete lymph node sections were fractioned and divided by the fraction of the area. Thereby, a value  $>1$  is regarded as enrichment.  $n=3$  for each time point.

## 5 Discussion

### 5.1 Kinetic of NP-KLH induced B cell subsets by analysis of their expression profile of cell surface markers after primary and secondary challenge

A number of previous studies have used flow cytometry or immunofluorescence microscopy to assess the NP specific immune response in C57BL/6 mice (Nossal and Tarlinton, 1996; Blink, 2005; Wolniak et al., 2006). These studies used a panel of markers to delineate either GC B cell populations or described the differentiation of cells dedicated to the plasma or memory B cell pool and were mainly confined to *one* lymphoid organ. However, a kinetic of B cell subsets after multiple challenges, including *different organs* has not yet been published so far. This investigation allowed the delineation of populations corresponding to distinct stages of GC B cell differentiation to memory B cells, plasmablasts and plasma cells. Furthermore, previously undescribed subsets were identified and assigned to different stages of GC B cell ontogeny within the corresponding organ.

#### 5.1.1 Identification of the GC B cell subset

Antigen driven peripheral B cell maturation in the mouse goes along with profound changes of their cell surface marker profile. In secondary lymphoid organs, activated B cells participating in the GC reaction are identifiable by binding high amounts of PNA (Rose et al., 1980; Kraal et al., 1982) and the downregulation of surface CD38 (Ridderstad and Tarlinton, 1998). Previous studies have uncovered extensive information regarding molecules that are typically expressed by murine GC B cells, hence can alternatively be used for their identification such as GL7 and CD95 (Martinez-Valdez et al., 1996; Cervenak et al., 2001). However, it was shown that the B220<sup>+</sup>PNA<sup>hi</sup> B cell subset is congruent with the identified GL7 and CD95 expressing cells (Shinall et al., 2000). The flow cytometric and immunofluorescence analyses in this work revealed the same result (data not shown). Therefore, B220, PNA and CD38 were used to identify the GC B cell population.

### 5.1.2 Kinetic of the GC B cell subsets

Consistent with previous studies (Wolniak et al., 2006), hapten-specific GCs appeared as soon as 4 days after primary immunization in the spleen and mesenteric lymph nodes, increased at day 8-16 and slightly declined until d50. Comparison of primary and secondary challenge revealed that aside from the earlier increase of the GC B cell subset after secondary challenge; their frequencies largely resembled the obtained GC B cell frequencies during primary challenge. The lymphocyte numbers in the spleen, however, exceeded the number calculated after the primary challenge. Thus, it appears that a secondary immunization essentially leads to a stronger response in terms of absolute GC B cell numbers. In order to delineate the GC B cell population, the GC B cells were divided into discrete subsets based on the expression of surface Ig (IgM or IgG1), binding to NP and the expression of the differentiation marker CD38.

Analysis of 5 consecutive time points during primary and secondary response revealed that throughout the GC reaction, expression of CD38, IgM, IgG1 and binding to NIP did not change significantly. However, frequencies of IgG1<sup>+</sup> and NP specific GC B cells were significantly higher than those of naïve animals from day 8 after primary and day 4 after secondary challenge. Throughout both responses, IgM was the major isotype expressed on GC B cells. Our results are in accordance with Wolniak and colleagues (Wolniak et al., 2006).

The specificity of the NP-KLH immune response was also verified by enumeration of NIP binding B cells after primary and secondary challenge. A population of NIP binding B cells appeared as early as 4 days after immunization in spleen and blood and increased in numbers as the response progressed. Induction of a secondary response led to the detection of higher numbers of NIP binding B cells. Immunofluorescence staining confirmed the formation of NP-specific GCs to be restricted to the NP-KLH immunized mice, as they were absent in naïve animals. However, GCs were also occasionally detected in naïve controls, reflecting the SPF conditions of the stock breeding.

### 5.1.3 Identification of the memory B cell subset

The murine memory B cell response has been the subject of lot of discussions in the past decades. Although many studies have suggested several characteristics to describe the memory B cell subset, there is no ultimate defining set of surface markers in the mouse which is in contrast to the well defined B220<sup>+</sup>CD27<sup>+</sup> human memory B cells (Lanzavecchia et al., 2006). Nevertheless, it has been widely accepted that murine memory B cells express B220, are antigen specific and contain V genes with somatic mutations consistent with a GC origin (Tarlinton, 2008). Furthermore, Tarlinton and colleagues have suggested CD38 as a marker to segregate memory B cells from other subsets, since restoration of CD38 levels is coincidental with the transition from GC to memory B cell. Another feature of NP-KLH induced memory B cells is the expression of surface IgG1; however, several reports suggest the formation of an IgM<sup>+</sup> memory subset (White and Gray, 2000; Nojima et al., 2011), upon immunization with different antigens. Therefore, in this work, murine memory B cells were defined as mononuclear cells, bearing the consensus B220<sup>+</sup>PNA<sup>lo</sup>CD38<sup>+</sup>IgG1<sup>+</sup> or IgM<sup>+</sup> phenotype.

### 5.1.4 Kinetic of the memory B cell subsets

In all analyzed organs, the majority of CD38<sup>+</sup> B cells were found to express surface IgM and their relative frequencies did not change appreciably over the ensuing 7 weeks of the primary and secondary response. Quantification of the kinetic and distribution of the IgG1 expressing potential memory B cell subset was in accordance with this finding. During both described immune responses, relative frequencies of isotype-switched cells underwent only minor changes. Induction of a secondary response did not give rise to a higher frequency, but led to an earlier emerge of IgG1<sup>+</sup> memory cells. The mainly unchanged frequencies presumably indicate that isotype switching occurs continuously throughout the GC response. If so, the formation and lifespan of these subsets must underlie a regulatory mechanism that would maintain equilibrium between the IgM and IgG1 cells. Alternatively, the stable frequencies can be explained by a longer lifespan of the B220<sup>+</sup>PNA<sup>lo</sup>CD38<sup>+</sup>IgG1<sup>+</sup> subset with probably no further differentiation in the sense of changing their phenotype. This would imply that an isotype switch appears at a very early time point of the GC response and is allowed to occur during a very short time frame. Once switched, such cells would not alter their surface marker expression profile

throughout the whole response. However, it remains unclear why these cells appear in the blood at a very early time point. While the current data do not address these possibilities directly, some observations can be made which will be described in the following sections.

### **5.1.5 Identification of the plasmablast and plasma cell subsets**

An important part of the immune response to the antigen is the production of antibodies. These are initially produced by plasma cells from extrafollicular foci found in secondary lymphoid organs such as the spleen and lymph nodes and are generally of low affinity (Jacob et al., 1991). Such antibodies are crucial for neutralization of the antigen (Ridderstad and Tarlinton, 1998). In the next step, the GC reaction generates high affinity antibody secreting plasmablasts and plasma cells (MacLennan, 1994). B cells committed to the plasma cell differentiation pathway are reported to down-regulate surface Ig, B220 and MHCII and acquire other cell surface molecules such as CD138 (Smith et al., 1996). In this population, dividing antibody forming plasmablasts and non proliferating antibody forming plasma cells can be distinguished by B220 and MHCII expression (Manz et al., 1998). Furthermore, these two subsets differ in their expression levels of CD22.2 (William et al., 2005). Whereas plasmablasts express high amounts of surface CD22.2, this marker is down regulated on differentiated plasma cells (section 4.1.4). In the present study, the mentioned markers above were combined for the first time, defining the  $B220^+CD138^+CD22.2^+MHCII^+Lambda/Kappa^{hi}$  cells as plasmablasts, and the  $B220^-CD138^+CD22.2^-MHCII^-Lambda/Kappa^{hi}$  subset as plasma cells.

### **5.1.6 Kinetic of the plasmablast and plasma cell subsets**

In this work, the plasma cell and plasmablast kinetic was conducted and the phenotypic forms they and their precursors may take were analyzed, focusing on their appearance in the spleen, blood and bone marrow at inductive, plateau and dissociative phases of the primary and secondary immune response.

The presented data show that the relative frequencies of plasmablasts in spleen and blood are nearly identical during the NP-KLH response, thus suggesting that the splenic

plasmablast subset gives rise to the blood plasmablasts. However, the bone marrow compartment was resided by low plasmablast numbers at all analyzed time points. It will be of great interest to know if further differentiation into plasma cells is the prerequisite of their entrance into the bone marrow or whether the circulating plasmablasts in blood migrate towards other organs. This question could be addressed by adoptive transfer of blood residing plasmablasts. Another inevitable question to address would be whether the entry of plasmablasts from the spleen into the blood is a stochastic or a selective process. A criterion for such a selective enrichment could be antigen specificity. The obtained data revealed that decrease of hapten-specific plasmablast numbers in spleen was accompanied by their disappearance from the blood circulation, thus suggesting an unselective enrichment in terms of hapten specificity. Further quantification showed the differentiation markers CD22.2 and MHCII to be uniformly expressed on all plasmablasts irrespective of their location.

Assessing the frequencies of plasma cells showed that the dynamics of this subset in blood resembles the observed dynamics in the bone marrow compartment. This observation possibly hints at the blood plasma cells being precursors of the bone marrow plasma cell compartment and supports previous reports from Tarlinton and colleagues (Blink, 2005). Interestingly, investigation of the hapten-specific plasma cell response led to the same results. The increasing frequency of  $\lambda^+$  plasma cells within the spleen by d16 p.i. was clearly reflected in blood and bone marrow.

Further characterization revealed a heterogeneous distribution of surface MHCII expression on the plasma cell subset. Detected plasma cells in spleen and bone marrow could be separated in two fractions with the following phenotype; i)  $B220^-CD138^+CD22.2^-MHCII^+$  and ii)  $B220^-CD138^+CD22.2^-MHCII^-$ . The bone marrow residing plasma cells, however, consisted almost exclusively of the  $MHCII^-$  fraction after immunization. One possible explanation would be the stricter regulation of CD22.2 compared to MHCII. In such a scheme the expression of surface CD22.2 would be probably coupled to the B220 expression and down regulated early during the differentiation process, as no distinct  $B220^+CD22.2^-$  cell subset could be detected. In contrast, MHCII is probably down-regulated on plasma cells later, resulting in a diverse expression profile in spleen and blood. It would be of great interest to study the



migratory behavior of both, MHCII<sup>+</sup> and MHCII<sup>-</sup> subsets, as it is reported that fully differentiated plasma cells are not migratory (Tarlington et al., 2008).

## **5.2 Detection of GC B cells in blood of NP-KLH immunized C57BL/6 mice**

A major finding of this work is the detection of GC B cells within the blood circulation of immunized C57BL/6 mice. This observation was surprising, as GC B cells are generally believed to be restricted to secondary lymphoid organs except in some autoimmune diseases, leading to the formation of ectopic GCs (Boer et al., 2000). The detected blood GC B cell subset displayed a number of characteristics that strongly suggest their derivation from the ongoing GC B cell reaction in secondary lymphoid organs. First, the blood GC B cell subset consists of fully matured B cells and has a follicular origin as shown by their B220<sup>+</sup>CD21<sup>+</sup>CD23<sup>+</sup>CD93<sup>-</sup> phenotype. Second, their kinetic resembles the monitored kinetic of splenic GC B cells. Third, a fraction of hapten-binding GC B cells appears in the blood by day 4 after immunization, much like the GC response in the spleen. This subset was not visible in naïve animals. Fourth, the NP-binding blood GC B cell subset displayed the same dynamics as splenic GC B cells during the primary and the secondary responses. However, GC B cells were not detectable within the bone marrow compartment at all analyzed time points. Thus, an arbitrary appearance of GC B cells in blood would be rather unlikely.

An interesting question to address would be whether the surface marker expression profile of blood released GC B cells differs from the originally described GC B cells in literature. Therefore, the phenotypic characteristics of the newly detected blood GC B cells were analyzed and compared to the splenic GC B cell subset. Interestingly, both subsets displayed similar traits, suggesting a rather unselected release into blood circulation in terms of isotype switch, hapten binding and CD38 expression. Addressing the question why these cells enter the blood circulation is of considerable interest. A possible explanation is that the assumed recycling of GC B cells suggested by Kepler and many others (Kepler and Perelson, 1993), (Oprea and Perelson, 1997), (Oprea et al., 2000), (Moreira and Faro, 2006), is not only restricted to secondary lymphoid organs but involves recirculation through the blood. The continuous introduction of GC B cells

into blood and their subsequent recirculation into secondary lymphoid organs would be a new way of iteration, complementing the occurring iteration within GCs. Notably, a recirculation involving all GCs within secondary lymphoid organs would be a practical approach to optimize affinity maturation and diversity in a shorter time frame as it would result in continuously reseeded and/or repopulated GCs. Despite the data shown in this work, there has been some experimental evidence published, supporting the theory of inter-GC recirculation. Tarlinton and colleagues have shown that emigration of B cells from GCs occurs during the immune response (Tarlinton, 2006). Furthermore, they showed that IgG1<sup>+</sup> B cells with accumulated mutations bearing a memory phenotype and antigen-specific plasma cells appear in blood one week after immunization (Blink, 2005). Despite the reports suggesting the emigration of GC products into the blood, it was shown that persisting GCs can be reutilized by hapten-specific transgenic B cells (Schwickert et al., 2009). Importantly, a pre-GC B cell population has been reported in the blood of children with SLE (Arce et al., 2001) and GC B cells were also detected in the blood of HIV infected drug-naïve Africans (Béniguel et al., 2004). Considering the mentioned data above and the hints from literature, the next inevitable step was to address the recirculation-hypothesis by direct evidence, which was adoptive transfer of the blood GC B cells.

### **5.3 Transferred blood GC B cells repopulate persisting GCs and differentiate into plasma cells**

The dynamics of the GC reaction in all its particulars has been the subject of several investigations over the last years. While the occurrence of somatic hypermutation and the selective retention of high-affinity clones are well-documented, the means by which the whole process of affinity maturation occurs remain unclear (Tarlinton, 1998, 2008; Anderson et al., 2009). Although the concept of inter-GC recirculation as a solution for affinity maturation within a short time period seems very plausible, so far it has not been documented by direct experimental evidence. The data presented here, strongly suggest the recirculation capacity of GC B cells via blood during the NP-KLH specific immune response.

To address this hypothesis by a direct approach, the blood GC B cell subset was isolated at a selected time point after immunization and their migration and differentiation was monitored by adoptive transfer. By choosing the recipients at two selected time points early into and right before the peak after challenge with NP-KLH, their different migratory behavior was assessed with respect to the stage of the immune response. A calculation of the detected absolute donor cell numbers revealed that the efficiency of transfer only slightly changed between the two chosen time points of transfer. In both transfer systems, numbers of donor cells increased about 6-fold within two days, showing their proliferation. However, transferred GC B cells differentiated in a different manner, depending on the time point of transfer. Whereas adoptive transfer into recipients at an early stage of response (d4 transfer) led to higher frequencies of isotype-switched donor cells, transfer into animals at the later time point (d8 transfer) favored an extensive differentiation into plasma cells. The latter was accompanied by detectable numbers of hapten-binding B cells. Taking into account the calculated lymphocyte numbers retrieved from kinetic experiments, the described observations held true with respect to absolute donor cell numbers. These data raise the interesting possibility that the observed GC B cell subset in the blood contains B cells which acquired this phenotype within GCs, survived the GC reaction and entered into the blood. Thus, they have the capability to differentiate further into isotype-switched non GC B cells or plasma cells, an attribute described for GC B cell emigrants.

Immunofluorescence analysis of *whole* mesenteric lymph nodes provided a detailed insight into the migratory and proliferative behavior of donor GC B cells and T cell interactions during the first week after transfer. In contrast to the obtained flow cytometric results from spleen, the counted absolute donor cell numbers in lymph nodes were higher after the transfer into day 8 p.i. mice. However, it should be considered that these two organs have disparate anatomical organizations and routes by which lymphocytes and antigens gain access to their lymphoid tissues. Despite the varying absolute numbers, the two transfer systems showed similar characteristics which can be summarized as follows: In both systems, no donor B cells were detected in the T cell zone, but accumulated at the T/B border and were in direct contact with T cells. This contact was particularly apparent at the early time points of analysis and often associated with proliferation, indicated by Ki67 staining. However, direct T cell contact

was not only constrained to the T/B borders, but also apparent in other regions of the lymph node. Another common feature of both transfers was their prescribed migratory route within 8 days. During this period donor cells successively entered the B cell follicles, accumulated within the dark zone and subsequently migrated to the GC light zones. Interestingly, their accumulation within the light zone was accompanied by their vanishing from the dark zone. Thus, by day 8 after transfer recipient GCs populated by donor cells became visible. The extent of this colonization differed depending on the applied transfer system. The presented data are in line with the recent *in vivo* imaging studies from Nussenzweig and colleagues who reported a purposeful GC B cell movement from the GC dark zones to the light zones (Victoria et al., 2010).

Additionally, the IF zone proved to be a locale for accumulation of a donor B cell fraction as soon as two days after transfer, confirming previous reports from Haberman and colleagues (Kerfoot et al., 2011). Notably, the IF zone was enriched during the entire analysis by donor cells which were frequently in T cell contact and were also subjected to proliferation. Thus, instead of concentrating at the border with the T cell zone, a fraction of the transferred GC B cells successively migrated into the follicle and the IF zone. It would be of great interest to know whether the GC entered cells originated from the follicle residing cells or came from the IF. This question would be hard to address, since the donor cell accumulation in both regions occurred simultaneously.

Widespread Bcl6 expression, however, was only evident in donor cells found within the GCs, confirming their participation in GC reaction of recipients.

The earliest evidence of progression toward the SCS was observed by day 2 after transfer into d8 p.i. immunized mice and 4 days after transfer into d4 immunized mice. Interestingly, these time points correspond to day 8 after challenge of recipient. However, 2 days later, in both transfers donor cells were absent from this locale. The migration toward SCS coincided by the localization of donor plasma cells in this area, as we proved by parallel staining of consecutive slides. A fraction of these cells expressed also Ki67, indicating their proliferation in this area. These results are in line with Haberman and colleagues, who reported the accumulation of a large number of transferred antigen specific B cells in the area adjacent to the SCS. These cells

proliferated and were not dedicated to the GC reaction (Kerfoot et al., 2011). Interestingly, such proliferating cells were found by Manser and colleagues (Coffey et al., 2009) in the outer follicle of the spleen. Haberman and colleagues affirmed this observation and claimed that they are analogous to the cells found adjacent to the SCS. However, in both of these works the phenotype of these cells was not analyzed further. The data presented in this work are consistent with the previous reports and further indicate that the SCS is a site for expansion of blood GC B cells which differentiated into plasma cells. Interestingly, this phenomenon seems to hold true across different experimental transfer systems and organs.

Collectively, these data support a model in which GC B cells leave the ongoing reaction and recirculate through blood “grazing” the secondary lymphoid organs for antigen and probably T cell help. In such a system, they would consequently improve affinity by their participation in ongoing GC reactions, particularly by competition with other B cell clones. Furthermore, studies explained above strongly suggest that the fate of these circulating GC B cells is determined by the time point of immune response.

#### **5.4 Transferred IgM and IgG1 potential memory B cells display different migration patterns**

An essential output of the GC response is the memory B cell subset (McHeyzer-Williams et al., 2006; Tarlinton, 2006; Tomayko et al., 2010). These populations are described to be enriched with varying degrees for cells with improved antigen binding capacity due to the expansion of clones with appropriate V gene somatic mutations within the GCs (Smith et al., 1997). Although it is generally believed that the “classical” memory B cell is isotype-switched, recent reports have been strongly suggesting this subset to contain both; IgM and IgG1 B cells (Dogan et al., 2009), (White and Gray, 2000). In line with these findings, the kinetic data presented in this work have shown that representatives of the two memory B cell subsets reside in blood of NP-KLH immunized C57BL/6 mice.

To compare the migration pattern of the previously described  $B220^+PNA^{lo}CD38^+IgG1^+$  and  $B220^+CD38^+PNA^{lo}IgM^+$  subset, these cells were isolated and subsequently

transferred into recipients at two previously described different time points after immunization (section 5.3).

The term “potential” was chosen to point out that this population may also contain other activated B cells, since their V region somatic mutations were not analyzed prior to transfer. Such an analysis was technically impossible, as it would completely destroy the cell membranes. Despite the mutated V region, however, the enriched and transferred population displayed all described characteristics for memory B cells: They were bigger than naïve B cells according to the forward and sideward scatter gate, had down-regulated surface IgD, were IgM<sup>+</sup> and bound low amount of PNA. Furthermore, they expressed high levels of CD38. The data presented here revealed that the IgM<sup>+</sup> and IgG1<sup>+</sup> memory B cell subsets display different homing capacities.

Upon transfer, the IgG1<sup>+</sup> B cells dominantly accumulated in the bone marrow compartment. Interestingly, the transfer of IgG1<sup>+</sup> B cells into recipients at an earlier time point p.i. resulted in their earlier appearance in the bone marrow. In both transfer systems, surface B220 was down-regulated on the detected donor cells over time, suggesting their differentiation into plasmablasts. It would be interesting to know whether this differentiation occurred within the bone marrow or if the plasmablasts that differentiated in other lymphoid organs immigrated into the bone marrow. If the bone marrow residing plasma cells originate from secondary lymphoid organs, a corresponding population should be detectable in spleen. This was not the case after transfer into d8 recipients, as numbers of IgG1<sup>+</sup> cells in spleen were below detection. However, the lymph nodes cannot be excluded as a potential site of differentiation, as this organ was not subjected to our analysis. Adoptive transfer of the IgG1<sup>+</sup> cells into d4 recipients resulted in their accumulation within bone marrow by day 2, whereas the earliest evidence of donor cells in spleen was found at day 4 after transfer and the majority of these cells had already down-regulated B220.

Taken together, these data support the idea that IgG1 memory B cells directly home to bone marrow and differentiate into plasma cells, thus are in line with Weill and colleagues (Dogan et al., 2009) .

Another vital part of the memory response to antigen is the production of IgM<sup>+</sup> memory B cells. Although the factors that regulate isotype-switching are well-known, little

attention has been paid to the functional diversity and distribution of IgM<sup>+</sup> memory B cells in vivo. This question was tried to address by transfer of blood-derived memory B cells. The IgM<sup>+</sup> potential memory B cell subset was isolated from the blood of C57BL/6 mice 8 days after their immunization with NP-KLH and transferred into recipients at an early time point (d4 p.i.), and right before the peak (d8p.i.) of the GC response. Consistent with the previously described data (shown in sections 4.2.3 and 4.3.3), the detected donor cell numbers differed between the two transfer systems. Whereas donor cell numbers remained nearly constant after their transfer into d4 recipients, transfer into the d8 recipients resulted in their sequential decrease over time. This phenomenon could be explained by the conditions the donor cells face whilst entering secondary lymphoid organs of the recipient. As the immunofluorescence microscopy studies of the spleen and the lymph nodes revealed, 4 days p.i. GC structures are fragmentary built and the recipients' B cell response has not matured yet, but Th cells are available in the follicle. Consequently, at day 4 the antigen is disposable on FDCs and Th cells are available whereas at day 8 the B cell response of recipient has matured and the donor B cells have to compete with the endogenous B cells.

A comparison of the surface and intracellular marker expression profiles of spleen and bone marrow residing IgM donor cells with the primal phenotype revealed insight into their preferred differentiation pathways and highlighted the role of antigen availability in these processes. Interestingly, a fraction of donor cells regained GC phenotype after both transfers, strongly suggesting their recruitment into the GC reaction of the recipient. This subset was detectable until day 12 p.i. of recipient and vanished afterwards. Another common feature was the fraction of hapten-binding donor cells which disappeared by day 16 p.i. of recipients.

Despite the described similarities between the IgM<sup>+</sup> transfers into day 4 and day 8 p.i. recipients, flow cytometric analysis revealed that the differentiation pathways of donor cells exhibited essential variation. Transfer of IgM<sup>+</sup> cells into day 4 p.i. recipients favored isotype switch, such that 2 days after transfer 10-15% of detected donor cells in the spleen and bone marrow expressed surface IgG1. Strikingly, as shown by flow cytometric data the transfer into day 8 p.i. recipients resulted in a rapid differentiation of two thirds of the donor cells into antibody secreting plasma cells. However, 4 days later,

the donor specific plasma cell response weaned, suggesting the vast majority of these cells to be rather short lived.

Analysis of whole mesenteric lymph nodes via immunofluorescence microscopy unveiled further details regarding the detailed migratory and proliferative behavior of donor IgM<sup>+</sup> cells during the first week after transfer.

The transferred IgM<sup>+</sup> cells into day 4 p.i. recipients accumulated within the IF zone and along the T/B cell zone border prior to migrating into the BCZ. The vast majority of the T/B border residing cells were in direct contact with T cells and partially proliferating. However, 2 days later donor cells had entered the follicle and become apparent in the GC dark and light zones, but were still detectable at the T/B border and the within the IF zone, albeit to a lesser extent. One week after transfer donor B cells had disappeared from the dark zones and was scarcely found within light zones. Instead, they re-accumulated within the IF and along the T/B borders. Notably, half of these cells were T cell associated while one fourth was proliferating. Additionally, a fraction of donor cells appeared for the first time within the area adjacent to the SCS.

In contrast, transferred IgM<sup>+</sup> cells into day 8 p.i. recipients were detected with less numbers in spleen, blood and bone marrow and followed a slightly different migration route. Although they also accumulated after 2 days within the IF zone, they were absent from the T/B cell zone borders. However, it remains to be addressed if the donor cells have moved along the borders before the first time point of analysis. Instead, donor cells accumulated in the B cell follicle and gradually moved to the GC dark zones and the adjacent area to the SCS. Finally, one week after transfer, cells had disappeared from the dark zones but were still enriched at the SCS borders. Notably by this time, similar to the previous observations, donor cells were found accumulated along the T/B cell zone borders. The transferred cells were not detected within light zones at any time point of this analysis. This could be explained by the two different transfer systems used. However, it should be taken into account that although as shown here blood released IgM<sup>+</sup> memory B cells have the capability to return into secondary lymphoid organs and getting recruited into the GC reaction, they may do so to a lesser extent than blood GC B cells which are per se dedicated to the GC response by their surface marker expression profile. It remains to be elucidated whether the induction of a secondary



response would increase the participation of IgM<sup>+</sup> and IgG1<sup>+</sup> memory B cells in the ongoing GC reaction as would be expected for IgM<sup>+</sup> memory B cells (Dogan et al., 2009).

In total, the data presented here show that during the NP-KLH response blood-derived IgM<sup>+</sup> potential memory B cells have the capability to enter secondary lymphoid organs through a prescribed migration route and participate in the ongoing GC reaction. These results are in line with Weill and colleagues who argued that transferred splenic IgM memory B cells reinitiate GC responses after induction of an immune response (Dogan et al., 2009). Hence, the blood residing IgM<sup>+</sup> B cells most probably originate from the described memory B cells outside the follicles. Our flow cytometric and immunofluorescence microscopy data revealed that a fraction of these cells differentiates further into plasma cells, which display a similar migration pattern, irrespective of the time point after immunization they get released into blood.

In conclusion, the results presented here demonstrate that a previously less described microenvironment within the IF zone of lymph nodes serves as an initial destination of circulating GC B cells and IgM<sup>+</sup> potential memory B cells and can promote initial proliferative stages during and after primary interactions with T cells at the interface of follicles. It would be important to understand the role of such a microenvironment as a potential site for clonal expansion, prior to the GC response. As Cohn mentioned many years ago (Cohn, 1972), unless a large pool of pathogen-specific lymphocytes was generated in a short period of time, the infection would overwhelm the host as a result of the high replicative capacity of most pathogens. Based on this idea, Manser and colleagues argue that if individual GCs are founded by only a small number of B cell precursors, subsequent generation of effector cell populations of sufficient size, expressing BCRs of the affinity and specificity necessary for rapid antigen (pathogen) clearance might not occur. They showed a rapid expansion of antigen specific B cells at the perimeters of the splenic follicles prior their introduction into the GCs (Coffey et al., 2009). This work support the idea that the IF zone would be the corresponding microenvironment in lymph nodes as suggested by Haberman and colleagues.

## 6 Summary and perspectives

In this work, the phenotypes of GC derived B cell subsets in the spleen, blood and bone marrow of C57BL/6 mice were evaluated at consecutive time points after their primary and secondary challenge with NP-KLH. Previous phenotypic studies have delivered significant information regarding the molecules expressed on GC derived B cell subsets and enable us to unambiguously identify GC B cells, plasmablasts and plasma cells in the corresponding organs (Ridderstad and Tarlinton, 1998; Shinall et al., 2000; McHeyzer-Williams and McHeyzer-Williams, 2004; Wolniak et al., 2006). In this study, these populations were resolved into discrete subsets by flow cytometry, based on the expression and distribution of Ig isotypes, activation markers and differentiation antigens. Furthermore, their formation, accumulation and their dissolve within the spleen, blood and bone marrow compartment were monitored in the course of primary and secondary immune response.

Taken together, the analyses revealed the following major points:

- The association between the expression of CD22.2 and MHCII, and the generation of plasmablasts and plasma cells were examined during the primary and secondary response to NP-KLH. Subsequently, CD22.2 was found to be a stricter marker for segregation of plasmablasts and plasma cells than MHCII. Whereas syndecan binding plasmablasts uniformly expressed CD22.2, this surface marker was homogenously down-regulated on plasma cells. In contrast the expression of MHCII on plasma cells was rather heterogeneous, comprising the two MHCII<sup>int</sup> and MHCII<sup>lo</sup> subsets.

It remains unclear whether these MHCII<sup>int</sup> and MHCII<sup>lo</sup> plasma cell populations are also functionally distinguishable. However, such questions could be addressed by adoptive transfer experiments and chemokine migration assays.

- Another major finding of this work was the detection of *GC B cells* in the circulating blood. The data presented here show that the newly detected blood-derived GC B cell subset consists of mature B cells, displaying a follicular phenotype. This finding was of particular importance, as it challenges the idea of

iteration within GCs by putting it in a new context. These data imply a complementary model to the traditional conception of an “internal iterative process” wherein GC B cell clones are “recycled” several times within single GCs. Thus, a “recirculation model” was postulated, wherein GC B cells leave the GC reaction after getting selected, entering the blood circulation, in order to getting recruited into the ongoing GC reaction in secondary lymphoid organs. Interestingly, these observations were reinforced by the detection of B cells with GC phenotype in blood of HIV infected patients (Béniguel et al., 2004). Furthermore, transfer experiments performed by Nussenzweig and colleagues (Schwickert et al., 2009) demonstrated that GCs are open structures and their seeding is probably an ongoing process. However, direct proof of recirculation and emigration of GC B cells is still missing.

- To test the concept of “recirculation” adoptive transfer experiments of the GC B cell subset detected in blood were implemented. The establishment of a functioning transfer system was particularly challenging, due to the limited numbers of lymphocytes in blood and the low frequencies of the GC B cell subset. Finally a particular cell enrichment and transfer procedure was established, allowing the efficient transfer of a few thousand cells, and their subsequent detection via flow cytometry and immunofluorescence microscopy. Nevertheless, dealing with such small numbers made it possible to make more funded predictions about how such processes take place in “real nature”. Hence; in this work a “wildtype” mouse model was chosen for conduction of these analyses. The resulting data clearly show that the blood-derived GC B cell subset can enter the secondary lymphoid organs and colonize the GCs of recipients. Additionally, the transferred blood derived GC B cells participate in the GC reaction as evidenced by their migration route from the dark zone to the light zone, which was associated with their proliferation and expression of the GC specific marker Bcl-6. Collectively, these data support a model wherein GCs are open structures (Schwickert et al., 2009), allowing the continuous immigration of GC B cells derived from other GCs via the bloodstream. Thus, during a response, individual GCs can be continuously repopulated by selected

clones from all secondary lymphoid organs. It could be speculated that such an interaction would result in an accelerated affinity maturation

- To address the question whether the capability to immigrate into secondary lymphoid organ is a blood GC B cell specific feature, adoptive transfers of two blood-derived B cells subsets, corresponding to later time points of GC B cell ontogeny were conducted. The data revealed a different migratory route for CD38<sup>hi</sup>IgG1<sup>+</sup> and CD38<sup>hi</sup>IgM<sup>+</sup> potential memory B cells. Whereas the IgG1<sup>+</sup> subset preferentially migrated toward the bone marrow compartment and subsequently down-regulated B220 surface expression, suggesting their differentiation into plasma cells, the IgM<sup>+</sup> cells were recruited to the spleen and were mainly found located within the B cell zones. A significant proportion of the IgM<sup>+</sup> cells differentiated into plasma cells. These results support the idea that after challenge, the IgG1<sup>+</sup> subset has immediate effector functions, the hallmark of B cell memory, but has little capacity to reinitiate the GC response, whereas the IgM<sup>+</sup> cells mobilize to the GCs and switch to IgG1 and thereby ensure the replenishment of the memory B cell pool (Dogan et al., 2009).

It would be interesting to see how the migratory behavior of these subset changes over time, and particularly if some of the differentiated plasma cells would acquire longevity. Another important question to address concerns the proliferative behavior of the blood derived GC B cell and potential memory B cell subsets. These questions could be addressed by BrdU labeling of donor B cell subsets and their subsequent analysis at much later time points (months). In such experiments a detailed localization of the different transferred cell subsets within the bone marrow compartment via immunofluorescence microscopy would deliver appreciable information. It would be of further interest whether these subsets have different potentials to induce B cell memory. This issue will be unveiled by induction of secondary of tertiary challenges.

## 7 Zusammenfassung

Keimzentren (GC) sind für die Entstehung des immunologischen Gedächtnisses und der Produktion hoch-affiner Antikörper von entscheidender Bedeutung. Hierbei handelt es sich um transiente Strukturen die nach Immunisierung mit einem T Zell-abhängigen Antigen in sekundär lymphatischen Geweben wie der Milz und den Lymphknoten entstehen. Im Laufe einer Immunantwort, wandern aktivierte B Zellen in die sekundär lymphatischen Organe ein und erreichen dann die T-Zell-Bereiche. Dort befinden sich für dasselbe Antigen spezifische, bereits aktivierte T-Zellen. Diese, ermöglichen den B-Zellen zu proliferieren. Ein Teil jener B-Zellen wandert zusammen mit den T-Zellen, von denen sie aktiviert wurden, zu den B-Zell-Follikeln, wo sie an der Grenze zur T-Zell-Zone Keimzentren bilden. Innerhalb der Keimzentren entstehen durch einer Reihe von mikro-evolutionären Prozessen, B-Zellen mit hoher Antigenaffinität, diese erhalten überlebenswichtige Signale von T-Zellen und können die Keimzentren verlassen um zu langlebigen Plasmazellen oder B-Gedächtniszellen zu differenzieren. Diese B-Gedächtniszellen sezernieren auch Antikörper anderer Immunglobulin-Klassen als IgM. Die Sezernierung solch „Klassengewechselter“ Antikörper ist für die Optimierung der Immunantwort von essentieller Bedeutung, da die „Immunglobulin-klasse“ eines Antikörpers bestimmend für seine Effektor-Funktion ist. Beispiele solcher Funktionen wären die Aktivierung des Komplementsystems, Opsonisierung, Neutralisation bakterieller Toxine oder Mastzellen Aktivierung.

Ogleich GCs unerlässlich für die Entstehung des immunologischen Gedächtnisses sind, spielen ektopische Keimzentren, also Keimzentren die sich außerhalb des sekundären lymphatischen Gewebes bilden, in der Entstehung und dem Verlauf diverser Erkrankungen wie z.B. Rheumatischer Arthritis, Hashimoto Thyreoiditis, Sjogren Syndrom, Multipler Sklerose, HIV und chronischer Hepatitis C eine große Rolle. Aus diesem Grund ist es unabdingbar, die Dynamik und die regulierenden Mechanismen, die dem Fortbestand und der Terminierung der Keimzentren zugrundeliegen zu verstehen. Deshalb wurden folgende Untersuchungen durchgeführt:

- i) Es wurde eine Kinetik sämtlicher wichtigen in der GC-Reaktion involvierten B Zellen mit Hilfe von durchflusszyometrischer Methoden erstellt. Diese Analyse umfasste die drei Organe, Milz, Blut und das isolierte Knochenmark aus Femur und Tibia, und wurde an mehreren aufeinanderfolgenden Zeitpunkten nach Induktion einer primären und sekundären Immunantwort mit dem Model Antigen NP-KLH vorgenommen.
- ii) Um das Migrationsverhalten von GC-B-Zell-Emigranten zu untersuchen, wurden verschiedene im Blut zirkulierende zu unterschiedlichen Zeitpunkten

der GC-B-Zell-Entwicklung gehörige B-Zell-Populationen isoliert und in Rezipienten transferiert die zu unterschiedlichen Zeitpunkten zuvor immunisiert waren. Die Lokalisierung und weitere Differenzierung der transferierten B-Zellen wurden in der Milz und im Knochenmark mittels Durchflusszytometrie und in den mesenterischen Lymphknoten mit Immunofluoreszenz-Mikroskopie innerhalb einer Woche nach dem Transfer bestimmt.

Diese Arbeit trägt durch folgende Erkenntnisse zum Verständnis der GC Entwicklung und Dynamik bei:

- 1) Eines der wichtigsten Erkenntnisse dieser Arbeit war die Detektion von B-Zellen mit einem GC Phänotyp im Blut. Die durchflusszytometrischen Untersuchungen zeigten dass diese Zellen eindeutig reife B-Zellen sind und folliculären Ursprung haben. Die Entdeckung von GC-B-Zellen im Blut führte zu der Hypothese der „Rezirkulation“; die besagt das eine Fraktion von GC-B-Zellen nach Verlassen der GC ins periphere Blut wandern, ohne ihren Phänotyp zu verlieren. Das Zirkulieren dieser Zellen im Blut ermöglicht es ihnen in jedes beliebige sekundäre lymphatische Gewebe einzuwandern um dort, in den lokalen GC Reaktionen teilzunehmen. Solch ein Schema würde zu einer höheren GC-Diversität und einer schnelleren Affinitätsreifung führen.
- 2) Um der „Rezirkulation-Hypothese“ eine experimentelle Basis zu geben, wurden die im Blut detektierten GC-B-Zellen isoliert und in Rezipienten transferiert, die sich in der frühen Phase oder kurz vor dem Höhepunkt der GC Reaktion befanden. Die Resultate zeigten dass die transferierten GC-B-Zellen in das sekundäre lymphatische Gewebe einwandern und an laufenden GC Reaktionen teilnehmen können um dann weiter zu Plasmazellen zu differenzieren.
- 3) Um zu prüfen ob die Fähigkeit in sekundär lymphatisches Gewebe zu immigrieren im Laufe der GC B-Zell Entwicklung beibehalten wird, wurden zwei weitere aus dem Blut gewonnene B-Zelltypen, die in einem späteren Entwicklungsstadium der GC B-Zellontogenese waren, auf dieselbe Weise transferiert. Hierbei handelte es sich um zwei potentielle Gedächtnis-B Zellpopulationen;  $CD38^{hi}IgG1^{+}$  und  $CD38^{hi}IgM^{+}$  B-Zellen. Die Analysen ergaben dass diese zwei B-Zellpopulationen in der Tat ein unterschiedliches Migrationsverhalten aufweisen. Während die  $IgG1^{+}$  B-Zellen bevorzugt in das Knochenmark einwanderten und zu Plasmazellen differenzierten, immigrierten die  $IgM^{+}$  B-Zellen auch in die Milz und die Lymphknoten wo sie teilweise an der laufenden GC Reaktion des Rezipienten teilnahmen.

## 8 Abstract

Development of B cell memory and generation of high affinity antibodies are crucially dependent on germinal centers (GC). GCs are transient structures which arise after challenge with a T cell-dependent antigen within secondary lymphoid organs, such as the spleen and lymph nodes. During the immune response activated B cells migrate to the T cell zones within the secondary lymphoid organs and acquire help from the residing antigen-specific, activated T cells. Some of these activated B cells migrate toward the B cell zones, expand rapidly and found the GCs. A number of micro-evolutionary processes occur within the GCs, leading to the production of high-affinity B cells which acquire the necessary survival signals from T cells and leave the GCs in order to differentiate into plasma cells and memory B cells. These memory B cells are able to produce antibodies other than IgM. The production of such “class switched” antibodies is important for optimizing the immune response to particular antigens, since the antibody class defines its effector functions, such as complement activation, opsonization, neutralization of bacterial toxins and mast cell activation.

GCs play a major role in the development of protective immunological memory; however, they are responsible for the pathogenesis of several autoimmune and infectious diseases, such as rheumatic arthritis, hashimoto thyroiditis, sjogren syndrome, multiple sclerosis, HIV and chronic hepatitis C. It is, therefore, of significant importance to understand the dynamic of GCs and the regulating mechanisms which underlie their progress and termination. This work delivers a deeper insight into the mentioned topics by performing the following analyses:

- i) A kinetic of the GC B cell subsets was conducted by means of flow cytometric analyses and immunofluorescence microscopy methods. This kinetic included the spleen, blood and isolated bone marrow from femur and tibia and comprised several time points after primary and secondary challenge with NP-KLH, a model antigen often used to analyze the T-dependent immune response.
- ii) To monitor the migratory behavior of GC B cell emigrants, different B cell subsets, corresponding to distinct stages of GC B cell ontogeny were isolated and enriched from blood. Subsequently, these subsets were transferred into recipients at an early time point and shortly before the peak of their GC response. The localization and differentiation status of the donor B cells within spleen, bone marrow and mesenteric lymph nodes of recipients were determined during one week after transfer via flow cytometry and immunofluorescence microscopy.

This thesis contributes the following insight into the development and dynamics of the GC response:

1. The major finding of this work was the detection of B cells bearing a GC phenotype in blood. The flow cytometric analysis revealed that these cells consist of mature B cells of a follicular GC origin. The detection of GC B cells within blood led to the postulation of the “recirculation” hypothesis, which states that a fraction of GC B cells exits the GCs and enters the peripheral blood without losing the GC B cell phenotype. Consequently, the circulation through blood enables such emigrants to enter any secondary lymphoid organ, enabling them to be re-admitted to the local GC reactions. Supposedly, such a scheme could lead to faster affinity maturation and a higher diversity of GC B cells.
2. To test the „recirculation“ hypothesis, a blood derived GC B cell fraction was isolated and transferred into recipients which were at an early time point, just before the peak of their GC response. The obtained results showed that the blood derived GC B cells immigrate into secondary lymphoid organs and are recruited to the already existing GC reaction. Furthermore, they differentiated into plasmablasts and subsequently plasma cells.
3. To address the question whether the capability to immigrate into secondary lymphoid organs is a GC B cell specific feature, additional transfer experiments were conducted with blood derived CD38<sup>hi</sup>IgG1<sup>+</sup> and CD38<sup>hi</sup>IgM<sup>+</sup> potential memory B cells, which correspond to later stages of GC B cell ontogeny. Interestingly, these two subsets displayed a different migratory behavior. Whereas CD38<sup>hi</sup>IgG1<sup>+</sup> B cells preferentially migrated into the bone marrow and differentiated into plasma cells, CD38<sup>hi</sup>IgM<sup>+</sup> B cells migrated into the spleen and the lymph nodes and participated in the ongoing GC reactions.



## 9 References

Anderson, S.M., Khalil, A., Uduman, M., Hershberg, U., Louzoun, Y., Haberman, A.M., Kleinstein, S.H., and Shlomchik, M.J. (2009). Taking advantage: high-affinity B cells in the germinal center have lower death rates, but similar rates of division, compared to low-affinity cells. *J. Immunol.* *183*, 7314–7325.

Anderson, S.M., Tomayko, M.M., Ahuja, A., Haberman, A.M., and Shlomchik, M.J. (2007). New markers for murine memory B cells that define mutated and unmutated subsets. *Journal of Experimental Medicine* *204*, 2103–2114.

von Andrian, U.H., and Mempel, T.R. (2003). Homing and cellular traffic in lymph nodes. *Nature Reviews Immunology* *3*, 867–878.

Arce, E., Jackson, D.G., Gill, M.A., Bennett, L.B., Banchereau, J., and Pascual, V. (2001). Increased Frequency of Pre-germinal Center B Cells and Plasma Cell Precursors in the Blood of Children with Systemic Lupus Erythematosus. *The Journal of Immunology* *167*, 2361–2369.

Bachmann, M.F., Odermatt, B., Hengartner, H., and Zinkernagel, R.M. (1996). Induction of long-lived germinal centers associated with persisting antigen after viral infection. *J. Exp. Med.* *183*, 2259–2269.

Beltman, J.B., Allen, C.D.C., Cyster, J.G., and de Boer, R.J. (2011). B cells within germinal centers migrate preferentially from dark to light zone. *Proc. Natl. Acad. Sci. U.S.A.* *108*, 8755–8760.

Berek, C., and Milstein, C. (1987). Mutation drift and repertoire shift in the maturation of the immune response. *Immunol. Rev.* *96*, 23–41.

Blink, E.J. (2005). Early appearance of germinal center-derived memory B cells and plasma cells in blood after primary immunization. *Journal of Experimental Medicine* *201*, 545–554.

Boer, B.A., Voigt, I., Kim, H.-J., Camacho, S.A., Lipp, M., Förster, R., and Berek, C. (2000). Affinity Maturation in Ectopic Germinal Centers. In *Lymphoid Organogenesis*, F. Melchers, ed. (Berlin, Heidelberg: Springer Berlin Heidelberg), pp. 191–195.

Béniguel, L., Bégaud, E., Cognasse, F., Gabrié, P., Mbolidi, C.D., Sabido, O., Marovich, M.A., deFontaine, C., Frésard, A., Lucht, F., et al. (2004). Identification of Germinal Center B Cells in Blood from HIV-infected Drug-naïve Individuals in Central Africa. *Clin Dev Immunol* *11*, 23–27.

Cervenak, L., Magyar, A., Boja, R., and László, G. (2001). Differential expression of GL7 activation antigen on bone marrow B cell subpopulations and peripheral B cells. *Immunol. Lett.* *78*, 89–96.

Cesta, M.F. (2006). *Normal Structure, Function, and Histology of the Spleen.*

Toxicologic Pathology *34*, 455–465.

Clarke, S.H., Huppi, K., Ruezinsky, D., Staudt, L., Gerhard, W., and Weigert, M. (1985). Inter- and intracloal diversity in the antibody response to influenza hemagglutinin. *J Exp Med* *161*, 687–704.

Coffey, F., Alabyev, B., and Manser, T. (2009). Initial Clonal Expansion of Germinal Center B Cells Takes Place at the Perimeter of Follicles. *Immunity* *30*, 599–609.

Cohn, M. (1972). Immunology: what are the rules of the game? *Cell. Immunol.* *5*, 1–20.  
Crotty, S., Johnston, R.J., and Schoenberger, S.P. (2010). Effectors and memories: Bcl-6 and Blimp-1 in T and B lymphocyte differentiation. *Nat. Immunol.* *11*, 114–120.

Debnath, I., Roundy, K.M., Weis, J.J., and Weis, J.H. (2007). Defining in vivo transcription factor complexes of the murine CD21 and CD23 genes. *J. Immunol.* *178*, 7139–7150.

Dogan, I., Bertocci, B., Vilmont, V., Delbos, F., Mégret, J., Storck, S., Reynaud, C.-A., and Weill, J.-C. (2009). Multiple layers of B cell memory with different effector functions. *Nature Immunology* *10*, 1292–1299.

Fooksman, D.R., Schwickert, T.A., Victora, G.D., Dustin, M.L., Nussenzweig, M.C., and Skokos, D. (2010). Development and Migration of Plasma Cells in the Mouse Lymph Node. *Immunity* *33*, 118–127.

González-Fernández, A., and Milstein, C. (1998). Low antigen dose favours selection of somatic mutants with hallmarks of antibody affinity maturation. *Immunology* *93*, 149–153.

Gray, D., and Skarvall, H. (1988). B-cell memory is short-lived in the absence of antigen. *Nature* *336*, 70–73.

Hannum, L.G., Haberman, A.M., Anderson, S.M., and Shlomchik, M.J. (2000). Germinal Center Initiation, Variable Gene Region Hypermutation, and Mutant B Cell Selection without Detectable Immune Complexes on Follicular Dendritic Cells. *J Exp Med* *192*, 931–942.

Hauser, A.E., Junt, T., Mempel, T.R., Sneddon, M.W., Kleinstein, S.H., Henrickson, S.E., von Andrian, U.H., Shlomchik, M.J., and Haberman, A.M. (2007). Definition of germinal-center B cell migration in vivo reveals predominant intrazonal circulation patterns. *Immunity* *26*, 655–667.

Jacob, J., Kassir, R., and Kelsoe, G. (1991). In situ studies of the primary immune response to (4-hydroxy-3-nitrophenyl) acetyl. I. The architecture and dynamics of responding cell populations. *The Journal of Experimental Medicine* *173*, 1165.

Kepler, T.B., and Perelson, A.S. (1993). Somatic hypermutation in B cells: an optimal control treatment. *J. Theor. Biol.* *164*, 37–64.

Kerfoot, S.M., Yaari, G., Patel, J.R., Johnson, K.L., Gonzalez, D.G., Kleinstein, S.H., and Haberman, A.M. (2011). Germinal center B cell and T follicular helper cell development initiates in the interfollicular zone. *Immunity* 34, 947–960.

Klein, U., Rajewsky, K., and Küppers, R. (1998). Human immunoglobulin (Ig)M+IgD+ peripheral blood B cells expressing the CD27 cell surface antigen carry somatically mutated variable region genes: CD27 as a general marker for somatically mutated (memory) B cells. *J. Exp. Med.* 188, 1679–1689.

Kraal, G., Weissman, I.L., and Butcher, E.C. (1982). Germinal centre B cells: antigen specificity and changes in heavy chain class expression. *Nature* 298, 377–379.

Lanzavecchia, A., Bernasconi, N., Traggiai, E., Ruprecht, C.R., Corti, D., and Sallusto, F. (2006). Understanding and making use of human memory B cells. *Immunol. Rev.* 211, 303–309.

MacLennan, I.C.M. (1994). Germinal centers. *Annual Review of Immunology* 12, 117–139.

MacLennan, I.C.M., Toellner, K., Cunningham, A.F., Serre, K., Sze, D.M. -Y, Zúñiga, E., Cook, M.C., and Vinuesa, C.G. (2003). Extrafollicular antibody responses. *Immunological Reviews* 194, 8–18.

Manz, R.A., Löhning, M., Cassese, G., Thiel, A., and Radbruch, A. (1998). Survival of long-lived plasma cells is independent of antigen. *Int. Immunol.* 10, 1703–1711.

Martinez-Valdez, H., Guret, C., de Bouteiller, O., Fugier, I., Banchereau, J., and Liu, Y.J. (1996). Human germinal center B cells express the apoptosis-inducing genes Fas, c-myc, P53, and Bax but not the survival gene bcl-2. *J. Exp. Med.* 183, 971–977.

McHeyzer-Williams, L.J., Malherbe, L.P., and McHeyzer-Williams, M.G. (2006). Checkpoints in memory B-cell evolution. *Immunol. Rev.* 211, 255–268.

McHeyzer-Williams, L.J., and McHeyzer-Williams, M.G. (2004). Analysis of antigen-specific B-cell memory directly ex vivo. *Methods Mol. Biol.* 271, 173–188.

McHeyzer-Williams, M.G., McLean, M.J., Lalor, P.A., and Nossal, G.J. (1993). Antigen-driven B cell differentiation in vivo. *J. Exp. Med.* 178, 295–307.

Moreira, J.S., and Faro, J. (2006). Re-evaluating the recycling hypothesis in the germinal centre. *Immunol. Cell Biol.* 84, 404–410.

Nojima, T., Haniuda, K., Moutai, T., Matsudaira, M., Mizokawa, S., Shiratori, I., Azuma, T., and Kitamura, D. (2011). In-vitro derived germinal centre B cells differentially generate memory B or plasma cells in vivo. *Nat Commun* 2, 465.

Nossal, G., and Tarlinton, D.M. (1996). The phenotype and fate of the antibody-forming cells of the splenic foci. *Eur. J. Immunol* 444, 448.

- Oprea, M., van Nimwegen, E., and Perelson, A.S. (2000). Dynamics of one-pass germinal center models: implications for affinity maturation. *Bull. Math. Biol.* *62*, 121–153.
- Oprea, and Perelson, A.S. (1997). Somatic mutation leads to efficient affinity maturation when centrocytes recycle back to centroblasts. *The Journal of Immunology* *158*, 5155–5162.
- Paus, D., Phan, T.G., Chan, T.D., Gardam, S., Basten, A., and Brink, R. (2006). Antigen recognition strength regulates the choice between extrafollicular plasma cell and germinal center B cell differentiation. *J. Exp. Med.* *203*, 1081–1091.
- Dal Porto, J.M., Haberman, A.M., Shlomchik, M.J., and Kelsoe, G. (1998). Antigen drives very low affinity B cells to become plasmacytes and enter germinal centers. *J. Immunol.* *161*, 5373–5381.
- Radbruch, A., Muehlinghaus, G., Luger, E.O., Inamine, A., Smith, K.G.C., Dörner, T., and Hiepe, F. (2006). Competence and competition: the challenge of becoming a long-lived plasma cell. *Nat. Rev. Immunol.* *6*, 741–750.
- Ridderstad, A., and Tarlinton, D.M. (1998). Kinetics of establishing the memory B cell population as revealed by CD38 expression. *J. Immunol.* *160*, 4688–4695.
- Roitt, I.M., Brostoff, J., and Male, D.K. (2001). *Immunology* (Mosby).
- Rose, M.L., Birbeck, M.S., Wallis, V.J., Forrester, J.A., and Davies, A.J. (1980). Peanut lectin binding properties of germinal centres of mouse lymphoid tissue. *Nature* *284*, 364–366.
- Rumfelt, L.L., Zhou, Y., Rowley, B.M., Shinton, S.A., and Hardy, R.R. (2006). Lineage specification and plasticity in CD19<sup>+</sup> early B cell precursors. *The Journal of Experimental Medicine* *203*, 675–687.
- Schitteck, B., and Rajewsky, K. (1990). Maintenance of B-cell memory by long-lived cells generated from proliferating precursors. *Nature* *346*, 749–751.
- Scholzen, T., and Gerdes, J. (2000). The Ki-67 protein: from the known and the unknown. *J. Cell. Physiol.* *182*, 311–322.
- Schwab, S.R., and Cyster, J.G. (2007). Finding a way out: lymphocyte egress from lymphoid organs. *Nat. Immunol.* *8*, 1295–1301.
- Schwickert, T.A., Alabyev, B., Manser, T., and Nussenzweig, M.C. (2009). Germinal center reutilization by newly activated B cells. *The Journal of Experimental Medicine* *206*, 2907.
- Shih, T.-A.Y., Meffre, E., Roederer, M., and Nussenzweig, M.C. (2002). Role of BCR affinity in T cell dependent antibody responses in vivo. *Nat. Immunol.* *3*, 570–575.

Shinall, S.M., Gonzalez-Fernandez, M., Noelle, R.J., and Waldschmidt, T.J. (2000). Identification of murine germinal center B cell subsets defined by the expression of surface isotypes and differentiation antigens. *The Journal of Immunology* *164*, 5729.

Smith, K.G., Hewitson, T.D., Nossal, G.J., and Tarlinton, D.M. (1996). The phenotype and fate of the antibody-forming cells of the splenic foci. *Eur. J. Immunol.* *26*, 444–448.

Smith, K.G., Light, A., Nossal, G.J., and Tarlinton, D.M. (1997). The extent of affinity maturation differs between the memory and antibody-forming cell compartments in the primary immune response. *Embo J* *16*, 2996–3006.

Strasser, A. (2005). The role of BH3-only proteins in the immune system. *Nature Reviews Immunology* *5*, 189–200.

Takahashi, Y., Dutta, P.R., Cerasoli, D.M., and Kelsoe, G. (1998). In situ studies of the primary immune response to (4-hydroxy-3-nitrophenyl) acetyl. V. Affinity maturation develops in two stages of clonal selection. *The Journal of Experimental Medicine* *187*, 885.

Takahashi, Y., Ohta, H., and Takemori, T. (2001). Fas is required for clonal selection in germinal centers and the subsequent establishment of the memory B cell repertoire. *Immunity* *14*, 181–192.

Tarlinton, D. (1998). Germinal centers: form and function. *Curr. Opin. Immunol.* *10*, 245–251.

Tarlinton, D. (2006). B-cell memory: are subsets necessary? *Nat Rev Immunol* *6*, 785–790.

Tarlinton, D., Radbruch, A., Hiepe, F., and Dörner, T. (2008). Plasma cell differentiation and survival. *Current Opinion in Immunology* *20*, 162–169.

Tarlinton, D.M. (2008). Evolution in miniature: selection, survival and distribution of antigen reactive cells in the germinal centre. *Immunology and Cell Biology* *86*, 133–138.

Tomayko, M.M., Steinel, N.C., Anderson, S.M., and Shlomchik, M.J. (2010). Cutting edge: Hierarchy of maturity of murine memory B cell subsets. *J. Immunol.* *185*, 7146–7150.

Victoria, G.D., Schwickert, T.A., Fooksman, D.R., Kamphorst, A.O., Meyer-Hermann, M., Dustin, M.L., and Nussenzweig, M.C. (2010). Germinal center dynamics revealed by multiphoton microscopy with a photoactivatable fluorescent reporter. *Cell* *143*, 592–605.

Wang, Y., Zhang, P., Li, W., Hou, L., Wang, J., Liang, Y., and Han, H. (2006). Mouse follicular and marginal zone B cells show differential expression of Dnmt3a and sensitivity to 5'-azacytidine. *Immunology Letters* *105*, 174–179.

Weiser, A.A., Wittenbrink, N., Zhang, L., Schmelzer, A.I., Valai, A., and Or-Guil, M. (2011). Affinity maturation of B cells involves not only a few but a whole spectrum of relevant mutations. *Int. Immunol.* *23*, 345–356.

White, H., and Gray, D. (2000). Analysis of immunoglobulin (Ig) isotype diversity and IgM/D memory in the response to phenyl-oxazolone. *J. Exp. Med.* *191*, 2209–2220.

William, J., Euler, C., and Shlomchik, M.J. (2005). Short-lived plasmablasts dominate the early spontaneous rheumatoid factor response: differentiation pathways, hypermutating cell types, and affinity maturation outside the germinal center. *J. Immunol.* *174*, 6879–6887.

Wolniak, K.L., Noelle, R.J., and Waldschmidt, T.J. (2006). Characterization of (4-hydroxy-3-nitrophenyl) acetyl (NP)-specific germinal center B cells and antigen-binding B220-cells after primary NP challenge in mice. *The Journal of Immunology* *177*, 2072.

---

## 10 Appendix

### Abbreviations

AFC	Antibody forming cell
APC	Antibody presenting cell
BCR	B cell receptor
BSA	Bovine serum albumin
CDR	Complementary determining region
DZ	Dark zone
EDTA	Ethylene diamine tetraacetate
FACS	Fluorescence activated cell sorting
Fc	Fragment crystallizable
FDC	Follicular dendritic cell
GALT	Gut associated lymphoid tissue
GC	Germinal center
Ig	Immunoglobulin
IgH	Immunoglobulin heavy chain
IgL	Immunoglobulin light chain
IHC	Immunohistochemistry
i.p.	Intraperitoneal
kDA	Kilo Dalton
KLH	Keyhole limpet hemocyanin
LZ	Light zone

---

MALT	Mucosa associated lymphoid tissue
MHC	Major histocompatibility complex
NIP	(4-hydroxy-3-iodo-5-nitrophenyl) acetyl
NP	(4-hydroxy-3-nitrophenyl) acetyl
PALS	Periarteriolar lymphoid sheath
PBA	PBS containing 0.5% bovine serum albumin
PBS	Phosphate buffered saline
PE	Phycoerythrin
PNA	Peanut agglutinin
SA	Streptavidin
SLE	Systemic lupus erythematosus
SHM	Somatic hypermutation
SRBC	Sheep red blood cells
V	Variable gene segment/region



---

## **Publications and presentations**

### **Publications**

Greiff, V., Redestig, H., Luck, J., Bruni, N., Valai, A., Hartmann, S., Rausch, S., Schuchhardt, J., and Or-Guil, M. (2012). A minimal model of peptide binding predicts ensemble properties of serum antibodies. *BMC Genomics* 13, 79.

Weiser, A.A., Wittenbrink, N., Zhang, L., Schmelzer, A.I., Valai, A., and Or-Guil, M. (2011). Affinity maturation of B cells involves not only a few but a whole spectrum of relevant mutations. *Int. Immunol.* 23, 345–356.

Valai, A., Uhlmann S., Greiff, V., Hauser A.E., and Or-Guil, M. (2012). Is there an alternative pathway for GC B cell recycling? Detection of germinal center B cells in murine blood after immunization with NP-KLH. Manuscript in preparation

### **Poster presentations**

Statistical analysis of murine derived antibody sequences from germinal centers. Valai, A., Weiser, A.A., Zhang, L., and Or-Guil M., M. ECI (European Congress of Immunology), Paris, 2006

Refined lineage tree analysis is compatible with dynamic open germinal centers and hints at short-scaled diversification processes. Valai, A., Wittenbrink N., Zhang, L., Weiser A.A., and Or-Guil, M., GCC (Germinal Center Conference), Frankfurt, 2009

Kinetic of murine GC derived B cell subsets in the course of primary and secondary response to NP-KLH. Valai, A., Uhlmann S., and Or-Guil, M., YRLS (Young Researchers in Live Sciences), Paris, 2011

## Acknowledgement

**Inhalt aus datenschutzrechtlichen Gründen entfernt.**

## **Curriculum Vitae**

**Inhalt aus datenschutzrechtlichen Gründen entfernt.**

**Inhalt aus datenschutzrechtlichen Gründen entfernt.**

## **Erklärung**

Hiermit bestätige ich, Atijeh Valai, geb. 29.05.1979 in Wien, dass ich die vorliegende Arbeit selbstständig angefertigt habe.

Ich versichere, dass ich ausschließlich die angegebenen Quellen und Hilfen in Anspruch genommen habe.

Berlin, den 12.03.2012

---

(Atijeh Valai)